Imperial College London
Department of Electrical and Electronic Engineering

Distributed Coordination of Flexible Devices in Power Networks

Xuan Gong

January 2020

Submitted in part fulfilment of the requirements for the degree of Doctor of Philosophy in Electrical and Electronic Engineering of Imperial College London and the Diploma of Imperial College London

Declaration of Originality

I declare that this thesis, titled "Distributed Coordination of Flexible Devices in Power Networks", is entirely my own work under the supervision of Dr David Angeli and Dr Antonio De Paola. Any ideas or quotations from the work of other people, published or otherwise, are appropriately referenced. This work has not been previously submitted, in whole or in part, to any other academic institution for a degree, diploma, or any other qualification.

Xuan Gong
Control and Power Research Group
Department of Electrical and Electronic Engineering
Imperial College London
January, 2020

Copyright Declaration

Abstract

The penetration of new types of devices, such as domestic storage and electric vehicles, offers increasing flexibility on demand side. This will bring both new opportunities and challenges to the operation of power systems. The aim of this thesis is to design novel distributed control strategies for large scale coordination of flexible devices. To this end, flexible devices are modelled as self-interested rational agents that aim at minimizing their individual costs in response to the broadcast price signals. This thesis mainly consists of three parts, considering that the price signals can be designed in different forms, and that flexible devices could operate in different markets (e.g. energy markets, and integrated energy and reserve markets).

The first part presents a multi-agent framework for the coordination of large populations of micro-storage devices in energy markets, under the assumption that the electricity price is some monotone increasing function of total power demand. The second part extends the work of the first part through taking into account the topology of power networks: the proposed modelling framework envisages heterogeneous groups of loads that operate at different buses, connected by transmission lines of limited capacity. The locational marginal prices of electricity are used as price signals, which are different in general for each bus and calculated through an optimal power flow problem. In the framework of the third part, it is envisioned that micro-storage devices and electric vehicles participate in an integrated energy-reserve market, and that they can contribute to the provision of reserve by being available to reduce their power consumption. These flexible devices autonomously schedule their operation in response to two kinds of price signals – the locational marginal prices of energy and reserve.

Iterative schemes for the coordination of the flexible devices are presented in the three parts. It is proved that the proposed coordination schemes can ensure the convergence to stable market configurations, characterized as aggregative equilibria at which each device cannot further reduce its cost by unilaterally changing its power profile. Distributed implementations of these proposed control strategies are discussed, and their performance is evaluated in simulations on large scale power systems.

Acknowledgements

First, I would like to express my biggest gratitude to my supervisor Dr. David Angeli for his continuous support and guidance throughout the duration of my PhD. He has always been professional, kind and understanding. I feel thankful and honored for the time I have spent in the study under his supervision. In my mind, he is the best supervisor in the world.

I would like to thank my second supervisor Dr. Antonio De Paola for the frequent discussion and specific guidance during my PhD study. Especially, I appreciate his patience, no matter in inspiring me to think or helping me modify academic papers.

Many thanks also to all my friends and colleagues at the Control and Power Research Group, with whom I have had a wonderful time at Imperial College London.

Special thanks to the Department of Electrical and Electronic Engineering that offered me full funding for overseas tuition fees, and China Scholarship Council that provided a stipend for living cost. Their sponsorship is a strong support that helps me complete my studies.

Finally, I want to thank my family for their unconditional love and encouragement. They are always willing to listen to me whenever I am frustrated or pleased. My deepest gratitude goes to Fanglin Guo, who has been my constant companion sharing my every joy and sorrow.

Contents

List of Tables

List of Figures

List of Abbreviations

EV	Electric Vehicle
LMP	Locational Marginal Price
DCOPF	Direct Current Optimal Power Flow
ACOPF	Alternating Current Optimal Power Flow
SCUC	Security-Constrained Unit Commitment
MINLP	Mixed-Integer Non-Linear Programming
OCGT	Open Cycle Gas Turbines
CCGT	Combined Cycle Gas Turbines
VPP	Virtual Power Plant
EMS	Energy Management System

Chapter 1

Introduction

1.1 Background and Motivation

Electricity demand is increasing in all sectors along with the economic development in recent decades, requiring enough generation capacity to meet the growing global electricity demand. At the same time, enhanced reliability is needed in the entire system and all its operation in order to provide high-quality electricity and avoid serious faults. Smart grids, which involve integration of low carbon generation, demand side response, energy storage devices, etc., are promising electrical systems to handle these challenges in a sustainable, reliable and economical way [1]. This thesis will explore the methods of incorporating demand side response into smart grids.

The increasing diffusion of new types of loads, such as electric vehicles and smart appliances, represents a crucial element in the ongoing transition of power systems towards the smart grid paradigm. The flexible devices can shift or reduce their power consumption according to users' needs (e.g. reducing energy cost) and the system requirement (e.g. matching the demand with supply). Utilities have mechanism to signal their customers at which time they can reduce or increase their

consumption, in return customers receive a monetary benefit from the utility companies. The flexible loads, if not coordinated, could bring a number of potential drawbacks [2, 3], such as causing new demand peaks and significant voltage deviations in the power grid. For example, if all flexible devices schedule their power consumption at the times when the energy price is the lowest during a day in order to reduce their individual energy costs, the aggregate residential demand will increase dramatically at those times. This phenomenon creates pronounced rebound peaks in the demand profile and consequently increases the energy price at those times, making the power schedule of the flexible devices suboptimal. However, if the devices are properly coordinated, the flexibility in the power consumption of private customers could be potentially exploited for multiple purposes, such as optimizing energy cost for domestic households, flattening demand profiles and providing ancillary services for the system [4, 5]. As for the provision of ancillary services, the transaction occurs in an ancillary service market. In this market, the flexible devices can make a profit by contributing to ancillary services such as spinning reserve, since they could provide their availability to reduce their power consumption if necessary. The clearing of energy and ancillary services is normally auctioned in the forms of integrated markets. In these markets [6], the energy market and ancillary service market are simultaneously cleared. The common feature of simultaneous market clearing of energy and ancillary services is the use of optimization model, usually a linear programming model. These models are formulated to optimize production cost [6], while balancing supply and demand and ensuring reliability. Energy price is associated to power balance equation while the price of ancillary service such as reserve is associated to ancillary service requirement constraint. Non-linear cases such as the optimization of costumer's payment are investigated in [7, 8]. Because of the strong interaction between the supply of energy and the provision of ancillary services [9], the integrated markets are considered to be reasonable. When participating in an integrated market, each flexible device has two cost components: energy cost for power consumption based on the energy price and ancillary service revenue

for ancillary service provision based on the ancillary service price.

Many schemes have been proposed in the literature to coordinate flexible loads [10]. In general, the coordination strategies are categorized into centralized and distributed approaches. Centralized strategies such as references [11, 12] envision a central entity that collects information from all flexible devices and centrally determines their power consumption in order to optimize some global objectives. However, these schemes become complicated to implement and computationally expensive for large numbers of flexible devices, making them unsuitable for big and complex systems. Better scalability is obtained with distributed schemes [13] that also preserve the privacy of the appliances. Game theory has been extensively applied to devise distributed control strategies for coordination of flexible devices. The associated games are designed to admit Nash equilibria, which normally correspond to the social optima of some auxiliary minimization programs. The connection between Nash equilibria and social optima has been investigated in [14].

1.2 Thesis Contributions

In order to rationally utilise the flexiblility from demand side (e.g. utilising it to reduce operational costs, minimize the energy cost of each device, avoid rebound peaks and provide ancillary services), this thesis designs novel distributed control strategies for large-scale deployment of flexible devices such as domestic storage devices and electric vehicles. Game-theoretic schemes are applied to coordinate these devices, which are modelled as self-interested agents that aim to reduce their own costs by changing their power profiles in response to the broadcast price signals. Iterative algorithms are proposed to coordinate the agents so that they can reach an aggregative equilibrium, where no agent can further reduce its cost by unilaterally adjusting its power profile. The main novelties of the proposed coordination strategies are listed as follows:

- A multi-agent system approach is proposed to coordinate large populations of micro-storage devices performing energy arbitrage. The modelling framework considers the storage devices with limited efficiency (accounting for power losses) and the bidirectionality of power flows.

- A similar coordination problem is investigated for electric vehicles, while taking into account network topology. In this case, the locational marginal price (LMP) of electricity at each bus, characterized as the Lagrange multiplier associated to an optimal power flow problem, is used as price signal broadcast to the electric vehicles. In order to solve the problem of the potential price discontinuity of the LMPs, a more complex pricing structure and a novel notion of equilibrium are introduced.

- The coordination problem of flexible devices is further extended in integrated energy-reserve markets, where, in addition to the energy cost, the devices could receive rewards by providing reserve. In these markets, flexible devices respond to two kinds of price signals - the LMPs of energy and reserve.

- The proposed coordination schemes guarantee the convergence to aggregative equilibra, minimized cost sustained by each single device and the optimality of some social welfare, for any penetration level of flexible devices and any grid topology.

1.3 Thesis Structure

The rest of the thesis is organized as follows. First, Chapter 2 presents the influence of the penetration of energy storage devices on the future power networks. Then, it designs a distributed price-based coordination strategy for the operation of micro-storage devices, assuming that the electricity price is a monotone increasing function of the total power demand. Chapter 3 considers a more realistic model compared to Chapter 2. It takes into account network topology, envisaging that loads operate

at a number of buses, connected by transmission lines of limited capacity. Additionally, the price signal broadcast to the flexible loads is the locational marginal price of electricity at each bus, which is calculated through an optimal power flow problem. The performance of the proposed coordination strategy is evaluated in the IEEE 24-bus system. In the modelling framework of Chapter 4, the flexible devices (including storage devices and electric vehicles) operate in an integrated energy and reserve market, where they can provide reserve by being available to reduce their power consumption. As a result, the flexible devices adjust their power profiles in response to both energy and reserve prices in order to minimize their own costs. Simulations are carried out on the PJM 5-bus system to verify the effectiveness of the coordination strategy in integrated energy-reserve markets. Finally, Chapter 5 summarizes the novelties of the thesis and discusses some relevant potential future work.

1.4 Publications

Journal Publications

- **X. Gong**, A. De Paola, D. Angeli and G. Strbac, "Distributed coordination of flexible loads using locational marginal prices", in IEEE Transactions on Control of Network Systems, vol. 6, no. 3, pp. 1097-1110, 2019.
- **X. Gong**, A. De Paola, D. Angeli and G. Strbac, "A game-theoretic approach for price-based coordination of flexible devices operating in integrated energy-reserve markets", in Energy, vol. 189, Dec. 2019, 116153.

Conference Publications

- **X. Gong**, A. De Paola, D. Angeli and G. Strbac, "A distributed price-based strategy for flexible demand coordination in multi-area systems", in 2018 IEEE PES Innovative Smart Grid Technologies Conference Europe (ISGT-Europe), pp. 1-6, 2018.
- A. De Paola, **X. Gong**, D. Angeli and G. Strbac, "Coordination of micro-storage devices in power grids: a multi-agent system approach for energy arbitrage", in 2018 IEEE Conference on Control Technology and Applications (CCTA), pp. 871-878, 2018.

Chapter 2

Distributed Coordination of Micro-storage Devices

2.1 Introduction

Energy storage devices are promising candidates in the process of transforming the conventional power grid into a smart and intelligent power system. It is expected that individual homes will be equipped with micro-storage devices which store electricity and charge their batteries when necessary. The adoption of energy storage devices can bring a number of benefits, which have been researched by a number of studies such as [15, 16, 17]. For example, storage devices can be utilised to facilitate the integration of intermittent renewable generations such as wind and solar, assist voltage regulation and reduce operation cost. However, some challenges still exist in the popularization of storage devices. For instance, if all micro-storage devices charge their batteries at the same time, a higher demand peak may occur in the electricity market, which requires more generation capacity and results in more carbon emissions. To coordinate the storage devices, a number of research has been carried out, among which game theoretic approaches have been extensively adopted [18, 19]. Although these approaches have different objectives, they all pursue an

equilibrium, at which some optimal solution to the relevant problem is obtained. In [20] a distributed scheme for the management of micro-storage devices, which uses the method of mean field games, is presented. In this scheme, the coordination problem of large storage populations are approximated as a differential game with infinite players that perform energy arbitrage. In [21], two game-theoretical approaches are proposed for the coordination of the storage devices in the future grid. One is played between self-interested consumers, which finally reaches a Nash equilibrium, while the other is played between the central entity and the consumers, which results in a Stackelberg equilibrium. In [22], a distributed algorithm based on welfare theory is proposed to calculate the optimal prices and demand schedules, in the case that households are equipped with different appliances including storage devices. To manage agent-based micro-storage devices, the framework proposed in [23] uses an adaptive mechanism based on predicted market prices to maximize the profit of each agent. In this framework, a Nash equilibrium is reached, at which peak demands and carbon emissions are reduced. However, the cited works do not consider efficiency models (for example with different power losses associated to charging and discharging) which is crucial in realistic modelling of storage operation.

This chapter presents a game-theoretic framework to coordinate the storage devices with power losses taking into account. The power losses limiting storage efficiency are expressed as fractions of the exchanged power, with different coefficients when charging and discharging are performed. As a result, nonlinearities appear in the model. In the game-theoretic framework, the storage devices are modelled as self-interested players aiming at minimizing their individual energy costs over a certain time interval. The proposed coordination scheme for micro-storage devices relies on the preliminary findings of [24]. Although the work in [24] studies the coordination of flexible demand without accounting for power losses, its proposed algorithm is a reference to design the coordination strategy of storage devices. The general idea is to update the power profiles of the devices sequentially in response to iterative broadcast price signals. These broadcast prices are assumed to be strictly monotone

increasing with respect to the demand level. It is proven that the proposed coordination scheme for micro-storage devices can always reach an aggregative equilibrium, at which no storage device can reduce its energy cost by unilaterally changing its power scheduling and the optimality of some social welfare is also reached.

2.2 Modelling of Micro-storage Devices and Electricity Market

A population $\mathcal{N} = \{1, \dots, N\}$ of micro-storage devices operate in the discrete time interval $\mathcal{T} = \{1, \dots, T\}$. The dynamics of the single device $j \in \mathcal{N}$ are described by the following equations:

$$E_{j,t+1} = E_{j,t} + u_{j,t}\Delta t \tag{2.1a}$$

$$E_{j,0} = E_j^0 \tag{2.1b}$$

where Δt is the considered time step. The quantity $E_{j,t}$ corresponds to the the energy level of the individual device $j \in \mathcal{N}$ at time $t \in \mathcal{T}$. It evolves dynamically according to (2.1a), where $u_{j,t}$ represents the power charged/discharged by the battery and is considered a control input to be determined by the device j. The proposed modeling framework envisages storage devices with limited efficiency: to account for power losses, only a fraction $\eta_- \leq 1$ of the discharged power is sold to the network. Similarly, when some battery is charging x amount of power, a larger amount $\eta_+ x$ with $\eta_+ \geq 1$ is bought from the system. This can be summarized by the following function:

$$\eta(x) = \begin{cases} \mu_+ & \text{if} \quad x \geq 0 \\ \mu_- & \text{if} \quad x \leq 0 \end{cases} \tag{2.2}$$

denoting by $y(u_{j,t})$ the power exchanged with the network by device j at time t:

$$y(u_{j,t}) = \eta(u_{j,t})u_{j,t}. \tag{2.3}$$

The above notation is extended in a vector sense, denoting by $E_j = [E_{j,1}, \ldots, E_{j,T}] \in \mathbb{R}^T$ the energy values of the device j across time. Similarly, $u_j \in \mathbb{R}^T$ and $y(u_j) \in \mathbb{R}^T$ denote the charge/discharge rate and the power exchanged with the network by the device j across time.

The individual device j is subject to the following operational constraints:

$$E_{j,T} = E_{j,0} = E_j^0 \tag{2.4a}$$

$$0 \leq E_{j,t} \leq \bar{E}_j \quad \forall t \in \mathcal{T} \tag{2.4b}$$

$$\underline{P}_j \leq u_{j,t} \leq \bar{P}_j \quad \forall t \in \mathcal{T}. \tag{2.4c}$$

In order to avoid full discharge of each device j, equation (2.4a) imposes that its charge level at the beginning and at the end of the considered time interval remains the same. This constraint is applicable for day-ahead markets: the time interval is set to $24h$ to implement daily cycles. In addition, (2.4b) and (2.4c) ensure that the charge level $E_{j,t}$ and charge/discharge rate $u_{j,t}$ are always within feasible bounds. From (2.1), the operational constraints (2.4) can equivalently be expressed with respect to u, as specified below:

Definition 2.1. *Let $\mathcal{U}_j$ denote the set of feasible charge/discharge profiles for device j. For the signal $u_j : \mathcal{T} \to \mathbb{R}$, it holds $u_j \in \mathcal{U}_j$ if the following conditions are fulfilled:*

$$\sum_{t=1}^{T} u_{j,t} = 0 \tag{2.5a}$$

$$0 \leq E_j^0 + \sum_{x=1}^{t} u_{j,x} \cdot \Delta t \leq \bar{E}_j \quad \forall t \in \mathcal{T} \tag{2.5b}$$

$$\underline{P}_j \leq u_{j,t} \leq \bar{P}_j \quad \forall t \in \mathcal{T}. \tag{2.5c}$$

In order to characterize the impact of the storage devices on the global quantities of the power grid, let $u = [u_1, \ldots, u_N] \in \mathbb{R}^{NT}$ represent the overall charge/discharge scheduling of the storage population and $\mathcal{U} = \mathcal{U}_1 \times \cdots \times \mathcal{U}_N$ the associated feasibility

set. The total power demand in the system at time t, when u is applied, is denoted as $D_t(u)$ and it has the following expression:

$$D_t(u) = d_t + \sum_{j=1}^{N} \eta\left(u_{j,t}\right) u_{j,t} = d_t + \sum_{j=1}^{N} y(u_{j,t}). \tag{2.6}$$

In other words, the demand $D_t(u)$ corresponds to the total power consumption d_t of all inflexible loads in the system (assumed to be known a priori) plus the total power variation introduced by the storage devices. The electricity market can then be abstracted as a monotone increasing function Π of total demand, expressing the electricity price p_t at time t as:

$$p_t = \Pi(D_t(u)). \tag{2.7}$$

Assumption 2.1. *The function $\Pi : \mathbb{R}_+ \to \mathbb{R}_+$ is strictly monotone increasing and Lipschitz continuous, with Lipschitz constant Γ.*

The choice of an increasing function of demand for the electricity price is common in a power system context, as the marginal cost of generation is generally higher when higher demand needs to be accommodated. The hypothesis of Lipschitz continuity has been introduced to simplify the analysis: weaker continuity notions can be considered with minor modifications.

2.3 Energy Arbitrage as a Competitive Game

The individual storage devices are modelled as self-interested rational agents that perform energy arbitrage and schedule their charge/discharge profile u_j in order to maximize their profit, charging energy at low prices and discharging when electricity is more expensive. The devices interact with each other through the changes in power demand and electricity price introduced by their operation strategies: the

higher is the total charge of the devices, the more expensive electricity will be (and vice versa). This setup can be characterized by a game-theoretical framework with the following elements:

- *Players*: The population $\mathcal{N} = \{1, \ldots, N\}$ of storage devices.
- *Strategies*: The set $\mathcal{U}_j$ of feasible charge/discharge profiles u_j.
- *Objective functions*: Each device $j \in \mathcal{N}$ aims to minimize its energy cost C_j (equivalently, maximize its profit $-C_j$), defined as follows:

$$C_j(u) = \sum_{t=1}^{T} \Pi(D_t(u)) y\left(u_{j,t}\right) \Delta t. \tag{2.8}$$

As expressed in (2.8), at each time t the individual device j trades with the system $y\left(u_{j,t}\right) \Delta t$ units of energy at price $\Pi(D_t(u))$. Note that the single term in the sum of (2.8) is positive when $y\left(u_{j,t}\right) > 0$ (the device is buying and charging energy) and negative when $y\left(u_{j,t}\right) < 0$ (the device is discharging and selling energy to the grid).

The main objective of the subsequent theoretical analysis and of the proposed control scheme is the convergence of the storage strategies to a stable market configuration, characterized by the following equilibrium notion:

Definition 2.2. *Consider the charge/discharge profile $u^* \in \mathcal{U}$ of the storage population, with $u^* = [u_1^*, \ldots, u_N^*]$. This corresponds to an aggregative equilibrium if the following holds for all $j \in \mathcal{N}$:*

$$\sum_{t=1}^{T} \Pi(D_t(u^*)) \cdot y\left(u_{j,t}^*\right) \cdot \Delta t = \min_{u_j \in \mathcal{U}_j} \sum_{t=1}^{T} \Pi(D_t(u^*)) \cdot y(u_{j,t}) \cdot \Delta t \tag{2.9}$$

where the aggregate demand profile $D_t(u^*)$ is equal to:

$$D_t(u^*) = d_t + \sum_{j=1}^{N} y\left(u_{j,t}^*\right) \tag{2.10}$$

The proposed aggregative equilibrium notion is expressed as a fixed point condition: each storage device minimizes its energy cost based on the electricity price $\Pi(D_t(u^*))$ associated to a certain power demand $D_t(u^*)$ (from (2.9)). In turn, the overall operation strategy u^* induces that very same demand profile, as imposed in (2.10).

Remark 2.1. *The aggregative equilibrium defined above is also known as a Wardrop equilibrium, which is a good approximation of the classical Nash equilibrium notion when the number of agents trends to infinity [25]. For the Wardrop equilibrium, the effect of an individual agent on the global quantities of the system is negligible. Since the power consumption u_j of the individual storage device (in the order of kWs) is orders of magnitude smaller than total power demand $D(u)$ (generally in the order of GWs), one can assume that each storage device has negligible market power and performs its cost minimization considering the electricity price to be fixed. As a result, the decision variable $u_{j,t}$ do not appear in the price $\Pi(D_t(u^*))$ in the right-hand side of (2.9). However, the Nash equilibrium considers the imperceptible changes in the value of the price $\Pi(D_t(u^*))$ caused by the power schedule $u_{j,t}$ of a single storage device. This is neither necessary in the present case nor applicable to mathematical analysis.*

In order to provide a more compact characterization of the equilibrium notion presented above, some functions of the charge/discharge profile u_j are preliminarily introduced:

$$\alpha(u,j,t) = \begin{cases} u_{j,t} & \text{if} \quad u_{j,t} > 0 \\ u_{j,t} - \underline{P}_j & \text{if} \quad u_{j,t} \leq 0 \end{cases} \tag{2.11a}$$

$$\beta(u,j,t) = \begin{cases} \bar{P}_j - u_{j,t} & \text{if} \quad u_{j,t} \geq 0 \\ -u_{j,t} & \text{if} \quad u_{j,t} < 0 \end{cases} \tag{2.11b}$$

$$e(u,j,\bar{t},\underline{t}) = \begin{cases} \frac{\min_{t\in\{\underline{t},\ldots,\bar{t}-1\}} E_{j,t}}{\Delta t} & \text{if } \underline{t} < \bar{t} \\ \frac{\bar{E}_j - \max_{t\in\{\bar{t},\ldots,\underline{t}-1\}} E_{j,t}}{\Delta t} & \text{if } \underline{t} > \bar{t} \end{cases} \tag{2.11c}$$

The equilibrium is now characterized through the following quantity:

$$\gamma(u, j, \bar{t}, \underline{t}) = \alpha(u, j, \underline{t}) \cdot \beta(u, j, \bar{t}) \cdot e(u, j, \bar{t}, \underline{t}) \cdot \left[\Pi(D_{\underline{t}}(u)) - \frac{\eta(u_{j,\bar{t}})}{\eta(u_{j,\underline{t}})} \Pi(D_{\bar{t}}(u)) \right] \quad (2.12)$$

The sign of $\gamma(u, j, \bar{t}, \underline{t})$ indicates whether a device j can swap a power amount from a time instant $t = \underline{t}$ to a time instant $t = \bar{t}$ to reduce its energy cost. There exists such a feasible power swap if $\gamma(u, j, \bar{t}, \underline{t}) > 0$. In the case of $\gamma > 0$, since the functions in (2.11) are always nonnegative, we have positivity of all factors in (2.12). It follows that u_j can be reduced at time $\underline{t}$ (since $a(u, j, \underline{t}) > 0$) and increased at time $\bar{t}$ (since $b(u, j, \bar{t}) > 0$) without violating the constraints (2.4b) on the charge level (since $e(u, j, \bar{t}, \underline{t}) > 0$). Moreover, the power swap is also cost reducing (since also the last factor in (2.12) is positive). This important result can be formalized as follows.

Proposition 2.1. *The charge/discharge profile $u^* \in \mathcal{U}$ corresponds to an aggregative equilibrium if and only if:*

$$\gamma(u^*, j, \bar{t}, \underline{t}) \leq 0 \qquad \forall j \in \mathcal{N}, \quad \forall (\bar{t}, \underline{t}) \in \mathcal{T} \times \mathcal{T}. \quad (2.13)$$

Proof. See Appendix A.1. □

In other words, this proposition means that at the aggregative equilibrium, no storage device can perform a feasible power swap to reduce its energy cost.

2.4 Strategy Update as Dynamical System

In order to properly coordinate the charge/discharge profiles of the storage devices and converge to an aggregative equilibrium, a novel distributed control strategy is proposed. It is envisioned that each device sequentially updates its strategy in response to an updated power signal, with the objective of reducing its energy cost.

2.4.1 Multi-valued Mapping

The update of the charge/discharge profiles is described by the evolution of the following dynamical system:

$$u(0) = u^0 \qquad u(k+1) \in F(u(k)) \tag{2.14}$$

where $F : \mathcal{U} \mapsto \mathcal{U}$ is a multi-valued correspondence and $u(k) \in \mathcal{U} \subseteq \mathbb{R}^{NT}$ denotes the strategies of the storage population after k updates. In order to formally define F, some relevant quantities are preliminarily introduced:

$$S_j(u) := \underset{(\bar{t},\underline{t})\in\mathcal{T}\times\mathcal{T}}{\arg\max}\, \gamma(u, j, \bar{t}, \underline{t}) \tag{2.15}$$

$$\Delta(u, j, \bar{t}, \underline{t}) := \min\left(\{\alpha(u, j, \underline{t}), \beta(u, j, \bar{t}), e(u, j, \bar{t}, \underline{t}), \lambda(u, j, \bar{t}, \underline{t})\}\right). \tag{2.16}$$

The functions α and β are defined in (2.11a) and (2.11b), respectively, whereas λ has the following expression:

$$\lambda(u, j, \bar{t}, \underline{t}) = \frac{\eta(u_{j,\underline{t}})\Pi(D_{\underline{t}}(u)) - \eta(u_{j,\bar{t}})\Pi(D_{\bar{t}}(u))}{\Gamma\left(\eta(u_{j,\underline{t}})^2 + \eta(u_{j,\bar{t}})^2\right)} \tag{2.17}$$

where Γ is the Lipschitz constant of the price function Π, as discussed in Assumption 2.1. The set $S_j(u)$ contains the pairs of time instants $(\bar{t}, \underline{t})$ that maximize the value of the function γ and can therefore be considered for cost-reducing power swaps. The problem of maximizing γ in (2.15) can be easily solved with enumeration method. The function $\Delta(u, j, \bar{t}, \underline{t})$ represents the associated amount of power variation. The terms α, β and e in (2.16) ensure feasibility of the power swap, whereas λ is an additional bound that preserves the original price order at $\bar{t}$ and $\underline{t}$ after the power swap, as required by the proof of the following Proposition 2.2. A multi-valued mapping $F_j : \mathcal{U} \mapsto \mathcal{U}$ is now defined for each device $j \in \mathcal{N}$:

$$F_j(u) = \bigcup_{s_j\in S_j(u)} f^{(s_j)}(u) \tag{2.18}$$

where each element $f^{(s_j)}(u) \in \mathcal{U} \subseteq \mathbb{R}^{NT}$ can equivalently be represented in a vectorial form as $f^{(s_j)}(u) = \left[f_{1,1}^{(s_j)}(u), \ldots, f_{N,T}^{(s_j)}(u)\right]$. Each single component $f_{i,t}^{(s_j)}(u) \in \mathbb{R}$ has the following expression when $s_j = (\bar{t}, \underline{t})$:

$$f_{i,t}^{(s_j)}(u) = \begin{cases} u_{i,t} + \Delta(u, j, \bar{t}, \underline{t}) & \text{if} \quad i = j, t = \bar{t} \\ u_{i,t} - \Delta(u, j, \bar{t}, \underline{t}) & \text{if} \quad i = j, t = \underline{t} \\ u_{i,t} & \text{otherwise} \end{cases} \tag{2.19}$$

When the mapping $F_j(u)$ is applied, the device j performs a cost-reducing operation, increasing its charge/reducing its discharge at time $t = \bar{t}$ and decreasing its charge/increasing its discharge a time $t = \underline{t}$. The amount of swapped power $\Delta(u, j, \bar{t}, \underline{t})$ associated to this strategy update ensures feasibility of the new strategy and convergence to equilibrium, as discussed later on. The application of $F_j(u)$ does not modify the strategies of all the other storage devices $i \in \mathcal{N} \backslash \{j\}$. The mapping F describing the iterative update mechanism of the storage population, with the devices sequentially updating their strategies one after another, can then be characterized by the following composition:

$$F(u) := \left(F_N \circ \cdots \circ F_1\right)(u). \tag{2.20}$$

The evolution of the devices' strategies $u(k)$ associated with the application of the mapping F is now formally defined:

Definition 2.3. *Given the dynamical system (2.14) with F as defined in (2.20), its solution set Φ is the following:*

$$\Phi := \left\{\phi : \mathbb{N}^+ \to \mathcal{U} \ : \ \phi(k+1) \in F(\phi(k)) \ \ \forall k \in \mathbb{N}^+\right\}. \tag{2.21}$$

2.4.2 Theoretical Results

The analysis on the convergence and optimality of the proposed mapping F is based on Lyapunov tools and considers the following function V of the players' strategies u:

$$V(u) := \sum_{t=1}^{T} \int_0^{D_t(u)} \Pi(x)\, dx. \tag{2.22}$$

In order to prove convergence and optimality of the proposed strategy update, the following preliminary results are introduced first:

Proposition 2.2. *For the function V in (2.22), evaluated along any solution $\phi \in \Phi$, it holds:*

$$V(\phi(k+1)) \leq V(\phi(k)) \qquad \forall k \in \mathbb{N} \tag{2.23a}$$

$$\phi(k+1) = \phi(k) \qquad \forall k : V(\phi(k+1)) = V((\phi(k)) \tag{2.23b}$$

$$\lim_{k\to\infty} V(\phi(k)) = V_\infty, \quad V_\infty \in \mathbb{R}_+ \tag{2.23c}$$

Proof. See Appendix A.2. □

It is now possible to provide the main results on the convergence and optimality of the proposed multi-valued mapping.

Theorem 2.1. *Let Ω^* denote the set of aggregative equilibria as presented in Definition 2.2 and indicate by $|x|_S$ the distance between some element $x \in \mathcal{U}$ and a set $S \subseteq \mathcal{U}$. For any solution $\phi \in \Phi$, it holds:*

$$\lim_{k\to+\infty} |\phi(k)|_{\Omega^*} = 0. \tag{2.24}$$

Proof. See Appendix A.3 □

Theorem 2.2. *For any feasible strategy $u \in \mathcal{U}$ and any aggregative equilibrium $u^* \in \Omega^* \subseteq \mathcal{U}$, it holds:*

$$V(u^*) \leq V(u). \tag{2.25}$$

Proof. See Appendix A.4. □

Theorem 2.2 states that the proposed update scheme converges to a set of points Ω^* which are not only aggregative equilibria but also global minima of the function V in (2.22). We wish to emphasize that V corresponds to the sum over time of the integral of the electricity price Π. Since Π can be interpreted as the marginal cost of generation, it follows that V quantifies the total generation costs of the power system. As a result, any point u^* not only constitutes a market equilibrium for the agents, but it is also optimal for the overall system.

Remark 2.2. *It has been proven in Appendix A.2 that a feasible power swap of each device j that reduces its own cost also ensures the reduction of the value of the global function V. This game is known as a potential game since the incentive of all storage devices to change their strategy can be expressed using a single global function. The global function is called the potential function, corresponding to the function V in the present work. The potential function is a useful tool to analyze equilibrium properties of games because of the strong connection between the optima of the potential function and the equilibria, as stated in Theorem 2.2.*

2.4.3 Pseudo-Code of the Coordination Scheme

The coordination scheme of micro-storage devices characterized by the mapping F is then presented in Algorithm 1, which consists of three main phases.

In the first **Initialization phase**, the algorithm sets the initial power scheduling $u(0)$ of the whole population of storage devices to some initial value u^0. In addition, two variables are initialized. The variable k is an iteration counter while the variable *conv* is used to detect whether a change in power scheduling has occurred at the latest iteration in the phase **Power scheduling update**. In this phase, each full execution of the **FOR** cycle in step 2.d) corresponds to the application of the mapping F in (2.20). In particular, each single iteration with index j is equivalent

to the application of F_j in (2.18). Specifically, a storage device j selects the time instants $\bar{t}^*, \underline{t}^* \in \mathcal{A}_j$ that maximize γ. If the maximized γ is positive, it implies that the cost of device j can be reduced by shifting the amount of power δ from time $\underline{t}^*$ to $\bar{t}^*$. After each **FOR** cycle, the iteration number k is increased by one as step 2.b). If no device j can perform a feasible power swap after a finite number of iteration k (i.e., $\gamma(u(k), j, \bar{t}, \underline{t}) \leq 0$ for all j and $(\bar{t}, \underline{t}) \in \mathcal{A}_j \times \mathcal{A}_j$), the variable *conv* remains equal to 1 throughout the **FOR** cycle and the final scheduling $u(k)$ is returned as the solution u^* of an aggregative equilibrium in the **Final Results** phase. This is consistent with Proposition 2.1.

Algorithm 1 Iterative scheme - Micro-storage device coordination

1. **Initialization phase.** An initial power scheduling is set for each storage devices and some flag variables are set:

$$u(0) = u^0 \in \mathcal{U} \qquad k = 0 \qquad conv = 0$$

2. **Power scheduling update.** The power scheduling of the micro-storage devices are iteratively updated:
WHILE $(conv = 0)$

   (a) $conv = 1$

   (b) $k = k + 1$

   (c) $u(k) = u(k-1)$

   (d) **FOR** $j = 1 : 1 : N$

      i. **FIND** $(\bar{t}^*, \underline{t}^*)$ such that:

$$(\bar{t}^*, \underline{t}^*) \in \underset{(\bar{t}, \underline{t}) \in \mathcal{A}_j \times \mathcal{A}_j}{\arg\max} \gamma(u(k), j, \bar{t}, \underline{t})$$

      ii. **IF** $\gamma(u(k), j, \bar{t}^*, \underline{t}^*) > 0$

$$\begin{array}{cc} conv = 0 & \delta = \Delta(u(k), j, \bar{t}^*, \underline{t}^*) \\ u_{j,\bar{t}^*}(k) = u_{j,\bar{t}^*}(k) + \delta & u_{j,\underline{t}^*}(k) = u_{j,\underline{t}^*}(k) - \delta. \end{array}$$

   END FOR

   END WHILE

3. **Final results**. The aggregative equilibrium solution is equal to the power scheduling at the last iteration:

$$u^* = u(k).$$

2.4.4 Distributed Implementation

The implementation of the coordination algorithm in practical contexts is now discussed. In particular, the proposed algorithm can be implemented in a distributed manner through a bidirectional communication scheme between the individual agents and some central entity (e.g. the system operator).

1. **Initialization Phase**: Each device $j \in \mathcal{N}$ initializes its charge/discharge profile $u_j = u_j^0$ autonomously. The information of the scheduled power profiles $u(0)$ of the devices is sent to the central entity, which calculates the total power demand $D(u(0))$ and the associate price $\Pi(D(u(0)))$.

2. **Power scheduling update**:

   (a) The price signal $\Pi(D(u))$ is broadcast by the central entity to a device j.

   (b) After receiving the price signal, the device j updates its strategy in order to reduce its energy cost. To do so, it selects a pair of advantageous time instants $s_j = (\bar{t}, \underline{t}) \in S_j(u)$ that maximize γ according to (2.15). If the maximized γ is positive, it implies that a feasible power swap can be performed by device j to reduce its cost. Then the device will swap the amount of power $\Delta(u, j, \bar{t}, \underline{t})$ in (2.16) from time $\underline{t}$ to time $\bar{t}$. The agent j has all the information to perform such cost-reducing operation, as $\gamma(u, j, \bar{t}, \underline{t})$ and $\Delta(u, j, \bar{t}, \underline{t})$ exclusively depend on the current charge/discharge profile u_j (known by agent j) and the electricity price $\Pi(D(u))$ (broadcast by the system operator). The power swap corresponds to the application of $f^{(s_j)}(u) \in F_j(u)$ according to the expression in (2.19).

   (c) The power swap is communicated to the system operator, which updates u as $f^{(s_j)}(u)$ and calculates the new price signal $\Pi(D(u))$.

   (d) Steps 2.a)-2.c) are repeated for the next device $j + 1$ (resetting the index to 1 when $j = N$).

3. The procedure is terminated until no device can perform a feasible power swap

to reduce its energy cost. In other words, $\gamma(u(k), j, \bar{t}, \underline{t})$ is not great than zero for all $j \in \mathcal{N}$ and $(\bar{t}, \underline{t}) \in \mathcal{A}_j \times \mathcal{A}_j$. This means that the aggregative equilibrium is reached according to Proposition 2.1.

Remark 2.3. *The above method has been chosen for its close correspondence with the theoretical formulation of the strategy update as composition of mappings F_j. An alternative implementation of a one-shot strategy with reduced communication requirements is available and is discussed in detail in [24] for the case of demand response. In this strategy, the flexible devices are coordinated through the broadcast of a single price signal (different in general for each device). To generate the price signal for each device, the central entity needs to collect all the information of the micro-storage devices and emulates a modified version of Algorithm 1. In response to its individual price signal, each device will schedule the power profile to minimize its energy cost. The resulting power scheduling of the whole population of the storage devices corresponds to an ϵ-approximate aggregative equilibrium. It should be noted that the privacy of the storage devices is divulged in the one-shot strategy.*

2.5 Case Studies

In this section, the distributed control strategy for the coordination of storage devices is applied to analyze a future scenario of UK power demand with a high penetration of micro-storage devices. The inflexible demand profile d_t of the future UK scenario (obtained from historical data) is represented by the blue curve in Fig. 2.1, and it is predicted that two different populations $\mathcal{N}_A$ and $\mathcal{N}_B$ ($\mathcal{N} = \mathcal{N}_A \cup \mathcal{N}_B$) of micro-storage devices will be installed in private households. It is assumed that the device numbers of populations $\mathcal{N}_A$ and $\mathcal{N}_B$ are that $N_A = N_B = 5 \cdot 10^5$. Furthermore, it is assumed that the devices of population $\mathcal{N}_A$ are with the same battery capacity and power rating such that $\bar{E}_A = 20kWh$ and $\bar{P}_A = -\underline{P}_A = 2kW$. With Similar assumption, the devices of population $\mathcal{N}_B$, which are with higher power rating and

battery capacity, have the following parameters: $\bar{E}_B = 30kWh$ and $\bar{P}_B = -\underline{P}_B = 3kW$. The value of the initial charge level E_j^0 of each storage device in the current case study is determined according to a uniform distribution with support $[0, \bar{E}_j]$. Besides, η_- and η_+ are set to 0.98 and 1.02, respectively.

A time interval of $24h$ and a time discretization of $0.25h$ (namely, $\mathcal{T} = \{1, \dots, 96\}$ and $\Delta t = 0.25$) are considered. To perform the coordination strategy, it is necessary to firstly determine initial charge/discharge profiles $u(0)$ for the storage devices. In this simulation, the initial charge/discharge profile $u_j(0)$ of each storage device is set as follows:

$$u_{j,t}(0) = 0 \quad \forall j \in \mathcal{N} \quad \forall t \in \mathcal{T}. \tag{2.26}$$

As $u_{j,t}(0) = 0$ for any device $j \in \mathcal{N}$, the aggregate demand profile $D_t(u(0))$ coincides with the inflexible demand d_t. Next, the coordination process is performed, during which each storage device aims at minimizing its energy cost.

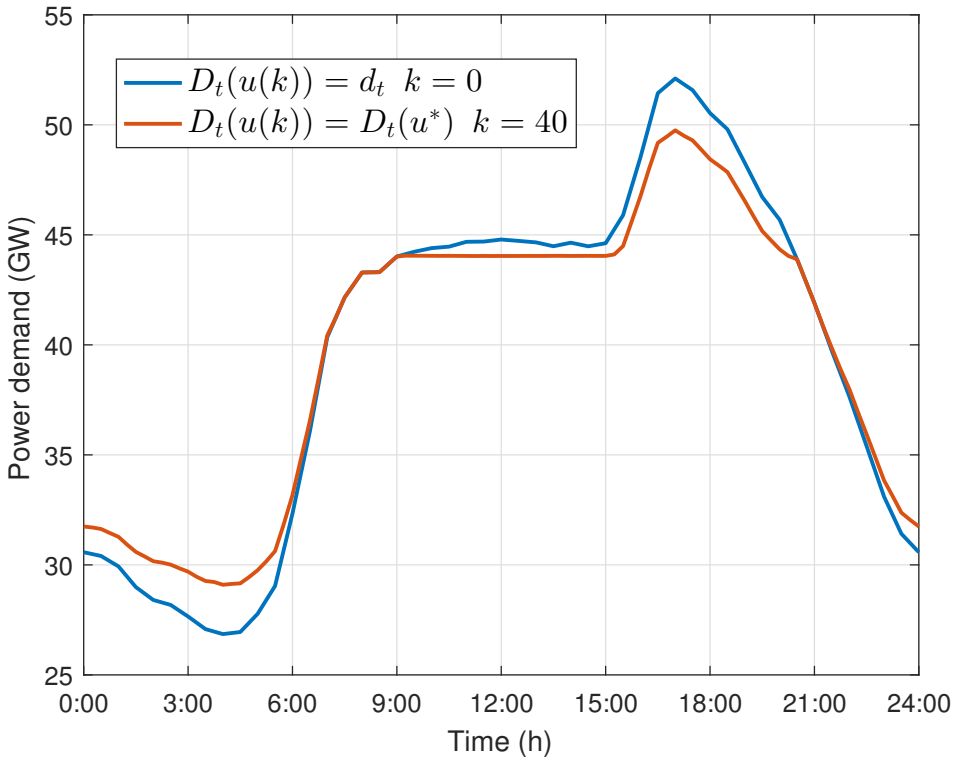

Figure 2.1: Initial (blue line) and final (red line) aggregate demand profiles.

The performance of the algorithm on the demand profile D_t is shown in Fig. 2.1, showing that the control strategy tends to shave demand peaks and fill demand valleys. This is reasonable since, in order to minimize their energy costs, the devices will charge at cheapest electricity prices (with lowest demand level) and discharge at highest prices (with highest demand level).

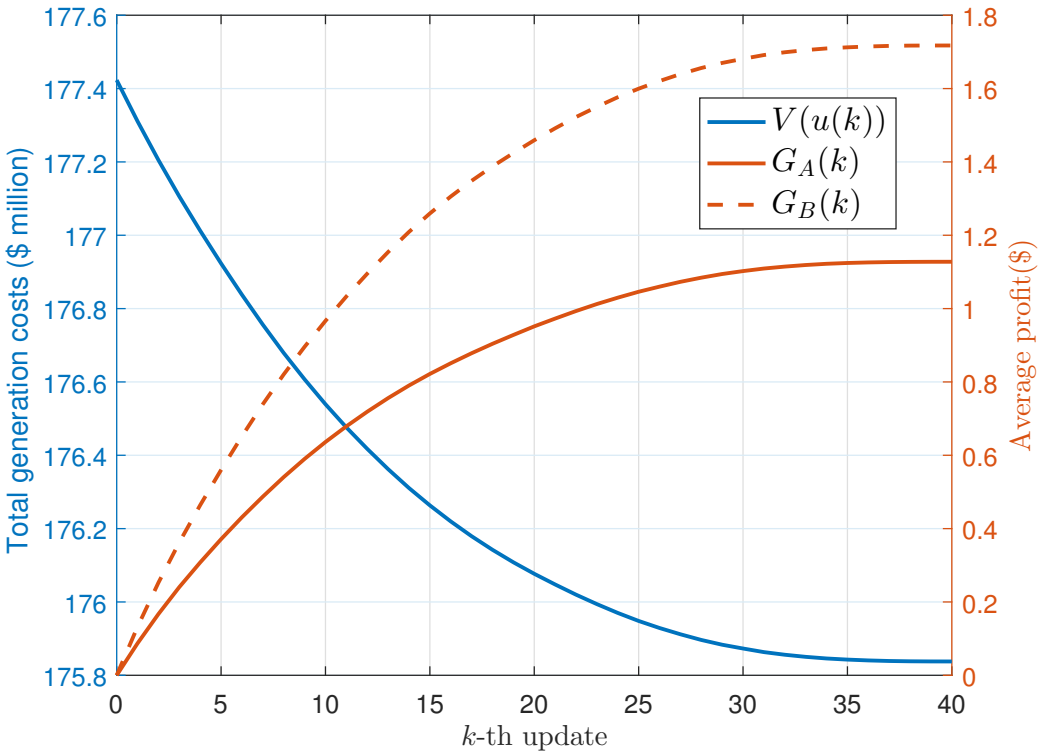

Figure 2.2: Total generation costs $V(u(k))$ and average profits $G_A(k)$ and $G_B(k)$ with respect to update count k.

The capability of increasing the average profit of storage devices and reducing total generation costs is also tested, considering the following price function Π for some positive constant a and b:

$$\Pi(D_t(u)) = aD_t(u) + b. \tag{2.27}$$

The function $\Pi(D_t(u))$ is obviously monotone increasing with respect to the aggregate demand $D_t(u)$, thus satisfying Assumption 2.1. For certain charge /discharge

profiles $u(k)$ at k-th update, the corresponding total generation cost can be expressed as follows:

$$V(u(k)) = \sum_{t=1}^{T} \left(\frac{1}{2} a \cdot D_t(u(k))^2 + b \cdot D_t(u(k)) \right) \Delta t. \tag{2.28}$$

The corresponding average profit $G_A(k)$ of the devices of population $\mathcal{N}_A$ is:

$$G_A(k) = -\frac{\sum_{j:j\in\mathcal{N}_A} \sum_{t=1}^{T} \Pi(D_t(u(k)))y(u_{j,t}(k))\Delta t}{N_A}. \tag{2.29}$$

Similar expression can be obtained for the average profit $G_B(k)$ of population $\mathcal{N}_B$. The values of $V(u(k))$, $G_A(k)$ and $G_B(k)$ at different updates are shown in Fig. 2.2. This figure shows that the control strategy terminates after $k = 40$ updates. It is seen that the total generation costs $V(u(k))$ gradually decrease with the increase in the update count k, which is consistent with Proposition 2.2. The profits $G_A(k)$ and $G_B(k)$ increase with k, and it is interesting to notice that higher profit is achieved by devices with higher power rating and battery capacity. Furthermore, the values of $V(u(k))$, $G_A(k)$ and $G_B(k)$ almost remain unchanged when the aggregative equilibrium is being approached (when k is approaching to 40).

Table 2.1: Total generation cost V, average profit G_A and G_B for individual devices in the scenarios of partial efficiency and full efficiency.

	Partial efficiency	Full efficiency
V	\$175.84 million	\$175.68 million
G_A	\$1.13	\$1.26
G_B	\$1.72	\$1.90

The values of V, G_A and G_B obtained in the above simulations (storage devices with partial efficiency) are compared to those in the scenario of storage devices with full efficiency, presented in Table 2.1. The latter case can easily achieved by setting both η_- and η_+ equal to 1. As expected, the consideration of partial efficiency increases the total generation cost and reduces the average profit of micro-storage devices (about 10% reduction with respect to the scenario of full efficiency). This can be straightforward explained: to charge a certain amount Δ of power, a storage device with partial efficiency needs to buy a larger amount $\eta_+\Delta$ ($\eta_+ > 1$) of power

from the grid, increasing the cost; Similarly, to discharge an amount Δ of power, a storage device with partial efficiency sells a smaller amount $\eta_-\Delta$ ($\eta_- < 1$) of power to the grid, decreasing the revenue. The increase of the total generation cost V can be explained with the same reason.

2.6 Summary

This chapter proposes a multi-agent system approach for the coordination of large populations of micro-storage devices performing energy arbitrage. The individual batteries are modelled as price-responsive self-interested agents that select their charge/discharge profile to maximize profit and interact between each other through the changes in power demand caused by their aggregate strategy. The main novelty is the design of an iterative control strategy that ensures asymptotic convergence to an optimal market equilibrium when partial efficiency of the agents (with ensuing nonlinearities), bidirectionality of power flows and state constraints are considered. Distributed schemes for its implementation and performance evaluation through case studies in large-scale power system are also provided.

Chapter 3

Coordination of Flexible Loads Considering Network Topology

3.1 Introduction

3.1.1 Relevant Work

In addition to the increasing number of micro-storage devices as introduced in Chapter 2, the penetration of flexible loads, such as smart appliances and electric vehicles, is also expected to increase significantly in the future. Unlike the micro-storage devices that can discharge their batteries to sell energy to the grid, the flexible loads, e.g. electric vehicles, only consume energy. The electrification of the transport sector can mitigate the shortage of fossil fuels and improve energy efficiency [26], whereas the increasing flexibility on the demand side can be explored and utilised in power systems for multiple purposes, such as reducing operational costs and avoid rebound peaks [27]. Chapter 3 will study the coordination of flexible loads. A large amount of research has been carried out to achieve flexible demand coordination, evaluating centralized and distributed approaches. Compared to distributed approaches, cen-

tralized control strategies are normally computationally expensive for large numbers of flexible loads. Multiple distributed approaches have been considered, including Lagrange relaxation methods [28], congestion pricing [29] and stochastic pricing [30]. Game theory has also been extensively applied to devise distributed control strategies for coordination of flexible loads [31, 32, 33, 34, 35, 36]. The general approach adopted in these papers is to model the flexible loads as self-interested players that compete for energy consumption at the cheapest prices. On this basis, distributed control actions are designed in order to converge to a stable market outcome (characterized as an equilibrium) and to possibly maximize some social welfare.

3.1.2 Motivation

It is worth emphasizing that all these works including Chapter 2 consider a unique price function throughout the grid, repartitioning total costs among the users proportionally to their fraction of total power consumption [31] or assuming that the electricity price, at a certain time instant, is some monotone increasing function of total power demand at the same time (e.g. [32, 33, 34, 35, 36] and Chapter 2). This choice captures a fundamental property of electricity markets, where the marginal cost of generation is increasing and higher supply corresponds to higher prices. However, the proposed modelling frameworks only consider distribution networks [32, 35, 36] or conduct a whole-system analysis (e.g. [33, 34] and Chapter 2) that does not account for any underlying network topology. In particular, the pricing schemes in [31, 32, 33, 34, 35, 36] and Chapter 2 neglect two fundamental characteristics of realistic power grids: the presence of multiple buses (connected by transmission lines of limited capacity) and, as a result, the arising of different locational marginal prices (LMPs) throughout the system if anyone of transmission lines is congested.

Recent work has proposed novel modelling approaches that incorporate the transmission network, investigating the impact of EVs [37, 38], and more generally de-

mand response [39, 40] on the locational marginal prices of the system. The interactions between distribution and transmission and the impact of uncertainties have also been assessed in [41] and [42], respectively. However, differently from [31, 32, 33, 34, 35, 36], all the cited papers [37, 38, 39, 40, 41, 42] do not provide any theoretical guarantee on the convergence to equilibrium of their coordination scheme, nor they can ensure social optimality of their solution.

3.1.3 Contributions

The objective of this chapter is to bridge the gap between the research approaches presented in [31, 32, 33, 34, 35, 36] and in [37, 38, 39, 40, 41, 42]. In particular, the framework presented in this work combines a rigorous theoretical analysis (guaranteeing convergence and optimality of the proposed coordination scheme) with an explicit modelling of the transmission infrastructure (accounting for the underlying network topology and assessing the impact of demand response on LMPs and generation costs).

These results are obtained considering heterogeneous price-responsive loads operating at distinct buses of the power system. The congestion of transmission lines is taken into account and the LMPs at each bus are characterized as the Lagrange multipliers associated to a linearized AC optimal power flow (ACOPF) problem, whose solution depends on the operation strategy of the flexible loads. The proposed coordination scheme for flexible demand relies on the preliminary findings of [43] and envisions iterative better-response updates by the price-responsive loads, which are characterized as the evolution of a multi-valued mapping. The formulation and the results of [43] have been expanded to explicitly consider a more complex pricing structure with LMPs. In order to account for the congestion of the transmission lines and the potential price jumps that this might cause, a more general class of aggregative games has been considered and a novel notion of variational aggregative equilibrium is introduced. Through the application of Lyapunov tools, it is

demonstrated that the proposed coordination scheme converges to an equilibrium and achieves global optimality for any penetration level of flexible demand and any grid topology. Distributed implementations of the proposed scheme and simulative results on the IEEE 24-bus system are also provided.

3.2 Modelling of Optimal Power Flow and Electricity Prices

The considered power system is composed by a finite set $\mathcal{M} = \{1, \dots, M\}$ of distinct buses. The set of transmission lines (of limited capacity) linking two buses is denoted as $\mathcal{L} = \{1, \dots, L\}$, with $s(l)$, $r(l) \in \mathcal{M}$ indicating the reference sending and receiving nodes of line l, respectively. As commonly assumed in theoretical analyses of electricity markets, the electricity price p_m at each bus m corresponds to the LMP associated to an optimal power flow problem [9]. A linearized ACOPF model in [44] is solved over the discrete time interval $\mathcal{T} = \{1, \dots, T\}$. Let $D \in \mathbb{R}^{MT}$ denote a vector of demand values whose individual component $D_{m,t}$ corresponds to the total active power demand at bus m at time t. A similar notation is adopted for the generation vector G, voltage angle vector θ and voltage magnitude v, representing by $G_{m,t}$, $\theta_{m,t}$ and $v_{m,t}$ their scalar values for bus m and time t. The linearized ACOPF in [44] can now be expressed as:

$$\varphi(D) = \min_{G,GQ,\theta,v^2} \sum_{m=1}^{M} \sum_{t=1}^{T} f_m(G_{m,t}) \tag{3.1}$$

subject to ($\forall l \in \mathcal{L}, m \in \mathcal{M}, t \in \mathcal{T}$):

$$P_{l,t} = g_l \frac{v_{s(l),t}^2 - v_{r(l),t}^2}{2} - b_l \left[\theta_{s(l),t} - \theta_{r(l),t}\right] + P_{l,t}^L \tag{3.2a}$$

$$Q_{l,t} = -b_l \frac{v_{s(l),t}^2 - v_{r(l),t}^2}{2} - g_l \left[\theta_{s(l),t} - \theta_{r(l),t}\right] + Q_{l,t}^L \tag{3.2b}$$

$$G_{m,t} - D_{m,t} = \sum_{\{l:s(l)=m\}} P_{l,t} - \sum_{\{l:r(l)=m\}} P_{l,t} + \left(\sum_{n=1}^{M} \mathcal{G}_{mn}\right) v_m^2 \tag{3.2c}$$

$$GQ_{m,t} - DQ_{m,t} = \sum_{\{l:s(l)=m\}} Q_{l,t} - \sum_{\{l:r(l)=m\}} Q_{l,t} + \left(\sum_{n=1}^{M} -\mathcal{B}_{mn}\right) v_m^2 \tag{3.2d}$$

$$\underline{G}_m \leq G_{m,t} \leq \bar{G}_m \tag{3.2e}$$

$$\underline{GQ}_m \leq GQ_{m,t} \leq \bar{GQ}_m \tag{3.2f}$$

$$\underline{v}_m^2 \leq v_{m,t}^2 \leq \bar{v}_m^2 \tag{3.2g}$$

$$\underline{\theta}_m \leq \theta_{m,t} \leq \bar{\theta}_m \tag{3.2h}$$

$$\begin{aligned}\left(sin\left(\frac{2\pi c}{a}\right) - sin\left(\frac{2\pi}{a}(c-1)\right)\right) P_{l,t} - \left(cos\left(\frac{2\pi c}{a}\right) - \right. \\ \left. cos\left(\frac{2\pi}{a}(c-1)\right)\right) Q_{l,t} - sin\left(\frac{2\pi}{a}\right) \bar{S}_l \leq 0\end{aligned} \tag{3.2i}$$

The Linearized ACOPF described in (3.1)-(3.2) determines the active power generation values G (and associated reactive power generation GQ, voltage angles θ and voltage magnitude v) that minimize total generation costs. It should be noted that the voltage variable is considered to be v^2 instead of v in order to keep the linearity of the constraints in (3.2). The function $f_m(g)$ in the objective function (3.1) represents the cost of generating g units of power at bus m and is assumed to be strictly convex. Conditions (3.2a) and (3.2b) are the linearized model of active power flow $P_{l,t}$ and reactive power flow $Q_{l,t}$ on line l with respect to θ and v^2, where g_l and b_l are the conductance and susceptance of line l, respectively. The last terms $P_{l,t}^L$ and $Q_{l,t}^L$ represent power losses on line l, which has been also linearized. Their expressions are not shown for complexity, but can be found in [44]. Constraints (3.2c) and (3.2d) are nodal power balance expressions. The last terms of (3.2c) and (3.2d) represent the power flows on the shunt elements, where $\mathcal{G}_{mn}$ and $\mathcal{B}_{mn}$ are the real and imaginary part of $\mathcal{Y}_{mn}$ in the admittance matrix. The limits of the variables G, GQ, v^2 and θ are shown in (3.2e), (3.2f), (3.2g) and (3.2h), respectively. Finally, the transmission line limits $P_{l,t}^2 + Q_{l,t}^2 \leq \bar{S}_l$ are approximated in (3.2i) by the piecewise

linearization method in [45]. The constraints hold for $c = 1, 2, ..., a$, where a is the side number of a convex regular polygon that approximates the circles associated to the line limits in $P - Q$ plane.

3.2.1 Electricity Prices

In order to characterize the locational marginal prices associated to a certain vector of demand values D, some properties of $\varphi(D)$ are preliminarily discussed.

Proposition 3.1. *The minimized generation cost $\varphi(D)$ is a strictly convex function on any set $[D_{min}, D_{max}]^{MT} \subset \mathbb{R}_{+}^{MT}$.*

Proof. See Appendix B.1. □

From the convexity result of Proposition 3.1, $\varphi(D)$ is Lipschitz continuous on the open interval $(D_{min}, D_{max})^{MT}$, where D_{min} and D_{max} can include all feasible values of demand. It straightly follows that $\varphi(D)$ is differentiable almost everywhere [46], with the exception of some zero-measure set $\mathcal{D} \subset (D_{min}, D_{max})^{MT}$. Introducing the notion of sub-differential, we can write:

$$\frac{\partial \varphi(D)}{\partial D_{m,t}} = \begin{cases} \varphi'_{m,t}(D) & \text{if} \quad D \notin \mathcal{D} \\ \left[\underline{\varphi}'_{m,t}(D), \bar{\varphi}'_{m,t}(D)\right] & \text{if} \quad D \in \mathcal{D} \end{cases} \tag{3.3}$$

where $\underline{\varphi}'_{m,t}(D)$ and $\bar{\varphi}'_{m,t}(D)$ are the left and right partial derivatives of $\varphi(D)$ with respect to $D_{m,t}$.

The electricity price $p_{m,t}$ is chosen as the Lagrange multiplier associated to the power balance constraint (3.2c), i.e. the marginal cost of providing an additional unit of power at bus m at time t. Within the considered theoretical framework, this price corresponds to the partial derivative presented in (3.3). To account for the points of non-differentiability of the optimized cost $\varphi(D)$, two distinct price signals are

considered:

$$\underline{p}_{m,t}(D) = \begin{cases} \varphi'_{m,t}(D) & \text{if} \quad D \notin \mathcal{D} \\ \underline{\varphi}'_{m,t}(D) & \text{if} \quad D \in \mathcal{D}. \end{cases} \tag{3.4a}$$

$$\bar{p}_{m,t}(D) = \begin{cases} \varphi'_{m,t}(D) & \text{if} \quad D \notin \mathcal{D} \\ \bar{\varphi}'_{m,t}(D) & \text{if} \quad D \in \mathcal{D}. \end{cases} \tag{3.4b}$$

Under the current formulation, $\bar{p}_{m,t}$ is the marginal cost of providing an additional unit of power at bus m. Conversely, $\underline{p}_{m,t}$ represents the marginal saving of reducing by one unit the power supplied to bus m.

We wish to emphasize that the double price formulation in (3.4) is not only a mathematical technical detail but it also represents a crucial element in correctly characterizing price variations and the cost minimization of the loads. In particular, the proposed formulation allows to formally account for the price "jumps" resulting from a marginal generator reaching its maximum capacity or the saturation of some line. In these cases, the electricity price will vary discontinuously. Considering the corresponding value of the demand vector D, the quantities $\underline{p}_{m,t}(D)$ and $\bar{p}_{m,t}(D)$ will represent the different price values at bus m and time t before and after the jump. It follows that $D \in \mathcal{D}$ and the minimized cost function $\varphi(D)$ will not be differentiable in these particular cases.

These price discontinuities are particularly relevant in the cost minimization problem of flexible demand. Each load, in order to correctly evaluate its cost variation, will have to consider $\underline{p}_{m,t}$ when its power consumption is reduced (thus reducing total demand D) and $\bar{p}_{m,t}$ when its power consumption is increased (thus increasing total demand D). This is consistent with the equilibrium formulation in the following Definition 3.2, where the considered prices are selected accordingly to the sign of the associated power scheduling variation.

3.2.2 Local Monotonicity of Prices

As a preliminary step in the definition of the proposed control scheme and in the theoretical assessment of its convergence and optimality properties, an important monotonicity property of the prices in (3.4) is presented.

Proposition 3.2. *Assume strict convexity of the generation cost functions $f_m(G)$ in (3.1). For any bus $m \in \mathcal{M}$ and time $t \in \mathcal{T}$, the corresponding electricity prices $\bar{p}_{m,t}(D)$ and $\underline{p}_{m,t}(D)$ are monotone increasing with respect to demand $D_{m,t}$ at the same bus m and time instant t.*

Proof. See Appendix B.2. □

We wish to emphasize that this monotonicity is only used to rigorously derive the convergence of the proposed coordination algorithm. The algorithm still works in reality even without this condition. This has been verified in the simulation of the IEEE 24-bus system, which does not use the monotonicity as a premise.

From the above considerations, the following power quantity can now be introduced:

Definition 3.1. *Consider a demand vector $D \in \mathbb{R}^{MT}$, a bus $m \in \mathcal{M}$ and two time instants $\bar{t}, \underline{t} \in \mathcal{T}$. The quantity $\epsilon(D, m, \bar{t}, \underline{t})$ is defined as follows:*

$$\epsilon(D, m, \bar{t}, \underline{t}) := \arg\min_{x \geq 0} \left(\left| \bar{p}_{m,\bar{t}}(D + x \cdot (\hat{\mathbf{e}}_{m,\bar{t}} - \hat{\mathbf{e}}_{m,\underline{t}})) - \underline{p}_{m,\underline{t}}(D + x \cdot (\hat{\mathbf{e}}_{m,\bar{t}} - \hat{\mathbf{e}}_{m,\underline{t}})) \right| \right) \tag{3.5}$$

where $\hat{\mathbf{e}}_{m,t}$ is the unit vector of the standard orthogonal basis associated to bus m and time t.

In the above definition, ϵ is the positive amount of power that can be swapped between $\underline{t}$ ant $\bar{t}$ in order to minimize their price differential. From the monotonicity of $\underline{p}_{m,t}$ and $\bar{p}_{m,t}$, when $\bar{p}_{m,\bar{t}} \leq \underline{p}_{m,\underline{t}}$ the quantity ϵ corresponds to the maximum power swap between $\underline{t}$ and $\bar{t}$ that preserves their original price order.

3.3 Modelling of Flexible Demand

This section presents the modelling framework of the flexible loads. These are described as price-responsive rational agents, characterizing their interactions through a game-theoretical set-up and introducing the concept of variational aggregative equilibrium.

3.3.1 Individual Devices and Impact on Aggregate Power Demand

A population $\mathcal{N} = \{1, \dots, N\}$ of price-responsive devices is considered, denoting by $\mu_j \in \mathcal{M}$ the power system bus in which the flexible load $j \in \mathcal{N}$ operates. The flexible loads are considered as self-interested rational agents that operate over the discrete time interval $\mathcal{T} = \{1, \dots, T\}$. In particular, each load $j \in \mathcal{N}$ schedules its power consumption over time $u_j = [u_{j,1}, \dots, u_{j,T}] \in \mathbb{R}^T$ in order to complete an assigned task at minimum energy cost. The task of agent j can be unequivocally characterized by three quantities:

- Its rated power P_j.
- The total energy E_j required to complete its task.
- The set of time instants $\mathcal{A}_j \subseteq \mathcal{T}$ during which it is available to operate.

Any feasible power consumption profile u_j guaranteeing task completion for agent j belongs to the set $\mathcal{U}_j$, defined as:

$$\mathcal{U}_j := \left\{ u_j \in \mathbb{R}^T : \sum_{t=1}^{T} u_{j,t} \cdot \Delta t = E_j \,, 0 \leq u_{j,t} \leq P_j \cdot \mathbb{1}_{\mathcal{A}_j}(t) \quad \forall t \in \mathcal{T} \right\} \tag{3.6}$$

where Δt denotes the time discretization step and $\mathbb{1}_{\mathcal{A}_j}(t)$ is the indicator function:

$$\mathbb{1}_{\mathcal{A}_j}(t) = \begin{cases} 1 & \text{if} \quad t \in \mathcal{A}_j \\ 0 & \text{if} \quad t \notin \mathcal{A}_j. \end{cases} \tag{3.7}$$

The equality in (3.6) ensures that the total energy consumed by load j is equal to the energy required to complete its task. The inequalities in (3.6) impose that the (positive) power consumption of load j cannot exceed its rated power P_j for t within the availability interval $\mathcal{A}_j$ and must be zero for t outside it. The proposed notation can be extended, representing by $u = [u_1, \dots, u_N] \in \mathbb{R}^{NT}$ the scheduled power profile of the whole population and by $\mathcal{U} = \mathcal{U}_1 \times \cdots \times \mathcal{U}_N$ the corresponding feasibility set.

Assumption 3.1. *The power scheduling problem admits at least one solution. In other words, the parameters $(P_j, E_j, \mathcal{A}_j)$ of each device j are such that $\mathcal{U} \neq \varnothing$.*

In order to account for the impact of the flexible loads on the power system quantities discussed in Chapter 3.2, it is sufficient to replace the demand vector $D \in \mathbb{R}^{MT}$ with a function $D(u) : \mathcal{U} \to \mathbb{R}^{MT}$ of the power scheduling u. For the individual demand component $D_{m,t}$, it holds:

$$D_{m,t}(u) = d_{m,t} + \sum_{\{j:\mu_j=m\}} u_{j,t} \tag{3.8}$$

where $d_{m,t}$ is the known inflexible demand at bus m at time t.

Remark 3.1. *The proposed modelling framework directly considers the impact of flexible demand at a transmission level and it does not specifically account for the effects on the underlying distribution network. This is consistent with previous works [37, 39, 40, 42, 38] on the subject and it is done in order to perform a theoretical high-level analysis that, by introducing the least degree of simplification and retaining structural aspects of the power system, ensures important properties of convergence and optimality for the proposed control scheme. As discussed in Chapter 5, an*

explicit characterization of the distribution network will be a key direction for further research in this area.

3.3.2 Game-theoretical Framework and Aggregative equilibrium

The coordination of the power scheduling by the flexible loads is analyzed within a game-theoretical framework. Each device is modeled as a self-interested player that aims to minimize its individual cost in response to broadcast price signals. The following competitive game is considered:

- *Players:* The set $\mathcal{N}$ of flexible devices.
- *Strategies:* The set $\mathcal{U}_j$ of feasible power profiles for a single flexible device $j \in \mathcal{N}$.
- *Objective function:* Energy cost of task completion. For a certain price signal $p : \mathcal{T} \to \mathbb{R}_+$, the following expression can be provided for the cost C_j of device j:

$$C_j = \sum_{t=1}^{T} p_t \cdot u_{j,t} \Delta t. \tag{3.9}$$

Within this framework, the flexible loads are rational agents competing for power consumption at cheap prices. In the next section, we propose a coordination strategy of the devices that ensures convergence to a stable market configuration. This is expressed as a variational aggregative equilibrium, defined as follows.

Definition 3.2. *The scheduled power consumption $u^* \in \mathcal{U} \subset \mathbb{R}^{NT}$ corresponds to a variational aggregative equilibrium if the following holds for all $u \in \mathcal{U}$:*

$$\Delta C_j = \sum_{t:\ u_{j,t} \geq u^*_{j,t}} \bar{p}^*_{\mu_j,t} \left[u_{j,t} - u^*_{j,t}\right] \Delta t - \sum_{t: u_{j,t} \leq u^*_{j,t}} \underline{p}^*_{\mu_j,t} \left[u^*_{j,t} - u_{j,t}\right] \Delta t \geq 0 \quad \forall j \in \mathcal{N} \tag{3.10}$$

$$\underline{p}^*_{m,t} = \underline{p}_{m,t}\left(D(u^*)\right) \quad \bar{p}^*_{m,t} = \bar{p}_{m,t}\left(D(u^*)\right) \quad \forall m \in \mathcal{M}, \forall t \in \mathcal{T}. \tag{3.11}$$

This definition represents an extension of the aggregative equilibrium, which has already been applied in the context of price-responsive demand coordination [33, 47, 25]. The general idea in these works is to characterize the equilibrium as a fixed point, which is similar to Definition 2.2 in Chapter 2: the power scheduling of each device is optimal for a certain price signal and, at the same time, the aggregate power consumption of all loads induces that very same price. This concept satisfyingly approximates a Nash equilibrium if the effect of the individual player on the global quantities of the system is negligible. This is true in the present case of large-scale deployment of flexible demand, as the power consumption of a single device is orders of magnitude smaller than total power demand.

Definition 3.2 proposes a generalization of the aggregative equilibrium concept for the case of non-differentiable global cost functions and discontinuous LMPs which, as underlined in our analysis, naturally arise from line congestion and maximum generation capacity when the proposed linearized ACOPF is considered. The left-hand side of (3.10) denotes the energy cost variation ΔC_j incurred by the single device j if it switches from the candidate equilibrium solution u^*_j to some other feasible power profile $u_j \in \mathcal{U}_j$. This cost variation is the difference between the costs of increased power consumption at certain time instants (priced at $\bar{p}^*$) and the savings from reduced power consumptions at other times (priced at $\underline{p}^*$). At equilibrium, as imposed in (3.10), the cost variations ΔC_j associated to a different strategy are always greater or equal than zero. Note that, if the minimized generation cost $\varphi(D)$ is a function differentiable everywhere, the signals $\bar{p}^*$ and $\underline{p}^*$ are the same, leading to the classical definition of aggregative equilibrium. The second part of the fixed point condition is given by (3.11), which ensures that the overall power consumption of the devices leads to same prices $\bar{p}*$ and $\underline{p}^*$ considered in (3.10).

In order to derive an equilibrium condition that is equivalent to the definition in

(3.10), to be used in the subsequent analysis, the following function similar to (2.12) in Chapter 2 is introduced:

$$\gamma(u, j, \bar{t}, \underline{t}) := \left(\underline{p}_{\mu_j,\underline{t}}(D(u)) - \bar{p}_{\mu_j,\bar{t}}(D(u))\right)(P_j - u_{j,\bar{t}})\, u_{j,\underline{t}}. \tag{3.12}$$

The sign of γ indicates the possibility by the single load to reduce its cost. If $\gamma(u, j, \bar{t}, \underline{t}) > 0$, the device j operating at bus μ_j, starting from a schedule u, can reduce its cost by swapping power from time $t = \underline{t}$ to time $t = \bar{t}$. In fact, considering the non-negativity of the factors $(P_j - u_{j,\bar{t}})$ and $u_{j,\underline{t}}$ in (3.12), the condition $\gamma(u, j, \bar{t}, \underline{t}) > 0$ implies three distinct inequalities:

$$\underline{p}_{\mu_j,\underline{t}}(D(u)) > \bar{p}_{\mu_j,\bar{t}}(D(u)) \qquad u_{j,\bar{t}} < P_j \qquad u_{j,\underline{t}} > 0.$$

The conditions above indicate, respectively, that:

- An advantageous price difference exists between $\underline{t}$ and $\bar{t}$.
- The device j can consume more power at time $\bar{t}$.
- The device j can consume less power at time $\underline{t}$.

The last two points make the power swap between $\underline{t}$ and $\underline{t}$ feasible, while the first one makes it cost-reducing for the device j. It follows that an equilibrium is reached when γ is always non positive and no device can perform a cost-reducing power swap. This is formalized by the following result:

Proposition 3.3. *The scheduled power consumption $u^* \in \mathcal{U}$ corresponds to a variational aggregative equilibrium, as presented in Definition 3.2, if and only if:*

$$\gamma(u^*, j, \bar{t}, \underline{t}) \leq 0 \quad \forall j \in \mathcal{N}, \quad \forall (\bar{t}, \underline{t}) \in \mathcal{A}_j \times \mathcal{A}_j. \tag{3.13}$$

Proof. See Appendix B.3. □

3.4 Distributed Coordination of Flexible Demand

This section proposes a distributed control strategy for flexible demand coordination. This is initially characterized in Chapter 3.4.1 as a multi-valued mapping (similar to Chapter 2.4.1), theoretically demonstrating with Lyapunov techniques and convexity arguments its asymptotic convergence to a variational aggregative equilibrium that is also socially optimal. An equivalent pseudo-code algorithm representation is given in Chapter 3.4.2, whereas Chapter 3.4.3 discusses the implementation of the proposed control strategy in practical contexts, envisioning a distributed scheme where individual loads iteratively update their power scheduling, on the basis of broadcast price signals, in order to reduce their energy cost.

3.4.1 Power Update as Evolution of Dynamical System

The power scheduling update of the flexible loads is described by the following discrete-time dynamical system:

$$u(0) = u^0 \in \mathcal{U} \qquad u(k+1) \in F(u(k)) \tag{3.14}$$

where $F : \mathcal{U} \mapsto \mathcal{U}$ is a multi-valued correspondence and $u(k)$ denotes the scheduled power consumption of the flexible loads after k iterations of the proposed coordination strategy. In order to characterize the multi-valued mapping F, the following quantities are preliminarily introduced:

$$S_j(u) := \underset{(\bar{t},\underline{t})\in\mathcal{A}_j\times\mathcal{A}_j}{\arg\max}\ \gamma(u, j, \bar{t}, \underline{t}) \tag{3.15}$$

$$\Delta(u, j, \bar{t}, \underline{t}) := \min\left(\left\{\epsilon(D(u), \mu_j, \bar{t}, \underline{t}), P_j - u_{j,\bar{t}}, u_{j,\underline{t}}\right\}\right) \tag{3.16}$$

The set $S_j(u)$ associates to a device $j \in \mathcal{N}$ the pairs of time instants $s_j = (\bar{t}_j, \underline{t}_j)$ that maximize the function γ under the current u and can therefore be considered

for cost-reducing power swaps. Considering the constraints in (3.6) and Definition 3.1 for ϵ, the function Δ returns the maximum feasible power swap that device j can perform between $\bar{t}$ and $\underline{t}$ while preserving their original price order.

The multi-value mapping F_j associated to the power scheduling update of a single device j is now defined:

$$F_j(u) = \bigcup_{s_j \in S_j(u)} f^{(s_j)}(u) = \bigcup_{s_j \in S_j(u)} \left[f_{1,1}^{(s_j)}(u), \ldots, f_{N,T}^{(s_j)}(u) \right] \tag{3.17}$$

where the single component $f_{i,t}^{(s_j)}(u)$ of $f^{(s_j)}(u)$ in (3.17), corresponding to the updated power consumption of device i at time t, has the following expression when $s_j = (\bar{t}, \underline{t})$:

$$f_{i,t}^{(s_j)}(u) = u_{i,t} + \Delta(u, j, \bar{t}, \underline{t}) \cdot \mathbb{1}_{\{j\}}(i) \left[\mathbb{1}_{\{\bar{t}\}}(t) - \mathbb{1}_{\{\underline{t}\}}(t) \right]. \tag{3.18}$$

When the mapping $F_j(u)$ in (3.17) is applied, a single element $s_j = (\bar{t}_j, \underline{t}_j)$ is selected within the set $S_j(u)$ and the device j swaps power from time $\underline{t}_j$ to $\bar{t}_j$. The amount of swapped power corresponds to Δ, defined in (3.16). The last two terms in its minimum function ensure that the updated power scheduling remains feasible, whereas the first term ϵ, defined in (3.5), guarantees that the power swap is performed (i.e. $\Delta > 0$) only if there is an advantageous price differential between the time instants $\bar{t}_j$ and $\underline{t}_j$. All other devices $i \in \mathcal{N} \backslash \{j\}$ maintain their previous power scheduling. The complete multi-valued correspondence F in (3.14) can now be expressed as the composition of N mappings F_j, iterated over the whole population of flexible loads $\mathcal{N} = \{1, \ldots, N\}$:

$$F(u) := \left(F_N \circ \cdots \circ F_1\right)(u). \tag{3.19}$$

The evolution of the power scheduling $u(k)$ according to the proposed update strategy can now be characterized as follows:

Definition 3.3. *Given the dynamical system (3.14), with F defined in (3.19), its*

solution set Ψ *can be expressed as:*

$$\Psi := \{\psi : \mathbb{N} \to \mathcal{U} \ : \ \psi(k+1) \in F(\psi(k)) \ \ \forall k \in \mathbb{N}\}\,. \tag{3.20}$$

This definition is similar to Definition 2.3. Some fundamental properties of the solution set Ψ are now demonstrated, showing that the proposed power update strategy (characterized by the mapping F) always converges to the variational aggregative equilibrium presented in Definition 3.2.

This is proved with Lyapunov arguments, selecting the optimized generation costs $\varphi(D)$ as the considered Lyapunov function. Similarly to the Lyapunov stability theorem in the discrete-time case, we aim to demonstrate that the function $\varphi(D)$ is always nonincreasing when evaluated over the state trajectories (3.19) of system (3.14), as shown in Proposition 3.4. This implies convergence to equilibrium – as demonstrated in Theorem 3.1.

The first step in our analysis is the following result:

Proposition 3.4. *For the optimized generation cost* φ *presented in (3.1), evaluated along any solution* $\psi \in \Psi$*, it holds:*

$$\varphi(D(\psi(k+1))) \leq \varphi(D(\psi(k))) \qquad \forall k \in \mathbb{N} \tag{3.21a}$$

$$\psi(k+1) = \psi(k) \qquad \forall k : \varphi(D(\psi(k+1))) = \varphi(D(\psi(k))) \tag{3.21b}$$

$$\lim_{k\to\infty} \varphi(D(\psi(k))) = \varphi_\infty, \quad \varphi_\infty \in \mathbb{R}_+ \tag{3.21c}$$

Proof. See Appendix B.4. □

Proposition 3.4 shows that the proposed power update of the flexible loads, characterized by the multivalued mapping F, has the fundamental property of reducing the total generation costs of the system at each iteration. As a result, the minimized

generation cost φ asymptotically converges to some finite value φ_∞. In addition, from (3.21b), the proposed strategy updates the power scheduling of the loads only if this ensures a reduction of total costs. The main equilibrium and optimality results can now be provided.

Theorem 3.1. *Let Ω^* denote the set of variational aggregative equilibria introduced in Definition 3.2. Indicating by $|x|_\Gamma$ the distance between some element $x \in \mathcal{U}$ and the set $\Gamma \subseteq \mathcal{U}$, it holds:*

$$\lim_{k\to\infty} |\psi(k)|_{\Omega^*} = 0 \qquad \forall \psi \in \Psi. \tag{3.22}$$

Proof. See Appendix B.5. □

This result ensures that the proposed scheme asymptotically converges to the set of variational aggregative equilibria. In other words, when the final power scheduling is applied, each device has no unilateral interest in modifying its power consumption in order to reduce its energy cost. This property holds for any grid topology, any penetration level of flexible demand and all parameters of the price-responsive loads. Global optimality of the equilibrium can also be demonstrated, under some mild assumptions:

Theorem 3.2. *If the optimized generation cost is differentiable at the aggregative equilibrium $u^* \in \Omega^*$, i.e. $D = D(u^*) \notin \mathcal{D}$ in (3.3), the following optimality property is verified:*

$$\varphi\left(D(u^*)\right) \leq \varphi\left(D(u)\right) \qquad \forall u \in \mathcal{U}. \tag{3.23}$$

Proof. See Appendix B.6. □

The theorem shows that any aggregative equilibrium u^* is also socially optimal if the function $\varphi(D)$ is differentiable at $D = D(u^*)$. In these cases, there exists no feasible power scheduling $u \in \mathcal{U}$ whose associated generation cost $\varphi(D(u))$ is lower than $\varphi(D(u^*))$ obtained at equilibrium.

3.4.2 Pseudo-Code and Flowchart Representation

Algorithm 2 Iterative scheme - Flex. demand coordination

1. **Initialization phase.** Starting values for power scheduling of the loads and flag variables are set:

$$u(0) = u^0 \in \mathcal{U} \qquad k = 0 \qquad conv = 0$$

2. **Power scheduling update.** The scheduled power profiles of the individual loads are iteratively updated:
WHILE $(conv = 0)$

   (a) $conv = 1$

   (b) $k = k + 1$

   (c) $u(k) = u(k-1)$

   (d) **FOR** $j = 1 : 1 : N$

      i. **FIND** $(\bar{t}^*, \underline{t}^*)$ such that:

$$(\bar{t}^*, \underline{t}^*) \in \underset{(\bar{t},\underline{t}) \in \mathcal{A}_j \times \mathcal{A}_j}{\arg\max} \gamma(u(k), j, \bar{t}, \underline{t})$$

      ii. **IF** $\gamma(u(k), j, \bar{t}^*, \underline{t}^*) > 0$

$$\begin{array}{cc} conv = 0 & \delta = \Delta(u(k), j, \bar{t}^*, \underline{t}^*) \\ u_{j,\bar{t}^*}(k) = u_{j,\bar{t}^*}(k) + \delta & u_{j,\underline{t}^*}(k) = u_{j,\underline{t}^*}(k) - \delta. \end{array}$$

   END FOR

   END WHILE

3. **Final results**. The aggregative equilibrium solution is equal to the power scheduling at the last iteration:

$$u^* = u(k).$$

The power scheduling update described by (3.19) and (3.17) can be performed through Algorithm 2, graphically summarized by the flowchart in Fig. 3.1.

The **Initialization phase** of the algorithm sets the power scheduling $u(0)$ of the whole population to some initial value u^0.

In the **Power scheduling update** phase, each full execution of the **FOR** cycle in step 2.b) corresponds to the application of the mapping F in (3.19). In particular, each single iteration with index j is equivalent to the application of F_j in (3.17).

First, the time instants $\bar{t}^*, \underline{t}^* \in \mathcal{A}_j$ which maximize γ are selected. Then, if the maximized γ is positive, the device j can reduce its energy cost by shifting the amount of power δ from $\underline{t}^*$ to $\bar{t}^*$. As established in Theorem 3.1, the algorithm converges to an aggregative equilibrium. When $\gamma(u(k), j, \bar{t}_j, \underline{t}_j) \leq 0$ for all $j \in \mathcal{N}$ and $(\bar{t}_j, \underline{t}_j) \in \mathcal{A}_j \times \mathcal{A}_j$, the logical variable *conv* remains equal to 1 throughout the **FOR** cycle and the final scheduling $u^* = u(k)$, returned in the **Final results** phase, fulfills (3.13) in Proposition 3.3.

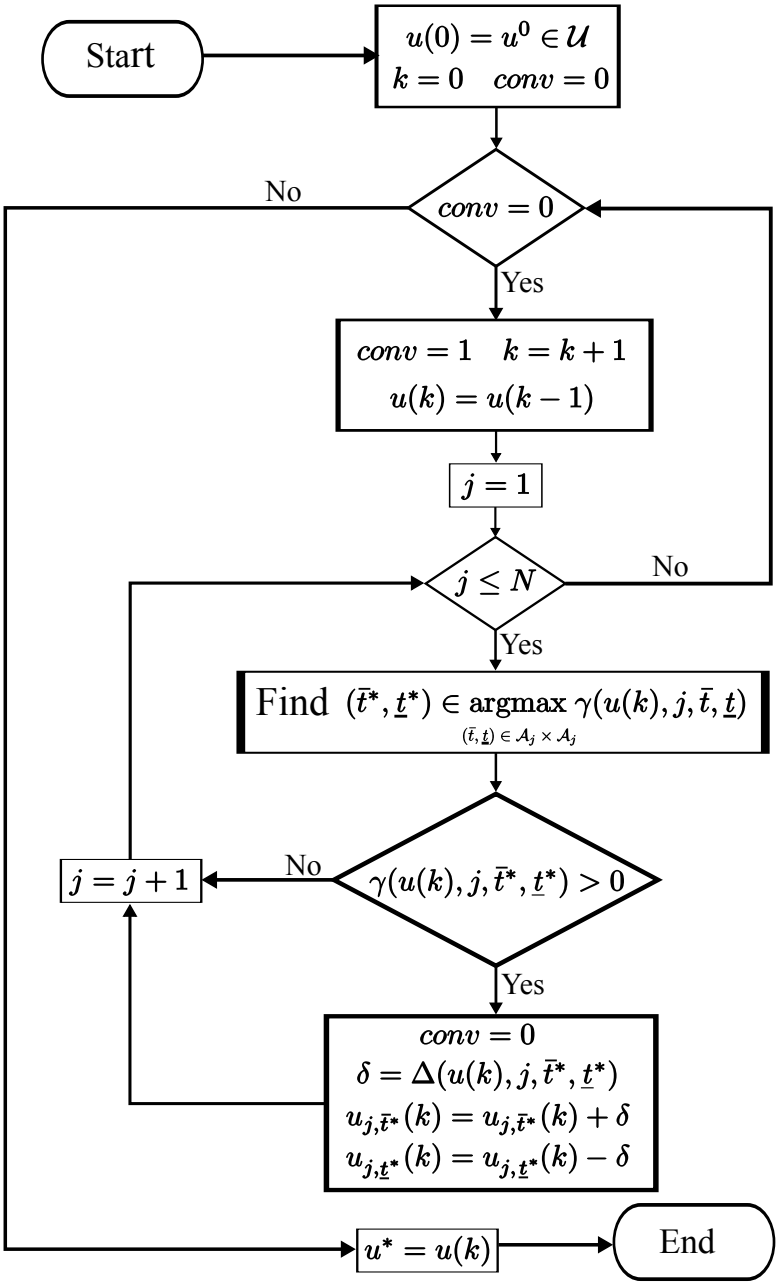

Figure 3.1: Flowchart of Algorithm 2.

3.4.3 Implementation Scheme

Algorithm 2 constitutes a pseudo-code representation of the iterated application of the multi-valued mapping F in (3.19). It details the steps required to calculate the modified power schedule by each individual load and specifies the stopping criterion for the iterative updates. In this section, we present an implementation scheme for the application of this algorithm in a distributed way, considering iterated broadcast of prices and individual devices that autonomously modify their power schedule to reduce their costs. Relying on a bi-directional communication scheme between the system operator and the flexible loads, the operations associated to each step of the algorithm can be performed as follows:

1. **Initialization phase**: Each device j determines an initial feasible power consumption profile $u_j(0) = u_j^0 \in \mathcal{U}_j$. This can be obtained by broadcasting a certain price signal p to all the loads and letting each device j schedule its power consumption $u_j(0) = u_j^0$ in order to minimize (3.9). The scheduled power profiles $u(0)$ are communicated to the central entity, which determines the resulting aggregate power demand $D(u(0))$ through (3.8).

2. **Power scheduling update**: Implementation of the **WHILE** cycle in step 2 can be performed as follows:

   - The price signals $\bar{p}_{\mu_j}(D(u(k)))$ and $\underline{p}_{\mu_j}(D(u(k)))$, i.e. the locational marginal prices at bus $m = \mu_j$ associated to the current demand profile D are calculated according to (3.4) and broadcast to device j. This device can then independently determine the time instants $\bar{t}^*, \underline{t}^* \in \mathcal{A}_j$ of an advantageous power swap reducing its energy cost (as in step 2.b.iii of Algorithm 2).
   - The device j applies (3.16) and independently calculates δ in step 2.b.iv of Algorithm 2, i.e. the maximum amount of power consumption that can be swapped in its power schedule from time $\underline{t}^*$ to $\bar{t}^*$.

- The device j communicates $\bar{t}^*$, $\underline{t}^*$ and δ to the central entity which in turn calculates the new demand profile $D(u(k+1))$ and the convergence flag *conv*.

3. **Final results**: When Algorithm 2 converges to an aggregative equilibrium, as proven in Theorem 3.1, the **WHILE** cycle described above is concluded and the devices cannot further reduce their energy costs. Their final power profiles u_j^* will be equal to $u_j(k)$ at the last iteration k.

In order to find out the communication scale of the practical implementation, the information exchanged at each iteration k of Algorithm 2 is firstly summarized in the Table 3.1.

Table 3.1: Communication between flexible loads and central entity at an iteration k of Algorithm 2.

k-th iteration	Information from entity to load j	Information from load j to entity
Load 1	Price signal (after power swap of load N)	Power swap of load 1
Load 2	Updated price after power swap of load 1	Power swap of load 2
Load 3	Updated price after power swap of load 2	Power swap of load 3
⋮	⋮	⋮
Load N	Updated price after power swap of load $N-1$	Power swap of load N

It is seen from the table that there are N times of communication between the central entity and the flexible loads at each iteration. At each time of the communication, the central entity broadcasts a price signal to a load j, and this load performs a power swap to reduce its energy cost in response to the price signal. The information of the power swap is then returned to the entity which will update the price accordingly. If the coordination algorithm terminates after a number $k = K$ of iterations, there will be $K \cdot N$ times of information exchanged between the entity and the loads.

3.4.4 Methods for Faster Algorithm Convergence

The coordination scheme in Algorithm 2 has been chosen for its simplicity and because it directly maps the multi-valued function F, introduced in (3.19) to analytically describe the scheduling update of the loads. Some alternative approaches that can ensure faster convergence are discussed below:

Best response strategy: Each load directly applies its cost-minimizing schedule in response to a price broadcast, with no impact of its previous power scheduling. This approach has exhibited fast convergence to equilibrium in simulation, but such result has not been formally proved.

One-shot strategy: With this method, discussed in detail in [24] for a simplified pricing structure, the flexible loads are coordinated through the broadcast of a single price signal (different in general for each load). These prices are calculated by the central coordinator, which receives the characteristics and task parameters of all the devices and internally emulates Algorithm 2 to calculate the final equilibrium solution. It should be mentioned that, in this case, one-shot convergence is obtained at the expenses of the loads' privacy.

3.5 Simulation Results

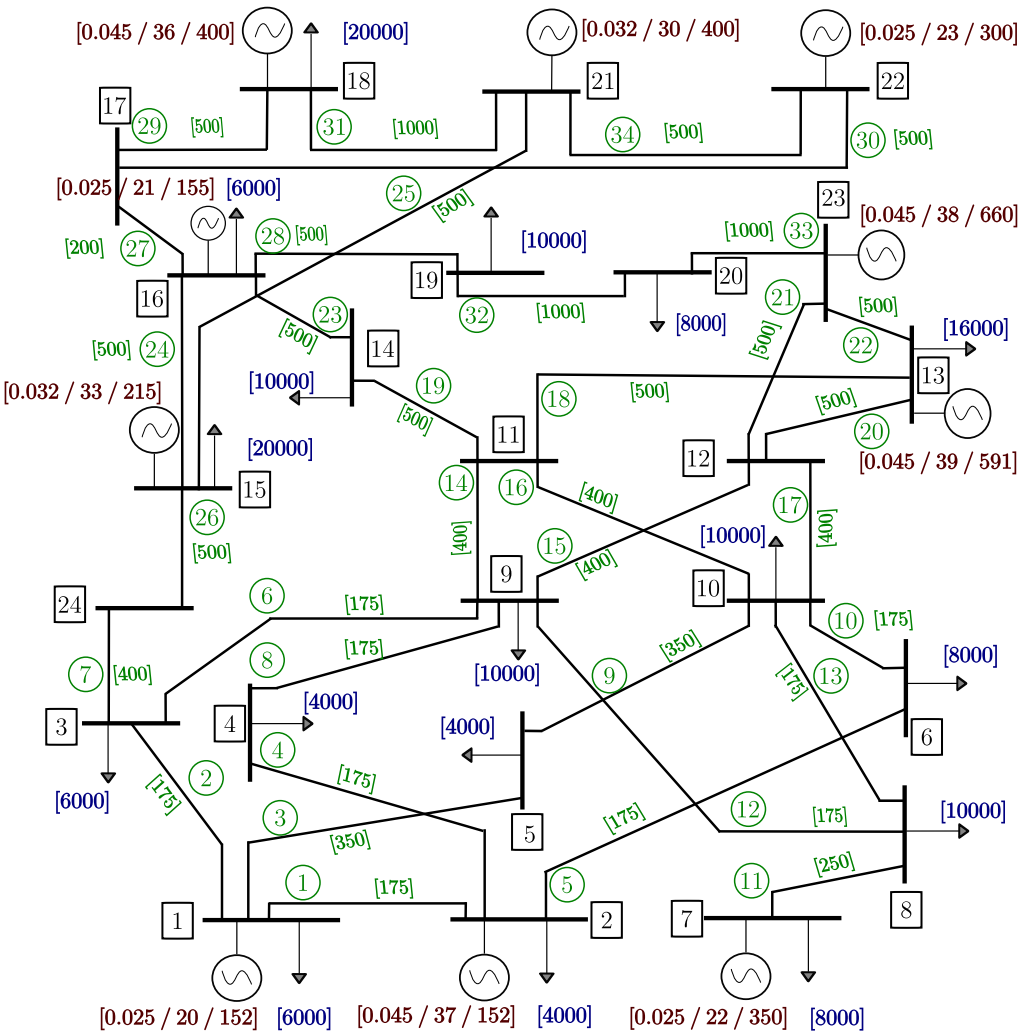

Figure 3.2: Diagram of the IEEE 24-bus system.

The performance of the proposed control scheme is assessed in simulation on the IEEE 24-bus system [48]. The generation cost $f_m(g)$ at each bus m is assumed to be a quadratic function of the power generation g, i.e. $f_m(g) = a_m g^2 + b_m g$. The diagram of the system and its relevant generation and parameters are shown in Fig. 3.2. Other parameters, such as reactive power generation limits of generators and resistance, reactance and susceptance of transmission lines, can be found in [48].

The inflexible active demand profiles $d_{m,t}$ are derived from historical data and are in general different for each bus. Their values are shown in Fig. 3.3 (left - black dashed lines). It is assumed that the inflexible demand at each bus operates at 0.95 lagging power factor and that the feasible range of voltage magnitude at each bus is between 0.9 p.u. and 1.1 p.u.. Additionally, the system model is considered to be power lossless, i.e. the terms $P^L_{l,t}$ and $Q^L_{l,t}$ are equal to zero in (3.2a) and (3.2b). A future scenario with high penetration of electric vehicles is considered: each vehicle j is modeled as a power load with unity power factor [49], aiming at charging its battery at minimum cost within its availability interval $\mathcal{A}_j$. The number N_m of EVs at each bus m is shown in Fig. 3.2. We denote by $\mathcal{N}_m \subseteq \mathcal{N}$ the subset of N_m devices operating at bus m. The required energy E_j of all devices $j \in \mathcal{N}_m$ is chosen according to a Gaussian distribution with mean x^E_m and standard deviation δ^E_m. In addition, it is assumed that all the vehicles at bus m have the same rated power P_m. For instance, the energy and power parameters for the EVs at bus 1 are selected as follows:

$$x^E_1 = 30 \text{ kWh} \qquad \delta^E_1 = \text{ 1kWh} \qquad P_1 = \text{ 10kW}.$$

The final time $T = 24h$ and time discretization step $\Delta t = 0.25h$ are chosen for the considered time horizon. It is assumed that each vehicle j can operate in a continuous time interval $[t_j, t_j + d_j]$. The equivalent availability window $\mathcal{A}_j$ of the single device j can be expressed in discrete time as:

$$\mathcal{A}_j = \{t \in \mathcal{T} : t_j \leq t \cdot \Delta t \leq t_j + d_j\}\,. \tag{3.24}$$

The values of t_j and d_j for all devices $j \in \mathcal{N}_m$ operating at bus m are also determined according to Gaussian distributions with mean values x^t_m and x^d_m and standard deviations δ^t_m and δ^d_m, respectively. For example, the availability parameters for the EVs at bus 1 are:

$$x^t_1 = 21:30 \text{ h} \qquad \delta^t_1 = 1.5 \text{ h} \qquad x^d_1 = 10 \text{ h} \qquad \delta^d_1 = 1.5 \text{ h}.$$

It should be noted that the normal distributions used to generate the EVs parameters E_j, t_j and d_j are properly truncated and rescaled in order to ensure feasibility and well-posedness of the considered scheduling problem.

3.5.1 Algorithm Implementation

The coordination of the flexible devices has been performed with Algorithm 2. The initial condition $u(0) = u^0$ in Step 1) envisages constant power profiles for all loads. The power update in Step 2) has been carried out by sequentially selecting a single device at each iteration. A single power swap is performed according to the expressions provided in step 2.d) before moving on to the next device.

The final results of the proposed coordination scheme, denoted by the star superscript, have been compared with the scenario **PG** (price-greedy). In this latter case, a more naive approach is applied and each load $j \in \mathcal{N}_m$ determines its power consumption profile according to the price $\bar{p}_m(d)$, i.e. the electricity price when only inflexible demand d is considered. The total power consumption of the flexible loads in this scenario is denoted as u^{PG}.

The demand and price profiles obtained with the two policies mentioned above are compared in Fig. 3.3, in which a limited number of relevant buses is considered. In the present case study, the two price signals $\bar{p}$ and $\underline{p}$ introduced in (3.4) coincide in all cases and therefore only the signal $\bar{p}$ is shown. The most relevant trend is that the electricity price $\bar{p}_m(D(u^*))$ obtained with the proposed algorithm is consistently flatter than $\bar{p}_m(D(u^{PG}))$. All the electric vehicles schedule their charge between 22:00h and 7:00h, when the electricity price at their bus is constant and minimum. As expected, at equilibrium no device can exploit any price differential to reduce its energy cost and therefore has no unilateral interest in changing its final power consumption profile. Note that the same flattening trend, albeit on a lesser scale, appears in the demand profiles $D_m(u^*)$, which do not exhibit the significant rebound

peaks of $D_m(u^{PG})$. The flattening of the demand profiles $D_m(u^*)$ in Fig. 3.3 is only partial since the iterative power update of the devices is based on differences in LMPs which, in general, do not exclusively depend on local demand but are also affected in non-trivial ways by the demand values at other buses.

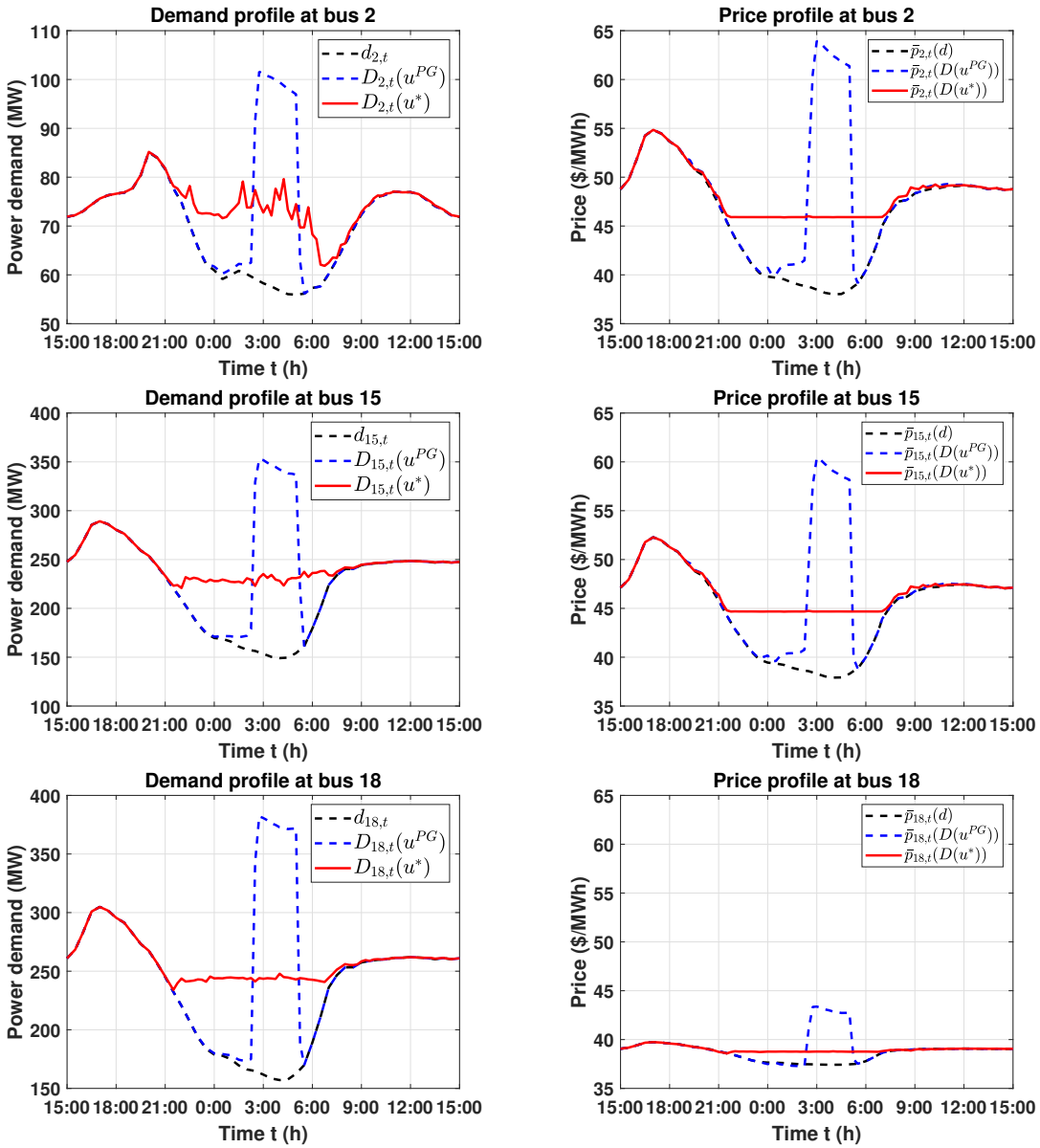

Figure 3.3: Demand profiles (left) and electricity prices (right): no flexible demand (black dashed trace), with proposed scheduling (red trace) and **PG** scenario (blue dashed trace).

The generation profiles with the proposed scheme and under the **PG** scenario are compared in Fig. 3.4. Differently from the significant variation in the **PG** case, the

algorithm completely flattens generation at each bus during night-time.

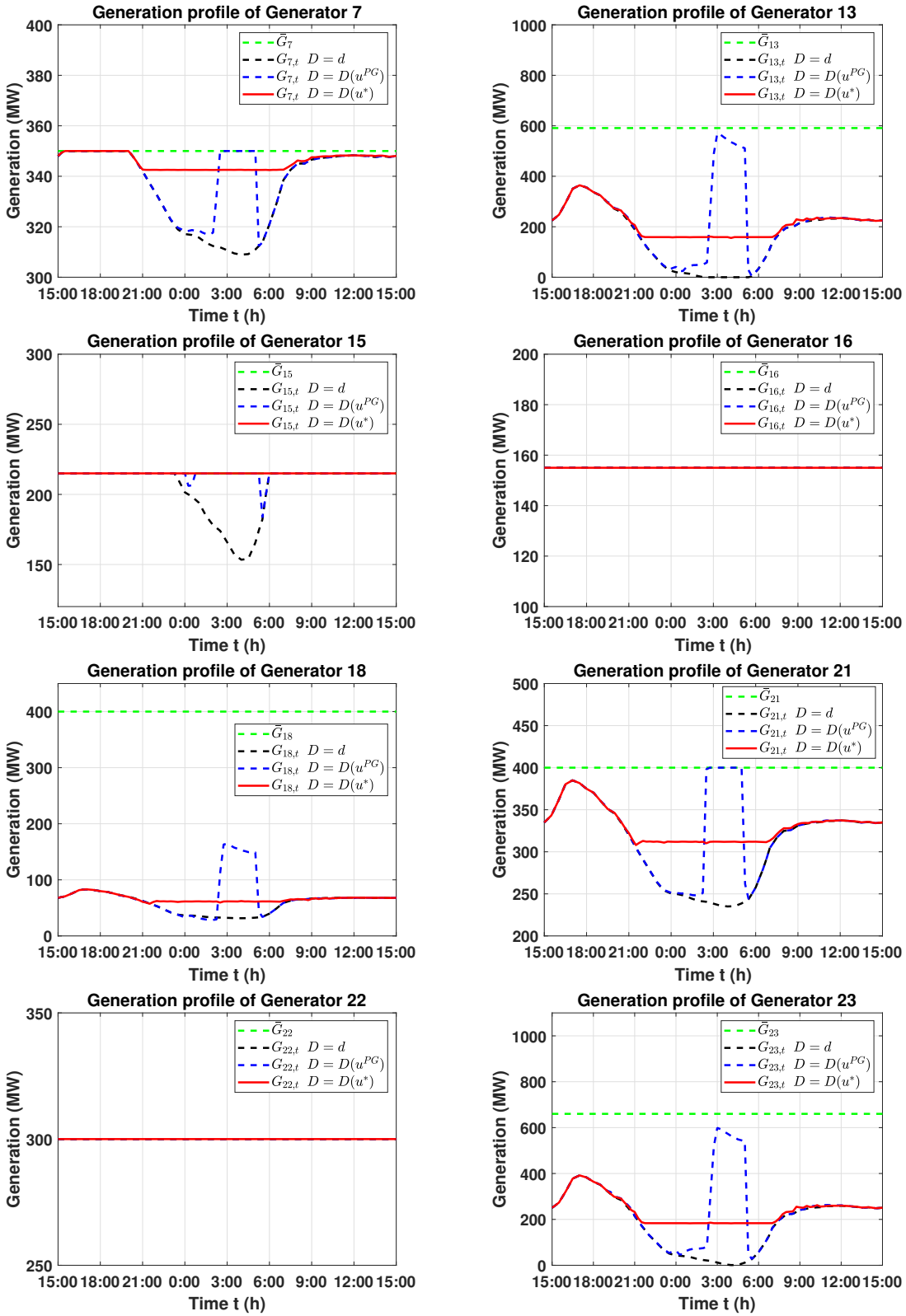

Figure 3.4: Generation profiles: no flexible demand (black dashed trace), with proposed scheduling (red trace), **PG** scenario (blue dashed trace) and generation capacity (green dashed trace).

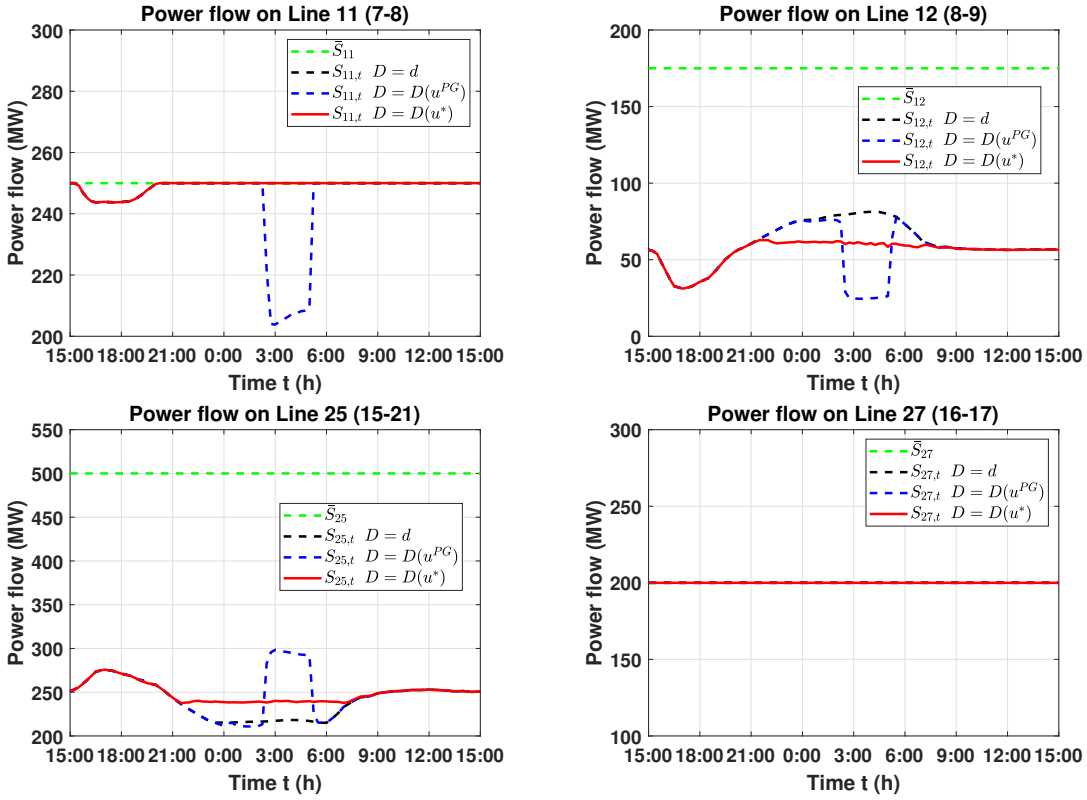

Figure 3.5: Power flows: no flexible demand (black dashed trace), application of proposed scheduling (red trace), **PG** scenario (blue dashed trace) and transmission capacity (green dashed trace).

Some relevant examples of apparent power flows (obtained with the proposed algorithm and in the **PG** case) are represented in Fig. 3.5. It can be seen that, in general, there are reduced variations over time when the final configuration with $D = D(u^*)$ is considered. Note that line 27 always works at its maximum capacity.

To assess the impact of generation capacity limits and lines congestion on the locational marginal prices, LMPs at buses 7 and 8 for $D = D(u^*)$ are plotted in Fig. 3.6. A few interesting trends can be underlined. As expected, the two prices $\bar{p}_{7,t}(D(u^*))$ and $\bar{p}_{8,t}(D(u^*))$ will be the same when there is no congestion on the line 11 connecting them (see top-left plot of Fig. 3.5). As soon as congestion appears on line 11, the prices become different: the LMP at bus 8 will vary continuously and its variations will be linked with the ones of other buses (i.e. buses 9 and 10), which are connected to bus 8 by lines 12 and 13 (not congested). Conversely, in this situation any additional unit of power at bus 7 can only be provided by generator 7

at its marginal generation cost, which leads to the negative price jump of $\bar{p}_{7,t}(D(u^*)$ (black trace).

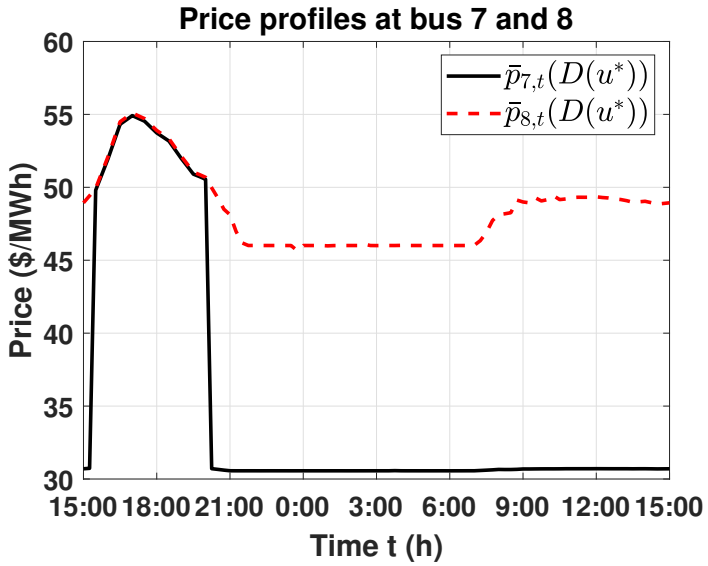

Figure 3.6: The comparison of price profiles at buses 7 and 8 for $D = D(u^*)$.

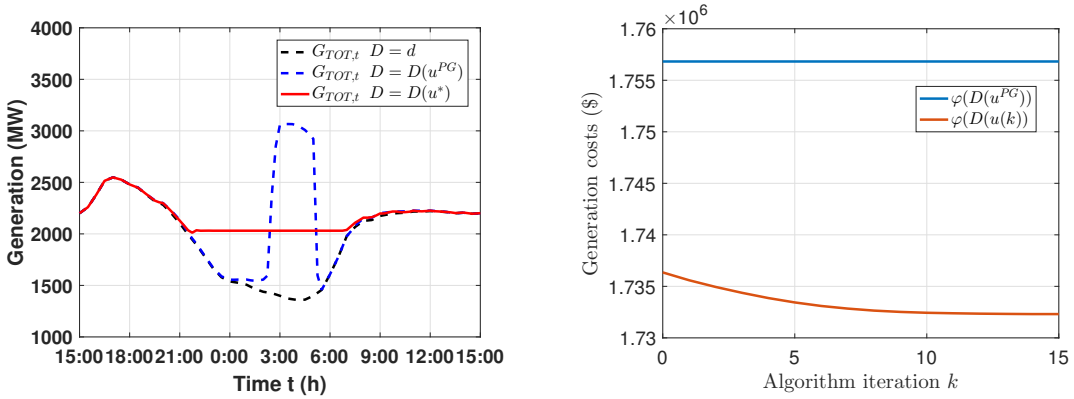

Figure 3.7: Profiles of total generation for the considered scenarios (left) and total generation costs as a function of algorithm iteration k (right).

The performance of the proposed algorithm is also assessed from a whole-system perspective. In particular, the profiles of total generation $G_{TOT,t} = \sum_{m=1}^{M} G_{m,t}$ for the different considered scenarios are compared on the left of Fig. 3.7. Interestingly, one can see that the proposed control strategy with $D = D(u^*)$ completely flattens the total generation profile G_{TOT}. This can be intuitively explained by the fact that, according to Theorem 3.2, the final configuration obtained with the proposed

coordination scheme not only is an equilibrium but it is also socially optimal. As we are considering strictly convex generation costs in (3.1) and the total generation over time is a fixed quantity, the generation profile will naturally tend to be flat at the optimum. In relation to this point, the generation costs φ are reported in Fig. 3.7 as a function of the number k of algorithm iterations. Consistently with the theoretical results of Proposition 3.4, the function $\varphi(D(u(k)))$ is decreasing over k. It can be seen that there is no further reduction of $\varphi(D(u(k)))$ after $k = 15$ iterations, and the algorithm has converged. As established in Theorem 3.2, the final value reached by $\varphi(D(u(k)))$ corresponds to the minimized generation costs of the system, which is smaller than the costs $\varphi(D(u^{PG}))$ in the **PG** scenario.

3.5.2 Robustness with respect to Uncertainties

In the above simulations, the inflexible demand d is known without uncertainties. To test the robustness of the control scheme with respect to forecast errors, it is now assumed that the coordination is performed with an estimate $\tilde{d}$ of inflexible demand. Denoting by $\tilde{d}_{m,t}$ the estimated inflexible demand at bus m and time t, the following expression is considered:

$$\tilde{d}_{m,t} = d_{m,t} + \eta_{m,t} \tag{3.25}$$

where $\eta_{m,t}$ represents the forecast error on inflexible demand at bus m at time t. Assuming that renewable generation has zero marginal cost and it is always dispatched first, the quantity $\eta_{m,t}$ can equivalently represent a negative error forecast in renewable generation. The error forecast η_m is characterized as a random walk $\eta_{m,t+1} = \eta_{m,t} + \sigma_m e_t$, where e_t represents uncorrelated white noise with zero mean and unitary variance. With this formulation, $\eta_{m,t}$ is a random variable with zero mean and standard deviation equal to $\sigma_m \cdot \sqrt{t}$, which is consistent with basic models for wind error forecast as shown for example in [50]. To account for error forecast

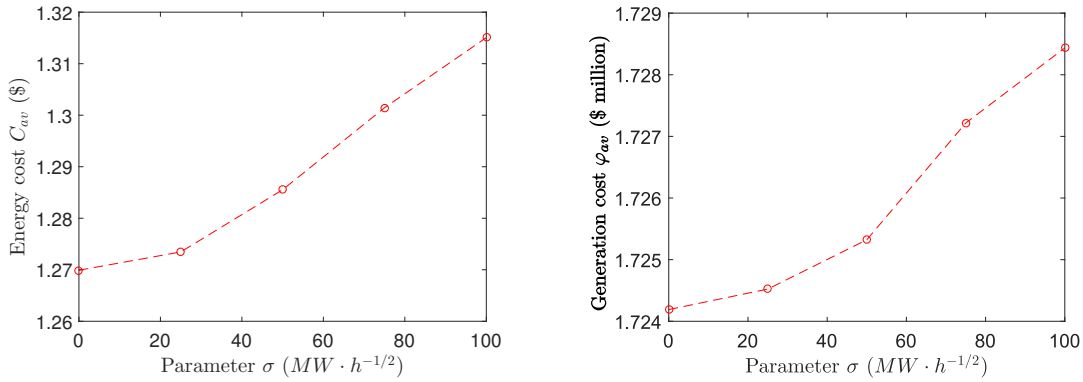

Figure 3.8: Average energy cost C_{av} (left) and average generation costs φ_{av} (right) as functions of the parameter σ.

correlation at the different buses due to geographical proximity, two independent noise signals e_t are considered for the South buses (e.g. buses 1-12) and for the North ones (buses 13-24). The value of σ_m at each node m is obtained as the rescaling of a unique parameter σ by the fraction of total demand at that node.

The coordination algorithm has been applied by considering the inflexible demand estimate $\tilde{d}$ rather than the actual profile d, denoting by $\tilde{u}^*$ the power scheduling of the loads at the final equilibrium solution. In this case of imperfect information, the total generation costs will be equal to $\varphi(D(\tilde{u}^*))$ and the energy cost $\tilde{C}_j$ sustained by the single device j will correspond to:

$$\tilde{C}_j = \sum_{t=1}^{T} p_{\mu_j,t}(D(\tilde{u}^*)) \cdot \tilde{u}^*_{j,t} \cdot \Delta t$$

The optimal scheduling $\tilde{u}^*$ has been calculated over $L = 50$ realizations of the estimated inflexible demand profile $\tilde{d}$. The resulting cost C_{av} (average of $\tilde{C}_j$ over all devices and demand realizations) and the total generation costs φ_{av} (average of $\varphi(D(\tilde{u}^*))$ over all demand realizations) are plotted in Fig. 3.8 as a function of the standard deviation parameter σ. As expected, for increasing values of σ (corresponding to higher forecast errors) the average energy cost C_{av} for the individual load and the average total generation costs φ_{av} increase. However, it can be seen that the performance degradation remains relatively small, even when large values of the standard deviation parameter σ are considered.

3.6 Summary

This chapter presents a novel distributed scheme for the coordination of large populations of flexible electric loads. A comprehensive modelling framework is proposed for demand response operating in multi-bus power systems, explicitly accounting for the congestion of transmission lines and the impact of flexible demand on the locational marginal prices at each bus. The main original contribution is a theoretical analysis that provides guarantees of convergence to a stable market outcome and global optimality, for any grid topology and penetration level of flexible demand. In addition, a double pricing structure and a novel concept of variational aggregative equilibrium are proposed to characterize stable market configurations in the case of discontinuous price functions. Practical implementation of the presented control scheme is discussed and its performance is evaluated in simulation on the IEEE 24-bus system with high penetration of electric vehicles.

Chapter 4

Coordination of Flexible Devices in Integrated Markets

4.1 Introduction

As mentioned in Introduction 1.1, flexible devices can contribute to the provision of ancillary services by being available to reduce their power consumption. However, the works in both Chapter 2 and Chapter 3 do not envision the possibility for the flexible devices to also provide ancillary services. Considering this factor, this chapter studies the coordination of flexible devices in an integrated market of energy and ancillary services. In addition, the flexible devices considered in this chapter include both the storage devices and flexible loads that have been introduced in Chapter 2 and Chapter 3, respectively.

This active participation of demand response to ancillary services has been assessed with different approaches. For example, centralized methods for primary frequency support in microgrids are presented in [51] and reward allocation mechanisms are proposed in [52] to enable provision of ancillary services by thermostatically controlled loads. Market frameworks have also been widely investigated for the pro-

vision of frequency response [53, 54] and reserve services [55, 56, 57, 58]. These papers consider flexible demand that actively participates to ancillary services markets. However, [53, 54, 55, 56, 57, 58] do not provide any theoretic guarantee of convergence and optimality of their proposed market setup.

This chapter bridges the gap between the game-theoretic schemes in [31, 32, 33, 34, 35, 36] and the market approaches proposed in [53, 54, 55, 56, 57, 58]. In particular, it considers large populations of flexible devices (EVs and storage) that individually participate to an integrated energy and reserve market. This scenario is analysed through a rigorous game-theoretic setup in order to formally demonstrate convergence of the proposed coordination scheme to an optimal configuration.

For simplicity, this chapter uses a DC optimal power flow (DCOPF) model to analyse the integrated market instead of using the linearized ACOPF in Chapter 3. The coordination problem is still analysed through an agent-based framework, similar to previous chapters: each individual device (either a domestic micro-storage or an electric vehicle) is modelled as a self-interested rational agent that responds to the price signals and determines its operational schedule in order to optimize its own objective function. In addition to the minimization of the energy cost, the individual device will also aim to maximize the rewards received for allocation of reserve. Using Lyapunov techniques, it is demonstrated that the proposed coordination strategy converges to a stable market configuration (characterized as an aggregative equilibrium) that is also socially optimal. Simulations are carried out on the PJM 5-bus system to test the validity of the proposed scheme and assess its performance.

4.2 System Model

The considered power system is composed by a set $\mathcal{M} = \{1, \dots, M\}$ of nodes connected by a set $\mathcal{L} = \{1, \dots, L\}$ of transmission lines. The reactance and maximum capacity of each line $l \in \mathcal{L}$ are denoted by X_l and $\bar{F}_l$, respectively. The analysis is performed over a discrete time interval $\mathcal{T} = \{1, \dots, T\}$, with a time discretization step Δt. Power demand is denoted by the vector $D \in \mathbb{R}^{MT}$, whose single component $D_{m,t}$ corresponds to the total power consumption at node m at time t. With a similar notation, $F_{l,t}$ indicates the power flow over line $l \in \mathcal{L}$ at time $t \in \mathcal{T}$ from the sending node $s(l) \in \mathcal{M}$ to the receiving node $r(l) \in \mathcal{M}$. Generation, reserve and voltage angle vectors are denoted as $G \in \mathbb{R}^{MT}$, $R^0 \in \mathbb{R}^{MT}$ and $\theta \in \mathbb{R}^{MT}$, respectively.

It is assumed that the power system operates under an integrated energy-reserve market. Consistently with the approach presented in [6] and [59], a DCOPF is solved to optimally dispatch power and procure reserve capacity. Similarly to [6], start-up times and costs are neglected, avoiding the use of binary variables. The presented formulation will be expanded in future work to consider a detailed unit commitment. Under the proposed framework, the DCOPF corresponds to the solution of the following minimization problem:

$$\varphi(D, R) = \min_{G, R^0, \theta} \sum_{m=1}^{M} \sum_{t=1}^{T} \left(f_m^G(G_{m,t}) + f_m^R(R_{m,t}^0) \right) \tag{4.1}$$

subject to:

$$D_{m,t} - G_{m,t} + \sum_{\{l:s(l)=m\}} F_{l,t} - \sum_{\{l:r(l)=m\}} F_{l,t} = 0 \quad \forall m \in \mathcal{M} \quad \forall t \in \mathcal{T} \tag{4.2a}$$

$$|F_{l,t}| = \left| \frac{1}{X_l} \cdot \left[\theta_{r(l),t} - \theta_{s(l),t} \right] \right| \leq \bar{F}_l \quad \forall l \in \mathcal{L}, \quad \forall t \in \mathcal{T} \tag{4.2b}$$

$$G_m \leq G_{m,t} \leq \bar{G}_m \qquad \forall m \in \mathcal{M}, \quad \forall t \in \mathcal{T} \tag{4.2c}$$

$$R^0_{m,t} \leq \bar{G}_m - G_{m,t} \qquad \forall m \in \mathcal{M}, \quad \forall t \in \mathcal{T} \tag{4.2d}$$

$$\sum_{m=1}^{M} \left(R^0_{m,t} + R_{m,t}\right) \geq \Delta G^{max}_L \quad \forall t \in \mathcal{T}. \tag{4.2e}$$

The objective function in the right-hand side of (4.1) corresponds to the sum (over all times t and buses m) of the generation cost $f^G_m(G_{m,t})$ for producing $G_{m,t}$ units of power and the cost $f^R_m(R^0_{m,t})$ for providing $R^0_{m,t}$ units of reserve. The functions f^G_m and f^R_m are assumed to be strictly convex.

Regarding the constraints, (4.2a) corresponds to the supply-demand balance. The inequalities in (4.2b) ensure that the power flow $F_{l,t}$ does not exceed the maximum line capacity $\bar{F}_l$, whereas (4.2c) imposes that generation at bus m is always within the minimum ($\underline{G}_m$) and maximum ($\bar{G}_m$) power capability. The amount of reserve $R^0_{m,t}$ that can be procured by generation at bus m at time t is constrained by (4.2d) and cannot exceed the extra available capacity. Finally, (4.2e) imposes that the total allocated reserve exceed some minimum quantity ΔG^{max}_L, which for example can correspond to the largest power unit capacity. Note that, in the left-hand side of (4.2e), the total procured reserve is calculated as the sum over all buses of two components: the reserve $R^0_{m,t}$ procured by the committed generation and the reserve $R_{m,t}$ provided by flexible demand and storage, which will be characterized in the next section.

Remark 4.1. *Compared with the linearized ACOPF in Chapter 3, the DCOPF neglects the reactive power and transmission losses while keeping the convexity and linearity. The neglect has little impact on the final results of the work, since the energy price and reserve price are related to the active power, and the transmission losses are quite small (due to high voltage at transmission level). It is also consistent with other works [37, 38, 39, 40] studying the interactions between price-responsive demand and the transmission network, where a DC formulation has been considered for the optimal power flow problem and the calculation of the LMPs. The DCOPF model is mostly used for the purpose of market clearing owing to its simplicity, robustness and less computation.*

We wish to emphasize that, if one assumes inelastic demand and perfect competition, the result of the OPF problem can be considered as the solution of a traditional centralized market mechanism [60]. Under this paradigm, one can define the prices for energy and reserve provision as the relevant Lagrange multipliers of the constraints in (4.2). For a formal characterization of these quantities, note that the optimized operational cost φ in (4.1) can be expressed as a function of the total power demand D and the reserve R procured by the flexible devices. These quantities do not appear as decision variables of the problem and depend instead on the aggregate behaviour of the flexible devices (described in Chapter 4.3). As a result, one can define the prices as follows:

$$p_{m,t}(D,R) = \frac{\partial \varphi(D,R)}{\partial D_{m,t}} \tag{4.3a}$$

$$\rho_{m,t}(D,R) = -\frac{\partial \varphi(D,R)}{\partial R_{m,t}}. \tag{4.3b}$$

The quantity $p_{m,t}$ represents the marginal cost of accommodating an additional unit of demand at node m at time t and it can be interpreted as the price of electricity at that bus and time instant. Similarly, the quantity $\rho_{m,t}$ represents the marginal saving obtained if flexible devices increase by an additional unit their allocated reserve $R_{m,t}$ at node m at time t (counterbalanced by an opposite reduction of $R^0_{m,t}$ from generators). As a result, $\rho_{m,t}$ can be considered the price at which the allocation of reserve by flexible devices is rewarded.

Assumption 4.1. *The function $\varphi(D,R)$ is differentiable with respect to $D_{m,t}$ and $R_{m,t}$ for any $m \in \mathcal{M}$ and $t \in \mathcal{T}$. Its derivatives $p_{m,t}(D,R)$ and $\rho_{m,t}(D,R)$ in (4.3) are Lipschitz continuous.*

The hypothesis of global differentiability of φ is introduced to simplify the subsequent analysis and ensure that the prices p and ρ in (4.3) are always well-defined. The results presented in the rest of this chapter can be extended to the case of φ differentiable almost everywhere by using the double-price framework presented in

Chapter 3 or reference [61].

4.3 Price-Responsive Flexible Devices

It is envisioned that a large population of storage devices and EVs operate in the considered power system. These devices have the capability to autonomously determine their power schedule during the considered time interval $\mathcal{T}$, according to their constraints and objectives. In addition, they also have the possibility to contribute to reserve, providing their availability to reduce their power consumption if necessary. This section proposes an agent-based modelling of these flexible devices, presenting their dynamics and objectives and characterizing their overall impact on the power system.

4.3.1 Dynamics and Constraints

Consider a population $\mathcal{N} = \{1, \dots, N\}$ of flexible devices partitioned into two groups: the set $\mathcal{N}^{EV}$ of EVs and the set $\mathcal{N}^{S}$ of storage batteries. Each device $j \in \mathcal{N}$ operates over the time interval $\mathcal{T}$ according to a scheduled power profile $u_j = [u_{j,1}, \dots, u_{j,T}] \in \mathbb{R}^T$, where $u_{j,t}$ denotes the power charged/discharged by device j at time t. The feasibility of the power schedules u_j for EVs and storage is the same as that presented in Chapter 2 and 3, which is shown as follows.

EVs: Each EV $j \in \mathcal{N}^{EV}$ has rated power $\bar{P}_j$ and requires a certain amount of energy E_j to fully charge its battery. Its charging can only occur within the interval $\mathcal{A}_j = \{T_j^s, T_j^s + 1, \dots, T_j^e\} \subseteq \mathcal{T}$, when the EV is plugged into the grid. Therefore, the set $\mathcal{U}_j$ of all feasible charging profiles u_j for an EV $j \in \mathcal{N}^{EV}$ can be defined as:

$$\mathcal{U}_j := \left\{ u_j \in \mathbb{R}^T : \ \sum_{t=1}^{T} u_{j,t} \cdot \Delta t = E_j \,, \ \ 0 \leq u_{j,t} \leq \bar{P}_j \cdot \mathbb{1}_{\mathcal{A}_j}(t) \quad \forall t \in \mathcal{T} \right\} \tag{4.4}$$

where $\mathbb{1}_{\mathcal{A}_j}(t)$ is the indicator function:

$$\mathbb{1}_{\mathcal{A}_j}(t) = \begin{cases} 1 & \text{if} \quad t \in \mathcal{A}_j \\ 0 & \text{if} \quad t \notin \mathcal{A}_j. \end{cases} \tag{4.5}$$

The equality in (4.4) guarantees that the energy charged by the EV j over the time interval $\mathcal{T}$ is equal to required amount E_j, while the inequalities indicate that the positive charging rate of the EV j cannot exceed its rated power $\bar{P}_j$ during the availability times $\mathcal{A}_j$ and should be zero outside $\mathcal{A}_j$. Note that the formulation (4.4) of the feasible set $\mathcal{U}_j$ is still valid if one considers other types of flexible loads.

Storage Devices: The storage device $j \in \mathcal{N}^S$ is characterized by the following parameters: its energy capacity $\bar{E}_j$, its maximum charging rate $\bar{P}_j$ and discharging rate $\underline{P}_j$. For a certain initial energy $E_{j,0}$ and charge/discharge profile u_j, the associated energy level $E_{j,t}$ of storage j at time t is expressed as:

$$E_{j,t} = E_{j,0} + \sum_{x=1}^{t} u_{j,x} \cdot \Delta t. \tag{4.6}$$

The set $\mathcal{U}_j$ of all feasible power profiles u_j for the storage device $j \in \mathcal{N}^S$ is defined as:

$$\mathcal{U}_j := \Bigg\{ u_j \in \mathbb{R}^T : \sum_{t=1}^{T} u_{j,t} = 0, \;\; 0 \leq E_{j,0} + \sum_{x=1}^{t} u_{j,x} \cdot \Delta t \leq \bar{E}_j, \\ \underline{P}_j \leq u_{j,t} \leq \bar{P}_j \quad \forall t \in \mathcal{T} \Bigg\}. \tag{4.7}$$

The equality in (4.7) is equivalent to the cyclic constraint $E_{j,0} = E_{j,T}$ from (4.6), ensuring that the initial and final storage energy levels are equal. The first and second chains of inequalities in (4.7) ensure that the energy level $E_{j,t}$ and charging/discharging rate $u_{j,t}$ remain within feasible limits.

The set $\mathcal{U}$ of feasible power schedule $u \in \mathbb{R}^{NT}$ for the whole population can be

characterized as follows:

$$\mathcal{U} = \mathcal{U}_1 \times \cdots \times \mathcal{U}_N. \tag{4.8}$$

4.3.2 Reserve Service Provision

It is envisioned that EVs and storage devices can contribute to the provision of reserve by being available to reduce their power consumption. For simplicity, it is assumed that this power reduction must last for a period of Δt, i.e. the considered time discretization step. For example, in the proposed case study, the time step Δt has been chosen equal to 30 minutes. The reserve amount r deliverable at time t by the single EV or storage is expressed as a function of the scheduled power consumption u. In particular, it is assumed that each device allocates the maximum feasible reserve amount, i.e. the maximum power reduction that does not violate the feasibility conditions expressed in (4.4) and (4.7).

EVs: At each time t, the maximum reserve amount r that can be provided by the EV j corresponds to a reduction of its power consumption from its scheduled value $u_{j,t}$ to 0.

$$r_{j,t}(u) = u_{j,t} \qquad \forall j \in \mathcal{N}^{EV}. \tag{4.9}$$

Storage Devices: The reserve r that can be allocated by the storage j at time t is determined by the feasibility constraints in (4.7) and must fulfill the following conditions:

$$r_{j,t}(u) \leq u_{j,t} - \underline{P}_j \tag{4.10a}$$

$$E_{j,t} - r_{j,t}(u)\Delta t = E_{j,0} + \sum_{x=1}^{t} u_{j,t}\Delta t - r_{j,t}(u)\Delta t \geq 0 \tag{4.10b}$$

Equation (4.10a) imposes that $r_{j,t}(u)$ is smaller than the maximum feasible power reduction $u_{j,t} - \underline{P}_j$ whereas (4.10b) ensures that a potential power reduction of $r_{j,t}(u)$ units by storage j at time t does not violate its energy constraints. The reserve r

can then be expressed as:

$$r_{j,t}(u) = \min\left(\frac{E_{j,t}}{\Delta t},\, u_{j,t} - \underline{P}_j\right) \qquad \forall j \in \mathcal{N}^S. \tag{4.11}$$

4.3.3 Aggregate Impact of Flexible Devices

It is now possible to express D and R, which appear as parameters of the minimized cost φ in (4.1), as functions $\tilde{D}(u)$ and $\tilde{R}(u)$ of the overall power schedule u of the flexible devices. The total demand $\tilde{D}_{m,t}(u)$ at bus m at time t is given by the sum of the power demand $d_{m,t}$ of the inflexible devices (assumed to be known a priori) and the total power consumption of the flexible devices. Denoting by $\mu_j \in \mathcal{M}$ the bus at which the device $j \in \mathcal{N}$ operates, it holds:

$$\tilde{D}_{m,t}(u) = d_{m,t} + \sum_{\{j:\mu_j=m\}} u_{j,t}. \tag{4.12}$$

Similarly, the total reserve $\tilde{R}_{m,t}(u)$ provided by the flexible devices at bus m at time t, when the scheduling u is applied, has the following expression:

$$\tilde{R}_{m,t}(u) = \sum_{\{j:\mu_j=m\}} r_{j,t}(u). \tag{4.13}$$

Replacing the generic terms D and R in (4.3) with the corresponding expressions $\tilde{D}(u)$ and $\tilde{R}(u)$ yields:

$$\tilde{p}_{m,t}(u) := p_{m,t}(\tilde{D}(u), \tilde{R}(u)) \tag{4.14a}$$

$$\tilde{\rho}_{m,t}(u) := \rho_{m,t}(\tilde{D}(u), \tilde{R}(u)). \tag{4.14b}$$

The functions $\tilde{p}_{m,t}(u)$ and $\tilde{\rho}_{m,t}(u)$ correspond, respectively, to the prices of electricity and reserve as functions of the overall power schedule u by the flexible devices.

4.4 Game-Theoretic Formulation

The power consumption and reserve service provision of the flexible devices is controlled in a distributed manner. Each device is modelled as a self-interested rational agent that autonomously schedules its power consumption and procured reserve to minimize its cost C, on the basis of broadcast price signals. For a certain device j, its cost C can be expressed as a function of the schedule u of the whole population and the power profile u_j of the considered device.

EVs: The cost C of EV j has the following expression:

$$C(u, u_j) = \sum_{t=1}^{T} [\tilde{p}_{\mu_j,t}(u) \cdot u_{j,t} - \tilde{\rho}_{\mu_j,t}(u) \cdot r_{j,t}(u)] + \psi(u_j) \quad \forall j \in \mathcal{N}^{EV} \tag{4.15}$$

Three distinct components appear in the cost expression:

- *Electricity cost*: the sum over all discrete time instants t of the power consumption $u_{j,t}$, multiplied by the electricity price $\tilde{p}_{\mu_j,t}(u)$.
- *Reserve revenue*: the sum over time of the allocated reserve $r_{j,t}(u)$, multiplied by the reserve price $\tilde{\rho}_{\mu_j,t}(u)$ with changed sign, since this represents a revenue for the device.
- *Discomfort cost*: summarized by the function ψ.

The function ψ is meant to represent the potential discomfort incurred by the EV owner if, by actually providing reserve, the vehicle battery is not fully charged by the end of the considered interval. Denoted by $\hat{E}(u_j, t)$ the final energy mismatch if reserve is provided by the EV j at time t, the following expression is considered for ψ:

$$\psi(u_j) = \sum_{t \in \mathcal{A}_j} \xi \cdot \hat{E}(u_j, t), \tag{4.16}$$

where ξ is a penalty factor. The missed energy $\hat{E}(u_j, t)$, if positive, will correspond

to the difference between the required energy E_j and the maximum energy that the EV can charge by operating at the maximum power rate $\bar{P}_j$ after the potential reserve service provision:

$$\hat{E}(u_j, t) = \min \left[0, E_j - \left(\sum_{\tau=T_j^s}^{t-1} u_{j,\tau} \Delta t + \sum_{\tau=t+1}^{T_j^e} \bar{P}_j \Delta t \right) \right]. \tag{4.17}$$

To capture the sensitivity of the cost C in (4.15) with respect to the power profile u_j of the single EV, the gradient $\nabla_{u_j} C(u, u_j) = \left[\frac{\partial C(u,u_j)}{\partial u_{j,1}}, \ldots, \frac{\partial C(u,u_j)}{\partial u_{j,T}} \right]$ is considered. Recalling from (4.9) that the provided reserve $r_{j,t}(u)$ is equal to the power consumption $u_{j,t}$ when $j \in \mathcal{N}^{EV}$, the individual components of $\nabla_{u_j} C(u, u_j)$ have the following expression:

$$\frac{\partial C(u, u_j)}{\partial u_{j,t}} = \tilde{p}_{\mu_j,t}(u) - \tilde{\rho}_{\mu_j,t}(u) + \frac{\partial \psi(u_j)}{\partial u_{j,t}} \quad \forall j \in \mathcal{N}^{EV}. \tag{4.18}$$

Storage Devices: In the present modelling framework, no extra cost ψ is considered for storage, as no customer discomfort is associated to its final energy level. As a result, the cost C sustained by the storage device j only consists of the first two components in (4.15).

$$C(u, u_j) = \sum_{t=1}^{T} \left[\tilde{p}_{\mu_j,t}(u) \cdot u_{j,t} - \tilde{\rho}_{\mu_j,t}(u) \cdot r_{j,t}(u) \right] \quad \forall j \in \mathcal{N}^{S}. \tag{4.19}$$

The individual components of the gradient $\nabla_{u_j} C(u, u_j)$ have the following expression:

$$\frac{\partial C(u, u_j)}{\partial u_{j,t}} = \tilde{p}_{\mu_j,t}(u) - \sum_{s=t}^{T} \tilde{\rho}_{\mu_j,s}(u) \frac{\partial r_{j,s}(u)}{\partial u_{j,t}} \quad \forall j \in \mathcal{N}^{S}. \tag{4.20}$$

Note that the partial derivatives $\frac{\partial r_{j,s}(u)}{\partial u_{j,t}}$ appear in (4.20) only for $s \geq t$. This is because changes in $u_{j,t}$ at time t only modify the energy level $E_{j,s}$ in (4.6) for $s \geq t$. Consequently, the reserve values $r_{j,s}(u)$ in (4.11) will be affected by changes in $u_{j,t}$ only if $s \geq t$, implying that $\frac{\partial r_{j,s}(u)}{\partial u_{j,t}} = 0$ when $s < t$.

Remark 4.2. *In the present framework, it is assumed that the storage devices have full efficiency and no energy loss is associated to their charge/discharge operation. This assumption is to avoid the nonlinearity introduced by the partial efficiency of storage devices, simplifying the mathematical analysis. For more accurate results, the case of storage devices with partial efficiency can be easily accommodated using the analytical approach presented in Chapter 2.*

4.4.1 Flexible Demand Operation as Competitive Game

On the basis of the modelling analysis presented above, the operation of the flexible devices can be characterized as a competitive game with the following elements:

- *Players:* The set $\mathcal{N}$ of EVs and storage devices.
- *Strategies:* The set $\mathcal{U}_j$ of feasible power profiles for each device $j \in \mathcal{N}$.
- *Objective Functions:* The cost C for EVs and storage devices presented in (4.15) and (4.19), respectively.

In other words, the flexible devices can be considered as price-responsive rational players that schedule their power profiles to minimize their own costs, competing for power consumption at times with lower price $\tilde{p}(u)$ and for reserve allocation at times with higher rewarded price $\tilde{\rho}(u)$. The devices interact with each other through the changes in prices introduced by their aggregate power profile. Notice in fact that variations in the individual power profiles u_j modify the overall power schedule u and change the price signals $\tilde{p}(u)$ and $\tilde{\rho}(u)$ in (4.14). For example, all devices will try to consume more power at times when $\tilde{p}(u)$ is low. However, by doing so, they will increase u and induce higher prices.

4.4.2 Aggregative Equilibrium

The power profile u^* scheduled by the flexible devices should correspond to a stable market configuration that satisfies each individual price-responsive agent. Within the proposed game-based framework, this can be characterized as an aggregative equilibrium of the game described in Chapter 4.4.1.

Definition 4.1. *Consider a feasible power schedule u^* with $u_j^* \in \mathcal{U}_j, \quad \forall j$. This corresponds to an aggregative equilibrium if the following conditions hold:*

$$C(u^*, u_j^*) \leq C(u^*, u_j) \qquad \forall u_j \in \mathcal{U}_j, \quad \forall j \in \mathcal{N}. \tag{4.21}$$

Condition (4.21) implies that, at the equilibrium u^*, no device j can unilaterally reduce its individual cost by changing its scheduled power u_j^* into any other feasible profile u_j. This equilibrium solution, as achieved according to the iteration scheme later proposed, has the following additional fairness features:

- Each device cannot unilaterally reduce its cost.
- Equal devices are charged equal cost.
- Flexibility is rewarded: larger availability windows imply cheaper cost.

Similarly to Definition 2.2 and 3.2, the concept of aggregative equilibrium is considered instead of the classic Nash formulation. It is assumed that the strategy variation of agent j from u_j^* to some other u_j has a negligible impact on the overall schedule u^* (i.e. the first variable of the cost C) and therefore on the prices $\tilde{p}(u^*)$ and $\tilde{\rho}(u^*)$. In other words, all devices are assumed to be price-takers.

4.5 Distributed Control Strategy

In this section we propose a distributed scheme that, by iterated price broadcasts and independent power schedule updates by the flexible devices, converges to the aggregative equilibrium introduced in Definition 4.1. Convergence will be proved with Lyapunov methods, demonstrating that a certain function V is reduced at each schedule update. In the present analysis, the chosen V has the following expression:

$$V(u) = \varphi(\tilde{D}(u), \tilde{R}(u)) + \sum_{j \in \mathcal{N}^{EV}} \psi(u_j). \tag{4.22}$$

Note that V corresponds to the sum of the minimized operational cost φ and the EV discomfort ψ, thus representing a global cost index for the considered problem.

4.5.1 Elementary Power Swap

It is envisioned that the flexible devices sequentially update their power profile in response to price signals, with the objective of reducing their cost function. The fundamental power update operation of device j consists of a power swap of Δ power units from time $\underline{t}$ to time $\bar{t}$. Starting from an initial power schedule $u \in \mathcal{U}$, the updated global power profile u^+ after the swap will have the following expression:

$$u^+_{i,s} = \begin{cases} u_{i,s} - \Delta & \text{if} \quad i = j, \ s = \underline{t} \\ u_{i,s} + \Delta & \text{if} \quad i = j, \ s = \bar{t} \\ u_{i,s} & \text{otherwise} \end{cases} \tag{4.23}$$

If one denotes by $\hat{\mathbf{e}}_{j,t}$ the vector of the standard orthogonal basis associated to the components j and t of $\mathbb{R}^{NT}$, the following equivalent compact expression can be provided:

$$u^+ = u + \Delta \left(\hat{\mathbf{e}}_{j,\bar{t}} - \hat{\mathbf{e}}_{j,\underline{t}} \right) \tag{4.24}$$

For a certain power schedule $u \in \mathcal{U}$, the amount of power Δ that can be swapped by the single device $j \in \mathcal{N}$ is limited by the quantity δ, defined as follows:

$$\delta(u, j, \bar{t}, \underline{t}) = \min\left\{a(u, j, \bar{t}), b(u, j, \underline{t}), c(u, j, \bar{t}, \underline{t}), d(u, j, \bar{t}, \underline{t})\right\}. \tag{4.25}$$

Each of the four terms of the minimum function in (4.25) is now described in detail:

- *Maximum feasible power increase* at time $\bar{t}$:

$$a(u, j, \bar{t}) = \bar{P}_j - u_{j,\bar{t}} \tag{4.26}$$

- *Maximum feasible power decrease* at time $\underline{t}$:

$$b(u, j, \underline{t}) = \begin{cases} u_{j,\underline{t}} & \text{if } j \in \mathcal{N}^{EV} \\ u_{j,\underline{t}} - \underline{P}_j & \text{if } j \in \mathcal{N}^{S} \end{cases} \tag{4.27}$$

The bounds a and b ensure that u_j^+ in (4.23), i.e. the new power schedule of device j after the elementary swap, always fulfils the power bounds in (4.4) and (4.7) when $\Delta \leq a$ and $\Delta \leq b$.

- *Maximum feasible power swap* that fulfils energy constraints:

$$c(u, j, \bar{t}, \underline{t}) = \begin{cases} \bar{P}_j & \text{if } j \in \mathcal{N}^{EV} \\ \min\limits_{t \in \{\underline{t}, \ldots, \bar{t}-1\}} \dfrac{E_{j,t}}{\Delta t} & \text{if } j \in \mathcal{N}^{S},\ \underline{t} < \bar{t} \\ \dfrac{\bar{E}_j - \max_{t \in \{\bar{t}, \ldots, \underline{t}-1\}} E_{j,t}}{\Delta t} & \text{if } j \in \mathcal{N}^{S},\ \bar{t} < \underline{t} \end{cases} \tag{4.28}$$

By imposing $\Delta \leq c$, the energy constraint in (4.7) is also fulfilled. For example, in the second case in (4.28), it is ensured that the minimum energy level of the storage device j between $\underline{t}$ and $\bar{t} - 1$, which is lowered by $c\Delta t$ as a result of the power swap, remains above the minimum zero value. The third case in (4.28) fulfils a similar purpose when $\bar{t} < \underline{t}$ and the state of charge of the storage is increased between $\bar{t}$ and

$\underline{t}-1$. Since no energy constraints are considered when $j \in \mathcal{N}^{EV}$, in the first case in (4.28) c corresponds to the maximum power $\bar{P}_j$.

- *Maximum cost-reducing power swap.*

The last term d in (4.25) ensures that $\Delta > 0$ only if the associated power swap reduces the cost of the individual device. This term can generally be defined as follows:

Proposition 4.1. *For all $j \in \mathcal{N}$, $(\bar{t}, \underline{t}) \in \mathcal{A}_j \times \mathcal{A}_j$, $u \in \mathcal{U}$, there exists $d(u, j, \bar{t}, \underline{t}) \geq 0$ such that, for any $\Delta \in [0, d(u, j, \bar{t}, \underline{t})]$, the following conditions hold:*

$$d(u, j, \bar{t}, \underline{t}) = 0 \quad \Longleftrightarrow \quad \nabla_{u_j} C(u, u_j) \left(\hat{\mathbf{e}}_{j,\bar{t}} - \hat{\mathbf{e}}_{j,\underline{t}} \right) \geq 0 \tag{4.29a}$$

$$C\left(u, u_j^+\right) - C(u, u_j) = \nabla_{u_j} C(u, u_j) \left(\hat{\mathbf{e}}_{j,\bar{t}} - \hat{\mathbf{e}}_{j,\underline{t}} \right) \Delta \tag{4.29b}$$

$$\exists\, \alpha > 0 : V(u^+) - V(u) = \nabla_{u_j} C(u, u_j) \left(\hat{\mathbf{e}}_{j,\bar{t}} - \hat{\mathbf{e}}_{j,\underline{t}} \right) \alpha \tag{4.29c}$$

Proof. See Appendix C.1. □

Condition (4.29a) imposes that d is positive (and therefore a power swap is performed by device j between times $\underline{t}$ and $\bar{t}$) only when the gradient of C is negative. This means that also the cost variation $C\left(u, u_j^+\right) - C(u, u_j)$ is negative, as established in (4.29b). Finally, (4.29c) ensures that the variations of C and V caused by the power swap have the same sign.

4.5.2 Coordination Algorithm

The proposed coordination strategy is described in Algorithm 3, which includes three main phases. In the **Initialization phase**, the power schedule of the devices is initialized to some arbitrary $u^{(0)} \in \mathcal{U}$. Two additional variables are also initialized:

k keeps track of the number of iterations in the algorithm, whereas the flag variable *conv* indicates whether an equilibrium has been reached and the update iterations can thus be terminated. In the **Power scheduling update**, the execution of a **FOR** cycle corresponds to a sequential strategy update by all devices, from $j = 1$ to $j = N$. After the update in step 2.a) of the relevant indexes, in step 2.b.i) the individual device j performs its strategy update by selecting a pair of time instants $(\bar{t}, \underline{t})$ that maximize the (non-negative) function δ and therefore are potentially associated to a cost-reducing power swap. This power swap is then performed in step 2.b.ii), where the power schedule u_j is updated. Finally, step 2.c.iii) is set to 0 if the current δ is greater than zero, to signal that the devices are still improving their strategy and convergence has not been reached yet. When the non-negative δ maximized in step 2.b.i) is equal to zero for all loads, the variable *conv* remains equal to one throughout the whole **FOR** cycle and the **Final results** phase is reached, returning the desired equilibrium solution u^*.

Algorithm 3 Iterative scheme - Flexible device coordination

1. **Initialization phase.** Set:

$$u_j(0) \leftarrow u_j^{(0)} \in \mathcal{U}_j \quad \forall j \qquad k \leftarrow 0 \qquad conv \leftarrow 0$$

2. **Power scheduling update**

   WHILE $(conv = 0)$

   (a) $conv \leftarrow 1 \qquad k \leftarrow k + 1 \qquad u(k) \leftarrow u(k-1)$.

   (b) **FOR** $j = 1 : 1 : N$

   i. $(\bar{t}, \underline{t}) \leftarrow \arg\max_{t_1, t_2} \delta(u(k), j, t_1, t_2)$

   ii. $u_{j,\bar{t}}(k) \leftarrow u_{j,\bar{t}}(k) + \delta(u(k), j, \bar{t}, \underline{t})$
   $u_{j,\underline{t}}(k) \leftarrow u_{j,\underline{t}}(k) - \delta(u(k), j, \bar{t}, \underline{t})$

   iii. **IF** $\delta(u(k), j, \bar{t}, \underline{t}) > 0 \;\; : \;\; conv \leftarrow 0$.

   END FOR

   END WHILE

3. **Final results**. The power schedule at the last iteration corresponds to the aggregative equilibrium:

$$u^* \leftarrow u(k).$$

The convergence and optimality of the proposed coordination scheme are now formally demonstrated.

Theorem 4.1. *Under Assumption 4.1, for any population $\mathcal{N}$ of flexible devices operating in the power system, Algorithm 3 asymptotically converges to an aggregative equilibrium u^*.*

Proof. See Appendix C.2. □

Theorem 4.2. *The final aggregative equilibrium u^* is a global minimizer of the function V:*

$$V(u^*) \leq V(u) \qquad \forall u \in \mathcal{U}. \tag{4.30}$$

Proof. See Appendix C.3. □

From these results, we can conclude that the coordination scheme returns a power schedule u^* which corresponds to a stable market configuration (i.e. an aggregative equilibrium). Recalling that V can be interpreted as a global cost index, it follows that u^* also represents a socially optimal solution for the coordination problem of flexible devices.

4.5.3 Practical Implementation

The proposed algorithm can be implemented in a distributed manner, assuming that each appliance is equipped with a smart controller and can receive price signals from a central entity. Such implementation is discussed for each of the three main phases of Algorithm 3.

1. **Initialization phase**: Each device j determines an initial feasible power profile $u_j(0) \in \mathcal{U}_j$. This can be induced in a distributed way by broadcasting some initial prices p_0 and ρ_0 and letting each device schedule its power profile $u_j(0) = u_j^0$, with

the objective to minimize its cost $C(u, u_j)$ in (4.15) or (4.19). The resulting power profiles $u_j(0)$ and the associated allocated reserve $r_j(u(0))$ of each device j are then communicated to the central entity, which can calculate the corresponding aggregate demand $D(u(0))$ and reserve $R(u(0))$ through (4.12) and (4.13). Resolution of the OPF problem (4.1)-(4.2) allows to derive the associated prices $\tilde{p}(u(0))$ and $\tilde{\rho}(u(0))$ through (4.3) and (4.14).

2. **Power scheduling update**: Each iteration of the **WHILE** cycle in Algorithm 3 can be implemented as follows:

   - The signals $\tilde{p}_{\mu_j}(u(k))$ and $\tilde{\rho}_{\mu_j}(u(k))$, i.e. the prices of energy and reserve at bus $m = \mu_j$ where device j operates, are broadcast to device j. In response to these prices, the device j selects the pair of time instants $(\bar{t}, \underline{t})$ that maximize the non-negative function δ (step 2.b.i)). The power amount δ is then shifted from time $\underline{t}$ to $\bar{t}$ (step 2.b.ii)), leading to a reduction of the energy cost C.
   - After the power swap, the device j communicates the changes of its power profile $u_j(k)$ and reserve amount $r_j(u(k))$ to the central entity, which updates the overall power schedule $u(k)$ and the prices $\tilde{p}_{\mu_j}(u(k))$ and $\tilde{\rho}_{\mu_j}(u(k))$ accordingly. The updated prices are then broadcast to the next device $j + 1$ and the operations described above are repeated.
   - After all the devices have updated their schedule once (corresponding to the completion of **FOR** cycle in step 2.b)), the iteration number k is increased by one (step 2.a)), and the next iteration is performed.

3. **Final results**: As demonstrated in the proof of Theorem 4.1, after a finite number of iterations, the maximized quantity $\delta(u(k), j, \bar{t}, \underline{t})$ is equal to zero and no advantageous power swap can be performed between $\underline{t}$ and $\bar{t}$. This implies that an equilibrium is reached and the algorithm is terminated. The final power schedule u^* will be equal to $u(k)$ at the last iteration k.

The information exchanged at each algorithm iteration k is summarized in Table

4.1. It can be seen that all the devices communicate with the central entity once at a single iteration. For a single device j, the central entity broadcasts the signals of energy price and reserve price to it, and then the device performs a power swap to reduce its cost in response to the price signals. The information of the changes in its power profile and reserve provision caused by the power swap is then returned to the entity which then updates the prices accordingly. When no device can perform a feasible power swap to reduce its cost after a finite number $k = K$ of iterations, the coordination algorithm terminates, and there are $K \cdot N$ times of information exchanged between the central entity and the devices.

Table 4.1: Communication between flexible devices and central entity at an iteration k of Algorithm 3.

k-th iteration	Information from entity to device j	Information from device j to entity
Device 1	Energy price and reserve price (after power swap of device N)	Changes in power and reserve amount caused by power swap of device 1
Device 2	Updated energy price and reserve price after power swap of device 1	Changes in power and reserve amount caused by power swap of device 2
Device 3	Updated energy price and reserve price after power swap of device 2	Changes in power and reserve amount caused by power swap of device 3
⋮	⋮	⋮
Device N	Updated energy price and reserve price after power swap of device $N-1$	Changes in power and reserve amount caused by power swap of device N

4.6 Computation Performance of Proposed Approach

In the case study presented in Chapter 4.7, a centralized approach would require the resolution of an optimization problem with a number of variables greater than $N \cdot T = 37,800 \cdot 48 = 1,814,400$. It is easy to see how this centralized formulation would

quickly become unsolvable for larger systems. On the other hand, by considering a distributed framework where each individual device operates independently in response to price signals, the proposed approach envisages the separate resolution of N smaller sub-problems, each with a much smaller number T of decision variables.

In relation to this point, it is worth discussing the computational complexity and the scalability of the proposed approach. The coordination algorithm presented in this work envisages sequential updates of the operational strategy by each individual device, in response to updated price signals. With the proposed approach, the time required to calculate the equilibrium solution is fundamentally linear with respect to the number $|\mathcal{N}|$ of smart controlled devices. In relation to this point, we wish to emphasize that this basic sequential approach has been chosen to facilitate the presentation of the proposed methodology and the subsequent theoretical analysis (i.e. the convergence and optimality results of Theorem 4.1 and 4.2). However, faster convergence and improved scalability can be obtained with some adjustments to the coordination algorithm. For example:

- **Simultaneous power updates by multiple devices**: instead of updating and broadcasting new price signals to a single device at each strategy update, a subset of devices can use the same price signal and modify their power profiles at once. This would reduce the number of required iterations and further enhance the scalability of the proposed method. Numerical convergence of this alternative method has been verified in simulation.

- **Jacobi iterative methods**: all devices (iteratively) update their operational strategies at once. Such schemes have been applied, for example, to the problem of EV charging coordination with no provision of ancillary services [32], [62]. With this approach, the convergence speed would still depend on the number of controlled devices, but the bi-directional exchange of information would be reduced.

- **One-shot strategy**: the central entity internally emulates the proposed coordination algorithm and then performs a one-shot broadcast of the final price signal, in order to directly induce the associated equilibrium solution. This scheme, initially presented in [24] for the simpler case of smart appliances not providing ancillary services, assumes that the central coordinator would possess some general knowledge of the devices' population, based for example on estimations or on historical data.

4.7 Simulations

4.7.1 System Model and Parameters

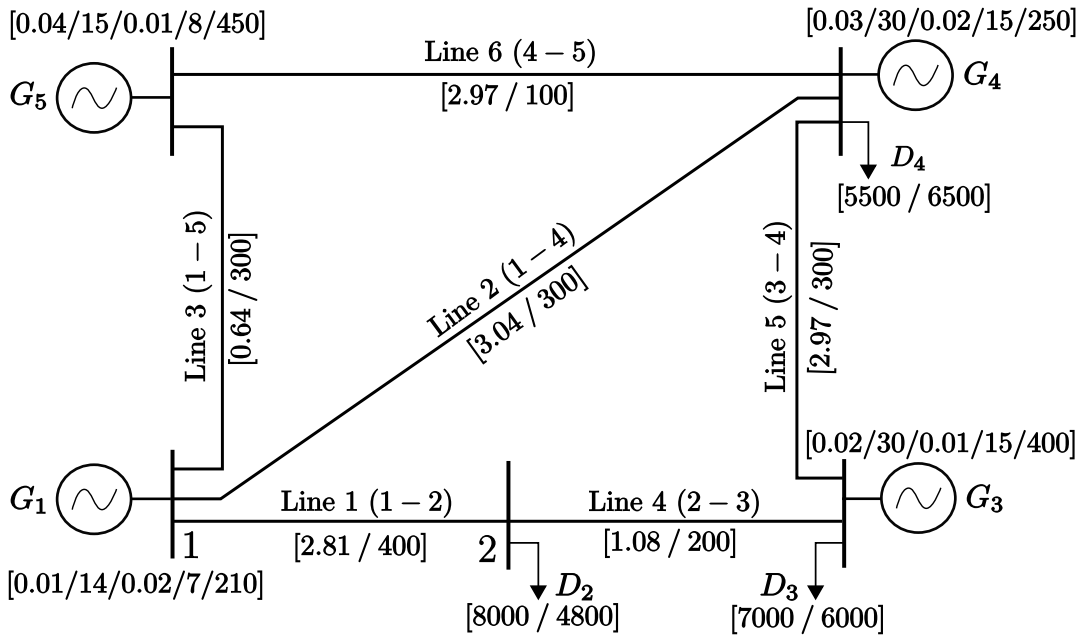

Parameters of Transmission Line l $(s(l)-r(l))$**:**
[*Reactance* X_l (p.u.) / *Capacity* $\bar{F}_l(MW)$]

Parameters of Generator m**:**
[*Quadratic coefficient* a_m $(\$/MW^2h)$ / *Linear coefficient* b_m $(\$/MWh)$/
Quadratic coefficient c_m $(\$/MW^2h)$ / *Linear coefficient* d_m $(\$/MWh)$ / *Capacity* $\bar{G}_m$ (MW)]

Parameters of Demand m**:**
[*EV number* $|\mathcal{N}_m^{EV}|$ / *Storage number* $|\mathcal{N}_m^{S}|$]

Figure 4.1: The PJM 5-bus system.

The proposed coordination algorithm is tested on the PJM 5-bus system [63] in Fig. 4.1. A time interval of $T = 24$h is considered, with time discretization $\Delta t = 0.5$h. The generation and reserve cost functions are assumed to be quadratic, i.e. $f_m^G(x) = \frac{1}{2}a_m x^2 + b_m x$ and $f_m^R(x) = \frac{1}{2}c_m x^2 + d_m x$. Relevant generation and transmission parameters are presented in Fig. 4.1. To fulfill the reserve service requirement (4.2d), the total allocated reserve must be greater than or equal to $\Delta G_L^{max} = \bar{G}_5 = 450$MW. Inflexible demand d_m at buses $m = 2, 3, 4$ has been derived from historical data [64]. As for flexible devices, we consider a population of EVs $\mathcal{N}_m^{EV}$ and storage batteries $\mathcal{N}_m^S$ at buses $m = 2, 3, 4$, with $\mathcal{N}^{EV} = \mathcal{N}_2^{EV} \cup \mathcal{N}_3^{EV} \cup \mathcal{N}_4^{EV}$ and $\mathcal{N}^S = \mathcal{N}_2^S \cup \mathcal{N}_3^S \cup \mathcal{N}_4^S$. A description of the two types of devices is provided below:

EVs: The required energy amount E_j for the EV j at bus m is determined according to a Gaussian distribution with mean value β_m^E and a standard deviation ω_m^E. Additionally, the rated power $\bar{P}_j$ is set to the same value $\bar{P}_j = 11$kW for all $j \in \mathcal{N}^{EV}$. Relevant parameters are listed below:

$$\beta_2^E = \beta_3^E = \beta_4^E = 30 \text{ kWh}$$

$$\omega_2^E = 1.0 \text{ kWh} \qquad \omega_3^E = 1.5 \text{ kWh} \qquad \omega_4^E = 1.5 \text{ kWh}.$$

It is assumed that each EV j at node m must complete its charging within a continuous time interval $[t_j, t_j + d_j]$. The start time t_j and the duration d_j also follow Gaussian distributions, with mean β_m^t and β_m^d and standard deviations ω_m^t and ω_m^d, respectively:

$$\begin{array}{llll} \beta_2^t = 20{:}30 \text{ h} & \omega_2^t = 1.5 \text{ h} & \beta_2^d = 10 \text{ h} & \omega_2^d = 1.0 \text{ h} \\ \beta_3^t = 21{:}30 \text{ h} & \omega_3^t = 1.5 \text{ h} & \beta_3^d = 11 \text{ h} & \omega_3^d = 2.0 \text{ h} \\ \beta_4^t = 21{:}00 \text{ h} & \omega_4^t = 1.0 \text{ h} & \beta_4^d = 11 \text{ h} & \omega_4^d = 1.5 \text{ h} \end{array}$$

Accordingly, the availability time interval $\mathcal{A}_j$ of EV j can be expressed in the discretized time horizon as:

$$\mathcal{A}_j = \{T_j^s, T_j^s + 1, \ldots, T_j^e\} = \{t \in \mathcal{T} : t_j \leq t \cdot \Delta t \leq t_j + d_j\}.$$

Storage Devices: An homogeneous population of storage batteries is considered,

with the following parameters:

$$\bar{P}_j = -\underline{P}_j = 2.5 \text{ kW} \qquad \bar{E}_j = 25 \text{ kWh} \qquad \forall j \in \mathcal{N}^S.$$

The total installed storage capacity is equal to $\bar{E}_j \cdot |\mathcal{N}^S| = 432.5$ MWh. The initial energy levels $E_{j,0}$ are determined stochastically, according to a uniform distribution with support $[0, \bar{E}_j]$.

4.7.2 Algorithm Implementation and Results

In the **Initialization phase** of Algorithm 3, the initial power schedule $u_j^{(0)} \in \mathcal{U}_j$ is chosen as a constant power profile over the availability interval $\mathcal{A}_j$ when $j \in \mathcal{N}^{EV}$ and is identically equal to zero when $j \in \mathcal{N}^S$. The **WHILE** cycle in the **Power scheduling update** phase is iterated $k = 15$ times in order to converge to the final equilibrium solution $u(n) = u^*$. This implies that $15N = 15 \cdot 37,800 = 567,000$ times of communication have occurred between the central entity and the flexible devices. Simulations have required about 90 minutes on a standard PC machine with a 4-core 2.40 GHz Intel(R) Xeon(R) E5620 processor and 12 GB of RAM. The final results are compared to a No-Flexibility scenario (denoted as **NF**), where the devices do not react to price signals, do not provide reserve and simply apply the initial power schedule $u^{(0)}$.

Fig. 4.2 compares the electricity price profiles (left) and the power demand (right) obtained with the proposed algorithm and in the **NF** scenario. It can be seen that prices are different at each node and are generally flattened when the proposed coordination scheme exploits the flexibility offered by EVs and storage. It is interesting to note that, at bus 2, the price $\tilde{p}_{2,t}$ is lower than $p_{2,t}^{NF}$ also during the first hours of the day, when the demand $\tilde{D}_{2,t}$ is higher than $D_{2,t}^{NF}$. This is due to the interplay between demand D and allocated reserve R in the price expressions (4.3) and the fact that, in the **NF** scenario, EVs and storage do not provide any reserve, thus indirectly impacting also electricity prices. A similar flattening trend can be seen in the demand profiles: when the equilibrium schedule u^* is applied, a substantial

peak-shaving/valley-filling is introduced. From the disaggregation of flexible demand $\tilde{D}(u^*)$ in its components $\tilde{D}^S(u^*)$ (from storage) and $\tilde{D}^{EV}(u^*)$ (from EVs), it can be seen that the electric vehicles schedule their charge during night-time, when electricity prices are lower. Similarly, the storage devices perform energy arbitrage by charging during night time and discharging at peak times.

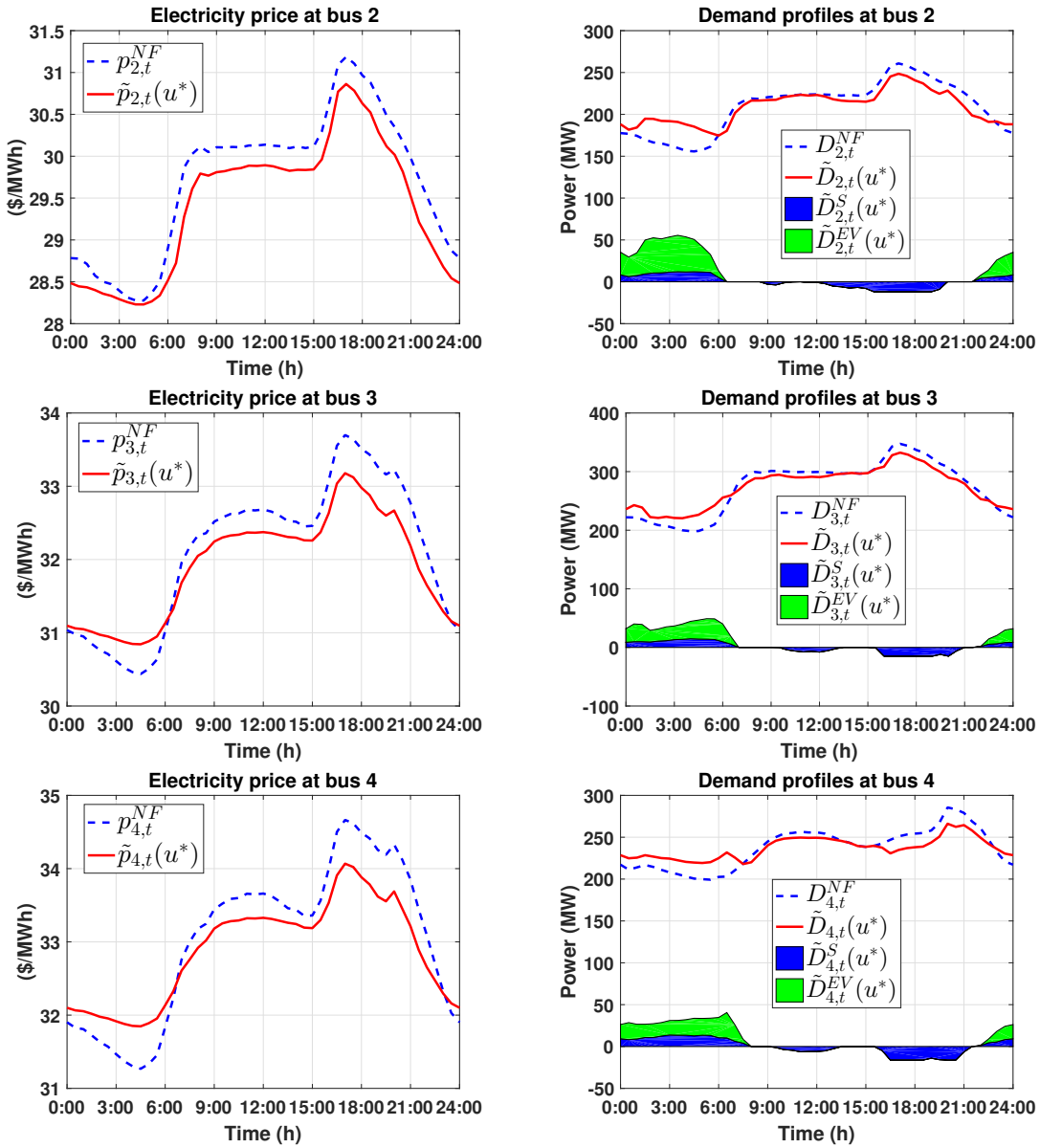

Figure 4.2: Electricity prices (left) and demand profiles (right) at each bus, when the **NF** scenario (blue dashed lines) and the proposed solution (red lines) are considered. For the latter, the coloured areas represent the net power contribution of storage (blue) and EVs (green).

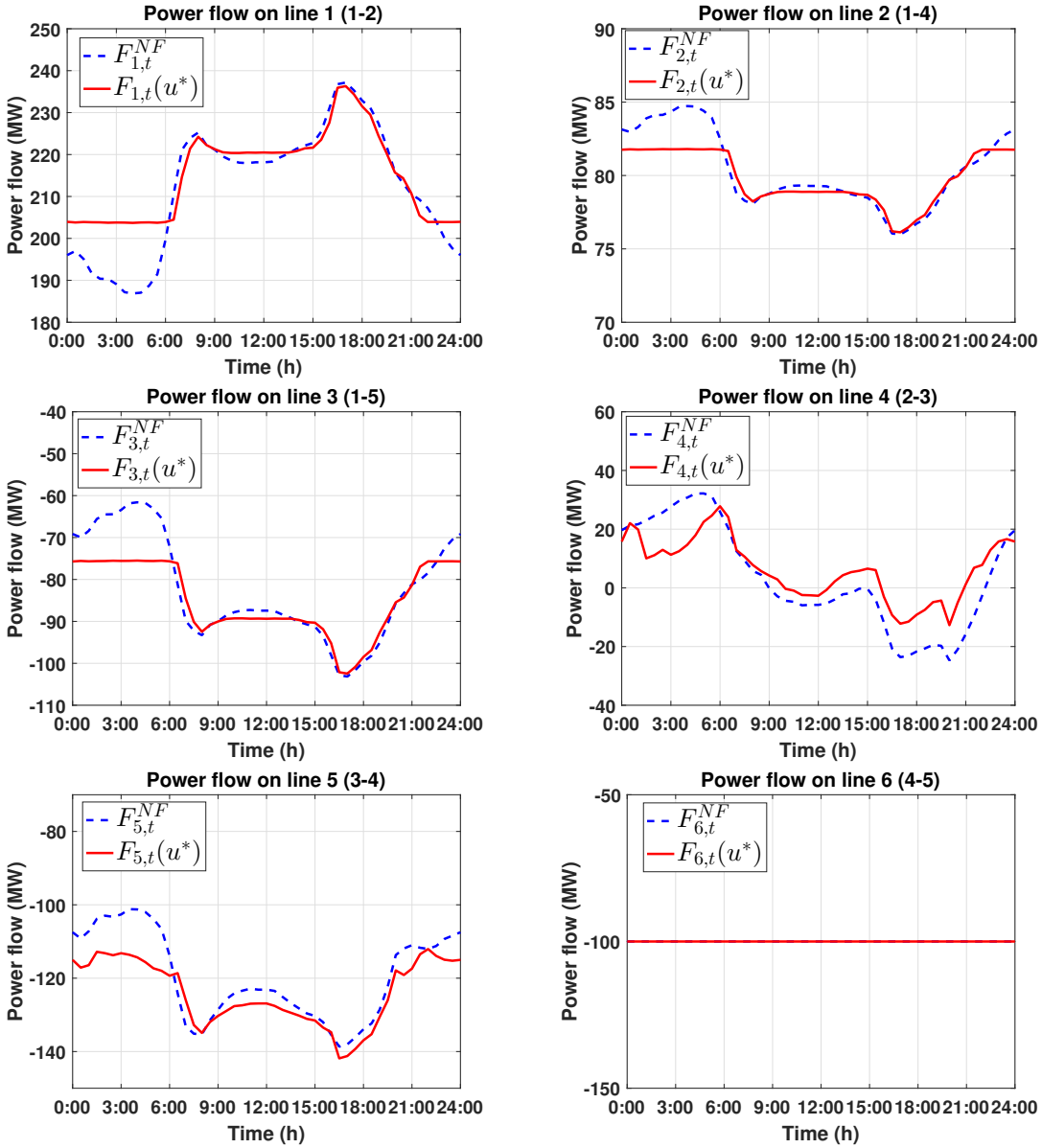

Figure 4.3: Power flows on the transmission lines when the **NF** scenario (blue dashed lines) and the proposed solution (red lines) are considered.

The power flows $F(u^*)$ and F^{NF}, obtained respectively with the proposed algorithm and in the No-Flexibility scenario, are compared in Fig. 4.3. The negative values on some of the lines indicate that power is flowing in the direction opposite to the conventional one considered on the line. For example, the negative values of $F_5(u^*)$ and F^{NF}_5 indicate that the power on line 5 is flowing from node 4 to node 3. A trend similar to the one for demand profile can be seen: the proposed algorithm is able to reduce the variation over time of the power flow. Note also that line 6 remains

congested and operates at its maximum capacity 100MW over the whole considered period of 24h. This leads to different locational marginal prices throughout the network, as shown in Fig. 4.2.

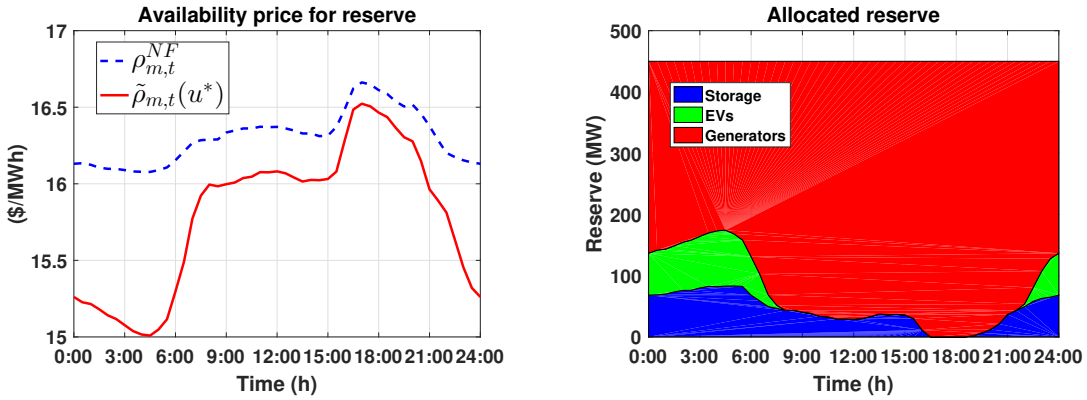

Figure 4.4: Reserve price (left) and allocated reserve (right).

Fig. 4.4 compares the prices for reserve provision at the final equilibrium solution and in the **NF** scenario (left) and shows the disaggregation of allocated reserve from different sources (right) when the considered algorithm is applied. Note that the reserve price $\tilde{\rho}_{m,t}(u^*)$ obtained with the proposed control strategy is always lower than the price $\rho^{NF}_{m,t}$ in the **NF** scenario. This is to be expected since, by providing reserve, the flexible devices reduce the marginal value (i.e. the price) of additional units of reserve. In the right part of Fig. 4.4, it can be seen how the EVs mostly provide reserve during the early hours of the day (when they are charging and therefore are available to reduce their power consumption). Conversely, the contribution of storage covers almost the whole day, with the exception of the interval between $t = 16:00$h and $t = 21:00$h, when the batteries are mostly discharging.

The power production and allocated reserve of the generators are shown in Fig. 4.5. Note that the capacity of the generator at bus 1 is fully allocated to power production (no reserve is provided). For the generators at the other buses, when Algorithm 3 is applied there is a reduction of reserve and an increase of power production during the early hours of the day (to accommodate the higher demand

from flexible devices).

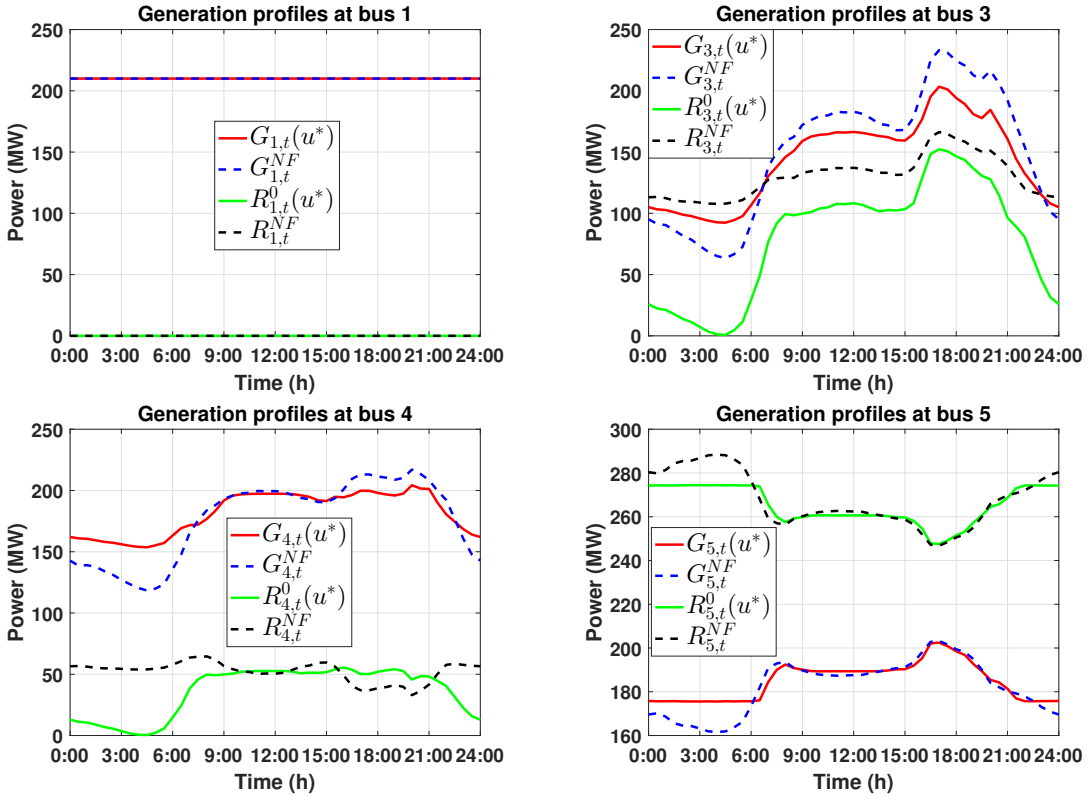

Figure 4.5: Power production and allocated reserve at each bus.

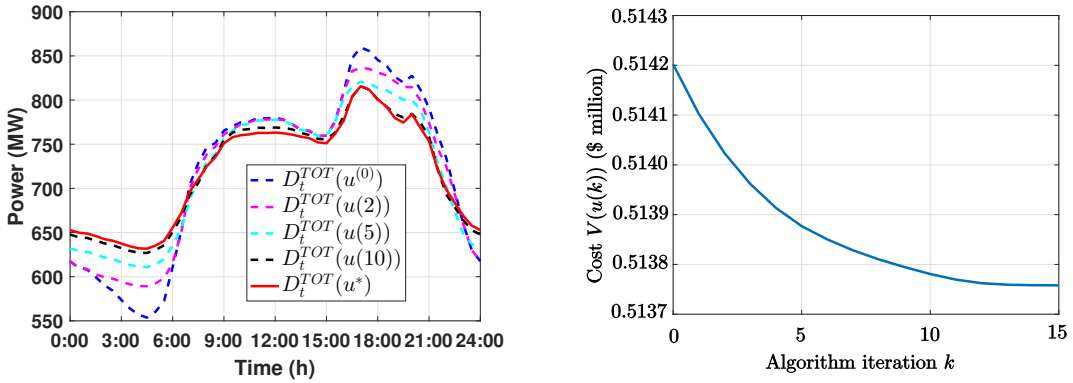

Figure 4.6: Comparison of total demand profiles (left) and global cost $V(u(k))$ as a function of the algorithm iteration k (right).

Finally, Fig. 4.6 evaluates the convergence of Algorithm 3 and its performance from a system perspective. On the left, the aggregate demand profiles $D_t^{TOT}(u(k)) = \sum_{m=1}^{M} \tilde{D}_{m,t}(u(k))$ – at different iterations k – are shown. It can be seen how the proposed sequential power swaps from the EVs and storage gradually flatten the

demand profile, consistently with the trends shown in Fig. 4.2. The right part of Fig. 4.6 shows the values of the function $V(u(k))$ in (4.22) at each algorithm iteration k. Note that $V(u(k))$ is reduced at each step and reaches a minimum at $k = 15$, as established in Theorem 4.2. From previous considerations, V represents a global cost index of the system, implying that the final equilibrium solution of the proposed algorithm is also socially optimal.

Table 4.2: Daily costs sustained by generators and single EV/storage devices in the **NF** scenario and with the proposed algorithm.

Scenario	No Flexibility (**NF**)			Proposed algorithm		
Cost ($)	Total	Energy	Reserve	Total	Energy	Reserve
Generation	$5.402 \cdot 10^5$	$4.118 \cdot 10^5$	$1.284 \cdot 10^5$	$5.133 \cdot 10^5$	$4.107 \cdot 10^5$	$1.026 \cdot 10^5$
EVs	0.92	0.92	0	0.47	0.91	-0.46
Storage	0	0	0	-0.96	-0.03	-0.93

A comparison of the daily costs sustained by generation and individual flexible devices under the **NF** scenario and with the proposed control strategy is presented in Table 4.2. From a generation perspective, it can be seen that our algorithm reduces total costs by approximatively 5%, with particularly lower costs for reserve allocation. It should be emphasized that the comparison does not consider the payments made in the proposed coordination scheme to EVs and storage for reserve allocation, which in the present case amount to \$25, 519 . From an EV perspective, it can be seen that total costs are halved with our control scheme: this is the result of substantial revenues for reserve allocation and a marginal reduction in the electricity costs. In this respect, note that the average total cost for single EV is not equal to the sum of the energy and reserve components, as EVs also incur in an average discomfort cost of \$0.02, as defined in (4.16). Regarding storage, this is assumed not to operate and have zero costs in the **NF** scenario. When the proposed algorithm is applied, as in the EV case, storage will obtain most of its revenues for reserve allocation. It is interesting to notice that low revenues from

energy arbitrage are caused by the flexible devices themselves, which tend to flatten the demand/price profiles and therefore reduce the price differentials that can be exploited for advantageous charge/discharging by the batteries.

4.8 Summary

This chapter presents a novel game-theoretic scheme for coordination of price responsive flexible devices operating in an integrated energy-reserve market. The proposed algorithm ensures the convergence to a stable market configuration which is also globally optimal, for any grid topology and penetration level of demand response. The algorithm is tested in simulation on the PJM 5-bus system, demonstrating its capability to flatten generation and demand profiles at each node while reducing the operational costs of the system.

Chapter 5

Conclusions and Future Work

5.1 Conclusions

Table 5.1: Comparison of different chapters

	Chapter 2	Chapter 3	Chapter 4
Object of study	Micro-storage devices	Flexible loads	Micro-storage devices and flexible loads
Whether considering network topology	No	Yes	Yes
Whether considering power losses	Yes	No	No
Whether considering ancillary services	No	No	Yes
Market clearing	Assuming price monotone increasing with demand	LMPs associated to a linearized ACOPF problem	LMPs associated to a DCOPF problem
Price signal	Energy price	Energy price	Energy price and reserve price

The penetration of flexible devices such as micro-storage devices and electric vehicles is increasing the flexibility of demand side. In order to coordinate these devices, this

thesis proposes novel distributed schemes using game-theoretical frameworks. In the frameworks, the flexible devices are modelled as self-interested players that aim at minimizing their individual costs in response to iterative broadcast price signals. The devices are coordinated through iterative algorithms, which converge to stable configurations (characterized as aggregative equilibria) where no device can further reduce its cost by unilaterally changing its power scheduling. The studies in Chapter 2, 3 and 4 are summarised in Table 5.1.

In Chapter 2, we analyse the coordination of large populations of micro-storage devices under a whole system framework (without considering network topology). The electricity price is assumed to be a monotone increasing function of total demand. Two main aspects have been considered: the bidirectionality of power flows and power losses. Power losses limiting storage efficiency are expressed as fractions of the exchanged power, with a charging coefficient and a discharging coefficient. The strategy update of storage devices is charaterized as a multi-valued mapping. It is demonstrated that the proposed scheme converges an aggreagtive equilibrium (at which each storage device minimizes its energy cost) and achieves global optimility (minimizing total generation costs). Meanwhile the peaks and valleys of the total demand profile are shaved and filled, respectively.

In Chapter 3, we investigate the coordination of flexible loads while expanding the work in Chapter 2 to take into account network topology. Because of the presence of network topology, the LMP of electricity at each bus is used as the price signal, instead of simply assuming like Chapter 2 that the electricity price is some monotone increasing function of total demand. The LMPs (generally different at different buses) correspond to the Lagrange multipliers associated to a linearized AC optimal power flow problem. Furthermore, we introduce a double pricing structure and a novel variation equilibrium to solve the problem of discontinuous LMPs. The iterative scheme for flexible demand coordination is analytically characterized as a multi-valued mapping. Its convergence to a stable market configuration (i.e.,

variational equilibrium) and global optimality are analytically demonstrated, for any penetration level of flexible demand and any grid topology. The simulations have verified that the proposed coordination strategy ensures flattened generation profile at each bus, reduced variations over time of power flow and minimized total generation costs.

In Chapter 4, we propose a novel coordination scheme for both micro-storage devices and flexible loads operating in an integrated energy-reserve market. Differently from previous chapters, these devices can also earn reserve revenue by being available to reduce their power consumption. In this case, we design a multi-price setup that includes energy price and reserve price. The price signals are obtained through the resolution of a DC optimal power flow problem that explicitly takes into account the impact of demand response on the optimal power dispatch and reserve procurement of generators. To simplify the mathematical analysis, it is assumed that the storage devices have full efficiency, rather than the partial efficiency considered in Chapter 2. The performance of the coordination scheme has been evaluated in simulations, demonstrating its capability to minimize the cost of flexible devices, flatten demand profiles and reduce the costs of generators.

5.2 Comparison with Centralized Approaches

Differently from centralized approaches, the proposed approaches in this thesis utilize a multi-agent framework which is a distributed approach. The coordination schemes assume that each flexible load and storage device can independently schedule its operational strategy in response to external price signals, with the unique objective of minimizing its own cost function. This framework exhibits relevant potential advantages with respect to centralized approaches:

- **Less computation**: the distributed approaches are able to break down the

complex task of coordinating large number of flexible devices into smaller sub-problems that are easier to solve. However, for centralized approaches, the resulting optimization problem would be extremely large and include a very high number of decision variables.

- **Economic optimality for single devices**: the final equilibrium solution obtained with the proposed schemes ensure cost minimization for each individual device, which cannot further reduce its energy cost by unilaterally changing its strategy. This might not be the case when using centralized approaches, since they will generally optimize only the overall operation of the devices' population.

- **Full control of the devices**: with the proposed approaches, customers preserve full control of their devices, whose operation is not determined by external entities.

- **Privacy:** the envisioned distributed structure of the coordination algorithm preserves the privacy of the customers. If the initial aggregate demand profile is known (or estimated), the coordination algorithm only requires the communication of the strategy changes adopted at each iteration by the agents, rather than their full power consumption profiles.

5.3 Future Work

Future work will focus on the following directions.

- The work in this thesis only considers the impact of price-responsive devices on the transmission infrastructure. Future work will try to build a bi-level optimization model to also account for the effect of flexible devices on distribution networks. The approach proposed by [41] that involves both transmission and distribution networks will initially be investigated. A theoretical study will

also be conducted, evaluating whether the presented results of convergence and optimality can be extended to a double-level network topology which accounts for transmission and distribution at the same time.

- Future work would expand the existing framework to conduct a stochastic optimization, which explicitly models and accounts for uncertainties on demand, generation and price. To do this, some relevant work could be first studied. For example, the work in [65] represents price uncertainty by means of scenarios when coordinating EVs. Generation uncertainty is considered in [66] to construct stochastic unit commitment and reserve scheduling problems.

- Instead of using DCOPF and linearized ACOPF model, future work will consider more complex models, e.g. a probabilistic security-constrained AC optimal power flow that guarantees N-1 security [67] or a security-constrained unit commitment (SCUC) model that determines the committed generation. In the SCUC model, some other relevant factors of individual unit operating constraints are included, such as ramping constraint and start-up cost. The SCUC problem belongs to a mixed-integer non-linear programming (MINLP) problem. In addition, multiple generation technologies such as nuclear, wind, open cycle gas turbines (OCGT) and combined cycle gas turbines (CCGT) could be also considered in the complex models.

- Flexible devices can provide not only spinning reserve but also some additional ancillary services (e.g. frequency control and non-spinning reserve). In this case, the flexible devices will respond to multiple prices and consequently the coordination scheme becomes more complex. The prices of ancillary services need to be calculated through building a proper model. Future work will focus on designing coordination schemes for flexible devices operating in the markets where they could contribute to several kinds of ancillary services, and evaluating whether the presented results of convergence and optimality still hold.

- In addition to coordinating flexible devices, future work will also manage distributed energy source generations (e.g. wind [68, 69] and solar energy) to achieve some objectives. This involves the concept of virtual power plants (VPPs). A VPP consists of a central IT control system and an integration of several power sources (such as distributed energy sources, flexible power consumer and batteries). VPP aims to operate these power sources as a unique plant and dispatches them through the central control system to trade energy in wholesale electricity market and provide ancillary services for system operation. The heart of a VPP is an energy management system (EMS) which coordinates the power flows coming from the generators, controllable loads and storages [70].

- All the proposed distributed algorithms in the thesis require a central entity to update the prices and broadcast them to individual devices. Future work will explore decentralized algorithms to coordinate the flexible devices. These algorithms belong to distributed algorithms, but they are tailored to the applications without a central authority, and communication is only limited among agents considered as neighbors.

Bibliography

[1] ABB. What is a smart grid. [Online]. Available: http://new.abb.com/smartgrids/what-is-a-smart-grid

[2] S. Rahman and G. Shrestha, "An investigation into the impact of electric vehicle load on the electric utility distribution system," *IEEE Transactions on Power Delivery*, vol. 8, no. 2, pp. 591–597, 1993.

[3] K. Clement-Nyns, H. Edwin, and J. Driesen, "The impact of charging plug-in hybrid electric vehicles on a residential distribution grid," *IEEE Transactions on Power Systems*, vol. 25, no. 2, pp. 371–380, 2010.

[4] G. Strbac, "Demand side management: Benefits and challenges," *Energy policy*, vol. 36, no. 2, pp. 4419–4426, 2008.

[5] M. H. Albadi and E. F. El-Saadany, "A summary of demand response in electricity markets," *Electric Power Systems Research*, vol. 78, no. 11, pp. 1989 – 1996, 2008.

[6] T. Wu, M. Rothleder, Z. Alaywan, and A. Papalexopoulos, "Pricing energy and ancillary services in integrated market systems by an optimal power flow," *IEEE Transactions on Power Systems*, vol. 19, no. 1, pp. 339–347, 2004.

[7] R. Fernańdez-Blanco, J. M. Arroyo, and N. Alguacil, "Network-constrained day-ahead auction for consumer payment minimization," *IEEE Transactions on Power Systems*, vol. 29, no. 2, pp. 526–536, 2014.

[8] N. Amjady, J. Aghaei, and H. Shayanfar, "Market clearing of joint energy and reserves auctions using augmented payment minimization," *Energy*, vol. 34, no. 10, pp. 1552–1559, 2009.

[9] D. S. Kirschen and G. Strbac, *Fundamentals of Power System Economics*. London, UK: John Wiley & Sons, 2004.

[10] J. Lavaei, S. Low, R. Baldick, B. Zhang, D. Molzahn, F. Dorfler, and H. Sandberg, "Guest editorial distributed control and efficient optimization methods for smart grid," *IEEE Transactions on Smart Grid*, vol. 8, no. 6, pp. 2939–2940, 2017.

[11] Y. He, B. Venkatesh, and L. Guan, "Optimal scheduling for charging and discharging of electric vehicles," *IEEE Transactions on Smart Grid*, vol. 3, no. 3, pp. 1095–1105, 2012.

[12] E. Sortomme, M. M. Hindi, S. J. MacPherson, and S. S. Venkata, "Coordinated charging of plug-in hybrid electric vehicles to minimize distribution system losses," *IEEE Transactions on Smart Grid*, vol. 2, no. 1, pp. 198–205, 2011.

[13] L. Deori, K. Margellos, and M. Prandini, "On decentralized convex optimization in a multi-agent setting with separable constraints and its application to optimal charging of electric vehicles," in *2016 IEEE 55th Conference on Decision and Control (CDC)*, Dec 2016, pp. 6044–6049.

[14] L. Deori, K. Margellos, and M. Prandini, "On the connection between nash equilibria and social optima in electric vehicle charging control games," *IFAC-PapersOnLine*, vol. 50, no. 1, pp. 14 320–14 325, 2017.

[15] N. Wade, P. Taylor, P. Lang, and P. Jones, "Evaluating the benefits of an electrical energy storage system in a future smart grid," *Energy Policy*, vol. 38, no. 11, pp. 7180–7188, 2010.

[16] J. Eyer and G. Corey, "Energy storage for the electricity grid: Benefits and market potential assessment guide," Sandia National Laboratories, USA, Tech. Rep., Feb. 2010.

[17] J. P. Barton and D. G. Infield, "Energy storage and its use with intermittent renewable energy," *IEEE transactions on energy conversion*, vol. 19, no. 2, pp. 441–448, 2004.

[18] Z. Fadlullah, Y. Nozaki, A. Takeuchi, and N. Kato, "A survey of game theoretic approaches in smart grid," in *Wireless Communications and Signal Processing (WCSP), 2011 International Conference on*, 2011, pp. 1–4.

[19] W. Saad, Z. Han, H. Poor, and T. Basar, "Game-theoretic methods for the smart grid: An overview of microgrid systems, demand-side management, and smart grid communications," *IEEE Signal Processing Magazine*, vol. 29, no. 5, pp. 86–105, 2012.

[20] A. D. Paola, D. Angeli, and G. Strbac, "Distributed control of micro-storage devices with mean field games," *IEEE Transactions on Smart Grid*, vol. 7, no. 2, pp. 1119–1127, 2016.

[21] H. Soliman and A. Leon-Garcia, "Game-theoretic demand-side management with storage devices for the future smart grid," *IEEE Transactions on Smart Grid*, vol. 5, no. 3, pp. 1475–1485, 2014.

[22] N. Li, L. Chen, and S. Low, "Optimal demand response based on utility maximization in power networks," in *Power and Energy Society General Meeting, 2011 IEEE*, 2011, pp. 1–8.

[23] P. Vytelingum, T. D. Voice, S. D. Ramchurn, A. Rogers, and N. R. Jennings, "Agent-based micro-storage management for the smart grid," in *Proc. 9th Int. Conf. Autonomous and Multiagent Systems*, Toronto, Canada, 2010, pp. 39–46.

[24] A. De Paola, D. Angeli, and G. Strbac, "Price-based schemes for distributed coordination of flexible demand in the electricity market," *IEEE Transactions on Smart Grid*, vol. 8, no. 6, pp. 3104–3116, 2017.

[25] D. Paccagnan, B. Gentile, F. Parise, M. Kamgarpour, and J. Lygeros, "Nash and Wardrop equilibria in aggregative games with coupling constraints," *IEEE transactions on Automatic Control*, vol. 64, no. 4, p. 13731388, 2019.

[26] T. H. Bradley and A. A. Frank, "Design, demonstrations and sustainability impact assessments for plug-in hybrid electric vehicles," *Renew. Sustain. Energy Rev.*, vol. 13, no. 1, pp. 115–128, 2009.

[27] F. Rahimi and A. Ipakchi, "Demand response as a market resource under the smart grid paradigm," *IEEE Transactions on Smart Grid*, vol. 1, no. 1, pp. 82–88, 2010.

[28] Y. Zhang, N. Gatsis, and G. B. Georgios, "Robust energy management for microgrids with high-penetration renewables," *IEEE Transactions on Sustainable Energy*, vol. 4, no. 4, pp. 944–953, 2013.

[29] Z. Fan, "A distributed demand response algorithm and its application to phev charging in smart grids," *IEEE Transactions on Smart Grid*, vol. 3, no. 3, pp. 1280–1290, 2012.

[30] L. Gan, U. Topcu, and S. H. Low, "Stochastic distributed protocol for electric vehicle charging with discrete charging rate," in *Power and Energy Society General Meeting, 2012 IEEE*, 2012, pp. 1–8.

[31] A. Mohsenian-Rad, V. Wong, J. Jatskevich, R. Schober, and A. Leon-Garcia, "Autonomous demand-side management based on game-theoretic energy consumption scheduling for the future smart grid," *IEEE Transactions on Smart Grid*, vol. 1, no. 3, pp. 320–331, 2010.

[32] L. Gan, U. Topcu, and S. H. Low, "Optimal decentralized protocol for electric vehicle charging," *IEEE Transactions on Power Systems*, vol. 28, no. 2, pp. 940–951, 2013.

[33] Z. Ma, D. Callaway, and I. Hiskens, "Decentralized charging control of large populations of plug-in electric vehicles," *IEEE Transactions on Control Systems Technology*, vol. 21, no. 1, pp. 67–78, 2013.

[34] B. G. Kim, S. Ren, M. van der Schaar, and J. W. Lee, "Bidirectional energy trading and residential load scheduling with electric vehicles in the smart grid," *IEEE Journal on Selected Areas in Communications*, vol. 31, no. 7, pp. 1219–1234, 2013.

[35] H. Chen, Y. Li, R. Louie, and B. Vucetic, "Autonomous demand side management based on energy consumption scheduling and instantaneous load billing: An aggregative game approach," *IEEE Transactions on Smart Grid*, vol. 5, no. 4, pp. 1744–1754, 2014.

[36] Z. Ma, S. Zou, X. S. L. Ran, and I. Hiskens, "Efficient decentralized coordination of large-scale plug-in electric vehicle charging," *Automatica*, vol. 69, pp. 35–47, 2016.

[37] M. González Vayá, T. Krause, R. A. Waraichand, and G. Andersson, "Locational marginal pricing based impact assessment of plug-in hybrid electric vehicles on transmission networks," in *CIGRE International Symposium*, Bologna, Italy, 2011.

[38] L. Wang, "Potential impacts of plug-in hybrid electric vehicles on locational marginal prices," in *IEEE Energy 2030 Conference*, Atlanta, GA, 2008.

[39] L. Wu, "Impact of price-based demand response on market clearing and locational marginal prices," *IET Generation, Transmission & Distribution*, vol. 7, no. 10, pp. 1087–1095, 2013.

[40] Y. Wang, L. Wu, and S. Wang, "A fully-decentralized consensus-based admm approach for dc-opf with demand response," *IEEE Transactions on Smart Grid*, vol. 8, no. 6, pp. 2637–2647, 2017.

[41] M. González Vayá, M. D. Galus, R. A. Waraich, and G. Andersson, "On the interdependence of intelligent charging approaches for plug-in electric vehicles in transmission and distribution networks," in *Proc. IEEE PES Innovative Smart Grid Technologies Europe*, Berlin, 2012.

[42] C. Zhao, J. Wang, J. Watson, and Y. Guan, "Multi-stage robust unit commitment considering wind and demand response uncertainties," *IEEE Trans. on Power Systems*, vol. 28, no. 3, pp. 2708–2717, 2013.

[43] A. De Paola, D. Angeli, and G. Strbac, "Convergence and optimality of a new iterative price-based scheme for distributed coordination of flexible loads in the electricity market," in *Proceedings of the IEEE Conference on Decision and Control*, Melbourne, 2017, pp. 1386–1393.

[44] Z. Yang, H. Zhong, A. Bose, T. Zheng, Q. Xia, and C. Kang, "Linearized OPF model with reactive power and voltage magnitude: a pathway to improve the Mw-only DC OPF," *IEEE Transactions on Power Systems*, vol. 33, no. 2, pp. 1734–1745, 2018.

[45] T. Akbari and M. T. Bina, "Linear approximated formulation of ac optimal power flow using binary discretisation," *IET Generation, Transmission & Distribution,*, vol. 10, no. 5, pp. 1117–1123, 2016.

[46] L. C. Evans and R. F. Gariepy, *Measure theory and fine properties of functions*. Boca Raton, FL: CRC, 1992.

[47] S. Grammatico, "Dynamic control of agents playing aggregative games with coupling constraints," *IEEE Transactions on Automatic Control*, vol. 62, no. 9, pp. 4537–4548, 2017.

[48] P. M. Subcommittee, "IEEE reliability test system," *IEEE Transactions on Power Apparatus and Systems*, vol. PAS-98, no. 6, pp. 2047–2054, 1979.

[49] P. Richardson, D. Flynn, and A. Keane, "Optimal charging of electric vehicles in low-voltage distribution systems," *IEEE Transactions on Power Systems*, vol. 27, no. 1, pp. 268–279, 2012.

[50] R. Doherty and M. O'Malley, "A new approach to quantify reserve demand in systems with significant installed wind capacity," *IEEE Transactions on Power Systems*, vol. 20, no. 2, pp. 587–595, May 2005.

[51] S. A. Pourmousavi and M. H. Nehrir, "Real-time central demand response for primary frequency regulation in microgrids," *IEEE Transactions on Smart Grid*, vol. 3, no. 4, pp. 1988–1996, Dec 2012.

[52] M. Vanouni and N. Lu, "A reward allocation mechanism for thermostatically controlled loads participating in intra-hour ancillary services," *IEEE Transactions on Smart Grid*, vol. 9, no. 5, pp. 4209–4219, 2018.

[53] A. D. Paola, V. Trovato, D. Angeli, and G. Strbac, "A mean field game approach for distributed control of thermostatic loads acting in simultaneous energy-frequency response markets," *IEEE Transactions on Smart Grid*, pp. 1–1, 2019.

[54] W. Li, P. Du, and N. Lu, "Design of a new primary frequency control market for hosting frequency response reserve offers from both generators and loads," *IEEE Transactions on Smart Grid*, vol. 9, no. 5, pp. 4883–4892, Sep. 2018.

[55] J. Wang, N. E. Redondo, and F. D. Galiana, "Demand-side reserve offers in joint energy/reserve electricity markets," *IEEE Transactions on Power Systems*, vol. 18, no. 4, pp. 1300–1306, Nov 2003.

[56] M. Parvania and M. Fotuhi-Firuzabad, "Demand response scheduling by stochastic SCUC," *IEEE Transactions on Smart Grid*, vol. 1, no. 1, pp. 89–98, 2010.

[57] F. Partovi, M. Nikzad, B. Mozafari, and A. M. Ranjbar, "A stochastic security approach to energy and spinning reserve scheduling considering demand response program," *Energy*, vol. 36, no. 5, pp. 3130 – 3137, 2011.

[58] N. G. Paterakis, O. Erdin, A. G. Bakirtzis, and J. P. S. Catalo, "Qualification and quantification of reserves in power systems under high wind generation penetration considering demand response," *IEEE Transactions on Sustainable Energy*, vol. 6, no. 1, pp. 88–103, Jan 2015.

[59] A. G. Vlachos and P. N. Biskas, "Simultaneous clearing of energy and reserves in multi-area markets under mixed pricing rules," *IEEE Transactions on Power Systems*, vol. 26, no. 4, pp. 2460–2471, Nov 2011.

[60] D. Papadaskalopoulos and G. Strbac, "Decentralized participation of flexible demand in electricity markets - part i: Market mechanism," *IEEE Trans. Power Syst.*, vol. 28, no. 4, pp. 3658–3666, Nov 2013.

[61] X. Gong, A. D. Paola, D. Angeli, and G. Strbac, "A distributed price-based strategy for flexible demand coordination in multi-area systems," in *2018 IEEE PES Innovative Smart Grid Technologies Conference Europe (ISGT-Europe)*, Oct 2018, pp. 1–6.

[62] L. Deori, K. Margellos, and M. Prandini, "Regularized jacobi iteration for decentralized convex quadratic optimization with separable constraints," *IEEE Transactions on Control Systems Technology*, vol. 27, no. 4, pp. 1636–1644, 2019.

[63] F. Li and R. Bo, "DCOPF-based LMP simulation: algorithm, comparison with acopf, and sensitivity," *IEEE Transactions on Power Systems*, vol. 22, no. 4, pp. 1475–1485, 2007.

[64] National Grid. (2018, Nov.) Historical demand data. [Online]. Available: http://www2.nationalgrid.com/UK/Industry-information/Electricity-transmission-operational-data/Data-Explorer/

[65] F. Fele and K. Margellos, "Scenario-based robust scheduling for electric vehicle charging games," in *2019 IEEE International Conference on Environment and Electrical Engineering and 2019 IEEE Industrial and Commercial Power Systems Europe (EEEIC/I&CPS Europe)*, 2019.

[66] K. Margellos, V. Rostampour, M. Vrakopoulou, M. Prandini, G. Andersson, and J. Lygeros, "Stochastic unit commitment and reserve scheduling: A tractable formulation with probabilistic certificates," in *2013 European Control Conference (ECC)*, Jul 2019, pp. 2513–2518.

[67] M. Vrakopoulou, M. Katsampani, K. Margellos, J. Lygeros, and G. Andersson, "Probabilistic security-constrained ac optimal power flow," in *2013 IEEE Grenoble Conference*, Jun 2013.

[68] K. Margellos, T. Haring, P. Hokayem, M. Schubiger, J. Lygeros, and G. Andersson, "A robust reserve scheduling technique for power systems with high wind penetration," in *International conference on probabilistic methods applied to power systems*, Jun 2012.

[69] M. Vrakopoulou, K. Margellos, J. Lygeros, and G. Andersson, "A probabilistic framework for security constrained reserve scheduling of networks with wind power generation," in *2012 IEEE International Energy Conference and Exhibition (ENERGYCON)*, Sep 2012, pp. 452–457.

[70] H. Saboori, M. Mohammadi, and R. Taghe, "Virtual power plant (vpp) definition concept components and types," in *Proc. Asia-Pacific Power and Energy Engineering Conf. (APPEEC)*, Wuhan, China, 2011.

[71] R. K. Sundaram, *A first course in optimization theory.* New York: Cambridge Univ. Press, 1996.

[72] F. H. Clarke, *Optimization and Nonsmooth Analysis.* New York: Wiley, 1983.

[73] R. Goebel, R. G. Sanfelice, and A. R. Teel, *Hybrid Dynamical Systems.* Princeton University Press, 2012.

[74] A. L. Dontchev and R. T. Rockafellar, *Implicit Functions and Solution Mappings*. Springer, 2009.

[75] C. D. Aliprantis and K. C. Border, *Infinite Dimensional Analysis*. Springer, 2007.

Appendix A

Appendix to Chapter 2

A.1 Proof of Proposition 2.1

To prove the proposition statement, an equivalent characterization of a feasible power profile u is first provided. Elementary variations of the candidate equilibrium solution u^* are then analyzed, proving their feasibility. Finally, the equilibrium property is demonstrated.

Characterization of feasible power profiles: It is first shown that any $u_j \in \mathcal{U}_j$ can be expressed as the sum of u_j^* and a finite number M of elementary variations $\delta^{(m)}$:

$$u_j = u_j^* + \sum_{m=1}^{M} \delta^{(m)}. \tag{A.1}$$

Each variation $\delta^{(m)} \in \mathbb{R}^T$ is characterized by two time instants $\underline{t}^{(m)}$, $\bar{t}^{(m)} \in \mathcal{T}$ and a power quantity $\Delta^{(m)}$, through the following expression:

$$\delta_t^{(m)} = \begin{cases} \Delta^{(m)} & \text{if } t = \bar{t}^{(m)} \\ -\Delta^{(m)} & \text{if } t = \underline{t}^{(m)} \\ 0 & \text{otherwise.} \end{cases} \tag{A.2}$$

To verify that (A.1) is always valid, we present a constructive method to calculate the functions $\delta^{(1)}, \ldots, \delta^{(M)}$. The power variation $\delta^{(1)}$ is defined first. Let $E_j^{(0)} = E_j^*$ and E_j denote the energy vectors associated by (2.1a) to $u_j^{(0)} = u_j^*$ and u_j, respectively. Given $\Delta u_j^{(1)} = u_j - u_j^{(0)}$ we have:

$$\bar{t}^{(1)} = \min_{t \in \mathcal{T}} \left\{ t : \Delta u_{j,t}^{(1)} > 0 \right\} \tag{A.3a}$$

$$\underline{t}^{(1)} = \min_{t \in \mathcal{T}} \left\{ t : \Delta u_{j,t}^{(1)} < 0 \right\} \tag{A.3b}$$

$$\Delta^{(1)} = \min \left\{ \left| \Delta u_{j,\bar{t}^{(1)}}^{(1)} \right|, \left| \Delta u_{j,\underline{t}^{(1)}}^{(1)} \right| \right\}. \tag{A.3c}$$

The following expression can then be provided for $\delta^{(1)}$:

$$\delta_t^{(1)} = \begin{cases} \Delta^{(1)} & \text{if } t = \bar{t}^{(1)} \\ -\Delta^{(1)} & \text{if } t = \underline{t}^{(1)} \\ 0 & \text{otherwise.} \end{cases} \tag{A.4}$$

The power profile resulting from the application of $\delta^{(1)}$ is expressed as $u_j^{(1)} = u_j^{(0)} + \delta^{(1)}$. It can be proven that $u_j^{(1)}$ and the associated charge level $E_j^{(1)}$ from (2.1a) are feasible and fulfill (2.4). To verify that (2.4a) holds for $E_j^{(1)}$, it is sufficient to note that, given the feasibility of $u_j^{(0)}$, the following holds:

$$E_{j,T}^{(1)} = E_j^0 + \sum_{t=1}^{T} u_{j,t}^{(1)} \Delta t = E_j^0 + \sum_{t=1}^{T} u_{j,t}^{(0)} \Delta t + \sum_{t=1}^{T} \delta_t^{(1)} \Delta t = E_j^0. \tag{A.5}$$

To check that (2.4c) holds for $u_j^{(1)}$, as we are assuming feasibility of $u_j^{(0)} = u_j^*$ and u_j, it is sufficient to show the following:

$$u_{j,t}^{(1)} = u_{j,t}^{(0)} \quad \forall t \in \mathcal{T} \setminus \left\{ \underline{t}^{(1)}, \bar{t}^{(1)} \right\} \tag{A.6a}$$

$$u_{j,\underline{t}^{(1)}} \leq u_{j,\underline{t}^{(1)}}^{(1)} < u_{j,\underline{t}^{(1)}}^{(0)} \tag{A.6b}$$

$$u_{j,\bar{t}^{(1)}}^{(0)} < u_{j,\bar{t}^{(1)}}^{(1)} \leq u_{j,\bar{t}^{(1)}}. \tag{A.6c}$$

Note that (A.6a) straightly follows from (A.4) whereas (A.6b) and (A.6c) derive from the expression of $\Delta^{(1)}$ in (A.3c), which ensures that $u_{j,t}^{(1)}$ is always a convex combination of $u_{j,t}^{(0)} = u_{j,t}^{*}$ and $u_{j,t}$ when $t \in \{\bar{t}^{(1)}, \underline{t}^{(1)}\}$. Finally, condition (2.4b) for $E_j^{(1)}$ is verified exploiting the feasibility of $u_j^{(0)} = u_j^{*}$ and u_j (with associated charge levels $E_j^{(0)}$ and E_j). For the case $\underline{t}^{(1)} < \bar{t}^{(1)}$, it is sufficient to check the following:

$$E_{j,t} \leq E_{j,t}^{(1)} < E_{j,t}^{(0)} \quad \forall t : \underline{t}^{(1)} \leq t < \bar{t}^{(1)} \tag{A.7a}$$

$$E_{j,t}^{(1)} = E_{j,t}^{(0)} \quad \forall t :\in \mathcal{T} \setminus \left\{ t : \underline{t}^{(1)} \leq t < \bar{t}^{(1)} \right\} \tag{A.7b}$$

Considering equation (2.5b), condition (A.7b) is a result of (A.6a) and equal total sum of $u^{(0)}$ and $u^{(1)}$, whereas (A.7a) straightly follows from (A.6a) and (A.6b). Similar checks can be performed for the opposite case with $\underline{t}^{(1)} > \bar{t}^{(1)}$, confirming that (2.4) holds for $u_j^{(1)}$ and associated charge level $E_j^{(1)}$ and therefore $u_j^{(1)} \in \mathcal{U}_j$.

All the other variations $\delta^{(m)}$ can be obtained with the same procedure detailed above, replacing $u_j^{(0)}$, $u_j^{(1)}$ and $\Delta u^{(1)}$ with $u_j^{(m-1)}$, $u_j^{(m)}$ and $\Delta u^{(m)}$, respectively. Similar arguments can be used to demonstrate that $u_j^{(m)} = u_j^{(m-1)} + \delta^{(m)} \in \mathcal{U}_j$. Note that, as a result of the power variation $\delta^{(m)}$, the modified vector $u_j^{(m)}$ is equal to u_j in its component $t = \bar{t}^{(m)}$ or $t = \underline{t}^{(m)}$. With each power variation, the cardinality of the support of $\Delta u_j^{(m)} = u_j - u_j^{(m)}$ is reduced by one, implying that there exists a finite number $M \leq T$ such that:

$$u_j^{(M)} = u_j^{*} + \sum_{m=1}^{M} \delta^{(m)} = u_j. \tag{A.8}$$

Feasibility of modified strategies: The following condition is now verified:

$$u_j^{*} + \delta^{(m)} \in \mathcal{U}_j \quad \forall m \in \{1, \ldots, M\}. \tag{A.9}$$

The case with $\underline{t}^{(m)} < \bar{t}^{(m)}$ in (A.2) is discussed first. It has been proven that $u_j^{(m)} = u_j^{(m-1)} + \delta^{(m)} \in \mathcal{U}_j$ when $u_j^{(m-1)} \in \mathcal{U}_j$. This is equivalent to state that, for

the positive power amount $\Delta^{(m)}$, it holds:

$$\Delta^{(m)} \leq \frac{E_{j,t}^{(m-1)}}{\Delta t} \quad \forall t \in \{\underline{t}^{(m)}, \dots, \bar{t}^{(m)} - 1\} \tag{A.10a}$$

$$\Delta^{(m)} \leq u_{j,\underline{t}^{(m)}}^{(m-1)} - \underline{P}_j \tag{A.10b}$$

$$\Delta^{(m)} \leq \bar{P}_j - u_{j,\bar{t}^{(m)}}^{(m-1)}. \tag{A.10c}$$

In fact, if $u_j^{(m-1)} \in \mathcal{U}_j$, condition (A.10a) is equivalent to (2.4b) with $E_j = E_j^{(m)}$, where $E_j^{(m)}$ is the charge level associated to $u_j^{(m)}$. Similarly, conditions (A.10b) and (A.10c) are equivalent to (2.4c), which is already fulfilled at all other time instants since $u_j^{(m-1)} \in \mathcal{U}_j$. Finally, condition (2.4a) is always verified for $u = u_j^{(m)}$ when $u_j^{(m-1)} \in \mathcal{U}_j$, since the total sum of the power profiles remains constant. With the same reasoning, $u_j^* + \delta^{(m)} \in \mathcal{U}_j$ if and only if the following holds for $\Delta^{(m)}$:

$$0 < \Delta^{(m)} \leq \min\left(\left\{\bigcup_{\{t:\underline{t}^{(m)} \leq t < \bar{t}^{(m)}\}} \frac{E_{j,t}^*}{\Delta t}, u_{j,\underline{t}^{(m)}}^* - \underline{P}_j, \bar{P}_j - u_{j,\bar{t}^{(m)}}^*\right\}\right). \tag{A.11}$$

To show that (A.11) holds and therefore $u_j^* + \delta^{(m)} \in \mathcal{U}_j$, from (A.10) it is sufficient to verify that:

$$E_{j,t}^{(m-1)} \leq E_{j,t}^* \quad \forall t \in \{\underline{t}^{(m)}, \dots, \bar{t}^{(m)} - 1\}. \tag{A.12a}$$

$$u_{j,\underline{t}^{(m)}}^{(m-1)} - \underline{P}_j \leq u_{j,\underline{t}^{(m)}}^* - \underline{P}_j \tag{A.12b}$$

$$\bar{P}_j - u_{j,\bar{t}^{(m)}}^{(m-1)} \leq \bar{P}_j - u_{j,\bar{t}^{(m)}}^* \tag{A.12c}$$

As a result of the proposed constructive method, the following inequalities hold:

$$u_{j,t}^* = u_{j,t}^{(0)} \geq u_{j,t}^{(1)} \geq \cdots \geq u_{j,t}^{(M)} = u_{j,t} \quad \forall t \in \underline{\mathcal{T}} \tag{A.13a}$$

$$u_{j,t}^* = u_{j,t}^{(0)} \leq u_{j,t}^{(1)} \leq \cdots \leq u_{j,t}^{(M)} = u_{j,t} \quad \forall t \in \bar{\mathcal{T}} \tag{A.13b}$$

where $\underline{\mathcal{T}} := \left\{t : u_{j,t}^* > u_{j,t}\right\}$ and $\bar{\mathcal{T}} := \left\{t : u_{j,t}^* < u_{j,t}\right\}$. Since $\underline{t}^{(m)} \in \underline{\mathcal{T}}$ and $\bar{t}^{(m)} \in \bar{\mathcal{T}}$, it follows that $u_{j,\underline{t}^{(m)}}^* \geq u_{j,\underline{t}^{(m)}}^{(m-1)}$ and $u_{j,\bar{t}^{(m)}}^* \leq u_{j,\bar{t}^{(m)}}^{(m-1)}$, thus proving (A.12b)

and (A.12c). Condition (A.12a) is now verified by contradiction. Suppose that there exists a time instant $s \in \{\underline{t}^{(m)}, \ldots, \bar{t}^{(m)} - 1\}$ such that:

$$E^*_{j,s} < E^{(m-1)}_{j,s}. \tag{A.14}$$

If such inequality holds, there must be at least one previous power variation $\delta^{(p)}$ with $p < m$ such that $\bar{t}^{(p)} \leq s$ and $\underline{t}^{(p)} > s$. The inequality $\underline{t}^{(p)} > s$ implies that $\underline{t}^{(p)} > \underline{t}^{(m)}$. However, by the constructive method, we have that $\underline{t}^{(1)} \leq \underline{t}^{(2)} \leq, \ldots, \leq \underline{t}^{(M)}$, which contradicts the inequality $\underline{t}^{(p)} > \underline{t}^{(m)}$ and consequently indicates that (A.14) does not hold. Hence (A.12a) is proven. Note that this proof considers the case $\underline{t}^{(m)} < \bar{t}^{(m)}$. Similar arguments can be used to obtain the same result when $\underline{t}^{(m)} > \bar{t}^{(m)}$, thus proving (A.9).

Equilibrium proof: Let C^*_j and C_j denote the energy cost of device j in (2.8) when u^*_j and u_j in (A.1) are applied, respectively. The following expression can be derived:

$$\begin{aligned} C_j = C^*_j + \sum_{m=1}^{M} \Big(& \Pi(D_{\bar{t}^{(m)}}(u^*)) \left[y\left(u_{j,\bar{t}^{(m)}}\right) - y\left(u^*_{j,\bar{t}^{(m)}}\right) \right] \\ & + \Pi(D_{\underline{t}^{(m)}}(u^*)) \left[y\left(u_{j,\underline{t}^{(m)}}\right) - y\left(u^*_{j,\underline{t}^{(m)}}\right) \right] \Big) = C^*_j + \sum_{m=1}^{M} \Delta C^{(m)} \end{aligned} \tag{A.15}$$

where $\Delta C^{(m)}$ corresponds to the m-th term of the sums in the second term of (A.15). Note that u^* is not an aggregative equilibrium if there exists $u_j \in \mathcal{U}_j$ such that $C_j < C^*_j$. From (A.15), this is the case if and only if there exists $m \leq M$ such that $\Delta C^{(m)} < 0$ (for the sufficiency, note that $u^* + \delta^{(m)}$ would be a cost-reducing strategy). As a result, the proposition statement is verified if it is proved that $\gamma(u^*, j, \bar{t}^{(m)}, \underline{t}^{(m)}) > 0$ if and only if $\Delta C^{(m)} < 0$. To prove it, the following case is analyzed first:

$$0 \notin \left(u^*_{j,\bar{t}^{(m)}}, u_{j,\bar{t}^{(m)}}\right) \cup \left(u_{j,\underline{t}^{(m)}}, u^*_{j,\underline{t}^{(m)}}\right) \tag{A.16}$$

In other words, it is first assumed that the control values at $t = \bar{t}^{(m)}$ and $t = \underline{t}^{(m)}$ do

not cross zero. As a result, from (2.2) , we have $\eta(u^*_{j,\bar{t}^{(m)}}) = \eta(u_{j,\bar{t}^{(m)}})$ and $\eta(u_{j,\underline{t}^{(m)}}) = \eta(u^*_{j,\underline{t}^{(m)}})$. This simplifies considerably the expression of the cost variation $\Delta C^{(m)}$, which from (2.3) can be rewritten as:

$$\Delta C^{(m)} = \Delta^{(m)} \left[\eta(u^*_{j,\bar{t}^{(m)}})\Pi(D_{\bar{t}^{(m)}}(u^*)) - \eta(u^*_{j,\underline{t}^{(m)}})\Pi(D_{\underline{t}^{(m)}}(u^*))\right]. \tag{A.17}$$

In this case, from (A.16) and feasibility of $u^* + \delta^{(m)}$, we have:

$$0 < \Delta^{(m)} \leq \alpha(u^*, j, \underline{t}^{(m)}) \tag{A.18a}$$

$$0 < \Delta^{(m)} \leq \beta(u^*, j, \bar{t}^{(m)}). \tag{A.18b}$$

$$0 < \Delta^{(m)} \leq e(u^*, j, \bar{t}^{(m)}, \underline{t}^{(m)}). \tag{A.18c}$$

Moreover, since $\Delta^{(m)} > 0$ and we are assuming negativity of $\Delta C^{(m)}$, it holds:

$$\eta(u^*_{j,\underline{t}^{(m)}})\Pi(D_{\underline{t}^{(m)}}(u^*)) - \eta(u^*_{j,\bar{t}^{(m)}})\Pi(D_{\bar{t}^{(m)}}(u^*)) > 0. \tag{A.19}$$

Note that the inequalities (A.18) and (A.19) correspond to positivity of the four factors of $\gamma(u^*, j, \bar{t}^{(m)}, \underline{t}^{(m)})$ in (2.12). Since its first three factors are always nonnegative, it follows that $\gamma(u^*, j, \bar{t}^{(m)}, \underline{t}^{(m)}) > 0$ if and only if $\Delta C^{(m)} < 0$. The proposition statement is verified if the above results also hold in the following case:

$$0 \in \left(u^*_{j,\bar{t}^{(m)}}, u_{j,\bar{t}^{(m)}}\right) \cup \left(u_{j,\underline{t}^{(m)}}, u^*_{j,\underline{t}^{(m)}}\right). \tag{A.20}$$

To check this, a smaller power swap $\tilde{\Delta}$ can be considered, with the following properties:

$$0 < \tilde{\Delta} < \Delta^{(m)} \tag{A.21a}$$

$$0 \notin \left(u^*_{j,\bar{t}^{(m)}}, u^*_{j,\bar{t}^{(m)}} + \tilde{\Delta}\right) \cup \left(u^*_{j,\underline{t}^{(m)}} - \tilde{\Delta}, u^*_{j,\underline{t}^{(m)}}\right). \tag{A.21b}$$

For the associated cost variation, it holds:

$$\Delta\tilde{C} = \tilde{\Delta}\left[\eta(u^*_{j,\bar{t}}) \cdot \Pi(D_{\bar{t}^{(m)}}(u^*)) - \eta(u^*_{j,\underline{t}}) \cdot \Pi(D_{\underline{t}^{(m)}}(u^*))\right]. \tag{A.22}$$

To extend the results obtained for (A.16) to the case in (A.20) and conclude the proof, it is sufficient to consider that $\Delta\tilde{C} < 0$ when $\Delta C^{(m)} < 0$. This is not formally proved for length reasons but it is straightforward to verify if one considers that the power increase at time $\bar{t}^{(m)}$ from u^*_j to u_j is associated to higher costs when the zero is crossed (coefficient $\mu_+ > 1$ is considered instead of $\mu_- < 1$) and the power decrease at time $\underline{t}^{(m)}$ from u^*_j to u_j is associated to lower savings when the zero is crossed (coefficient $\mu_- < 1$ is considered instead of $\mu_+ > 1$).

A.2 Proof of Proposition 2.2

Proof of (2.23a): The following equivalent property is verified:

$$V(u^+) \leq V(u) \qquad \forall u^+ \in F(u), \ \forall u \in \mathcal{U}. \tag{A.23}$$

As the mapping F is defined in (2.20) as the composition of N submappings F_j, it is sufficient to prove the following stronger condition:

$$V(y) \leq V(u) \qquad \forall y \in F_j(u), \forall j \in \mathcal{N}, \ \forall u \in \mathcal{U}. \tag{A.24}$$

Note that (A.24) is verified if the following holds for all $s_j(u) = (\bar{t}, \underline{t}) \in S_j(u)$:

$$V(y) = V(f^{(s_j)}(u)) < V(u) \quad \text{if } \gamma(u, j, \bar{t}, \underline{t}) > 0 \tag{A.25a}$$

$$V(y) = V(f^{(s_j)}(u)) = V(u) \quad \text{if } \gamma(u, j, \bar{t}, \underline{t}) \leq 0 \tag{A.25b}$$

The case with positive γ is analyzed first. In this scenario, given the nonnegativity of the functions α, β and e in (2.11), it holds:

$$\Pi(D_{\underline{t}}(u)) > \frac{\eta(u_{j,\bar{t}})}{\eta(u_{j,\underline{t}})} \Pi(D_{\bar{t}}(u)). \tag{A.26}$$

From the expression of $\gamma(u, j, \bar{t}, \underline{t})$ in (2.12), it follows that also $\Delta(u, j, \bar{t}, \underline{t})$, as defined in (2.16), is positive. Given (2.22), expression (2.19) for the single components of $f^{(s_j)}(u)$ and definition (2.6) of the aggregate demand $D_t(u)$, it holds:

$$V(f^{(s_j)}(u)) - V(u) = \int_{D_{\bar{t}}(u)}^{D_{\bar{t}}(u) + \eta(u_{j,\bar{t}})\Delta(u,j,\bar{t},\underline{t})} \Pi(x)\, dx - \int_{D_{\underline{t}}(u) - \eta(u_{j,\underline{t}})\Delta(u,j,\bar{t},\underline{t})}^{D_{\underline{t}}(u)} \Pi(x)\, dx. \tag{A.27}$$

Let $W(z) : \mathbb{R} \to \mathbb{R}$ denote the function returning the right-hand side of (A.27) when $\Delta(u, j, \bar{t}, \underline{t})$ is replaced by z. Its derivative takes the following expression:

$$\dot{W}(z) = \frac{dW(z)}{dz} = \eta(u_{j,\bar{t}})\Pi\left(D_{\bar{t}}(u) + \eta(u_{j,\bar{t}})z\right) - \eta(u_{j,\underline{t}})\Pi\left(D_{\underline{t}}(u) - \eta(u_{j,\underline{t}})z\right). \tag{A.28}$$

The following conditions are fulfilled:

$$\dot{W}(0) = \eta(u_{j,\bar{t}})\Pi\left(D_{\bar{t}}(u)\right) - \eta(u_{j,\underline{t}})\Pi\left(D_{\underline{t}}(u)\right) < 0 \tag{A.29a}$$

$$\dot{W}(z) < 0 \qquad \forall z \in \left[0, \frac{\eta(u_{j,\underline{t}})\Pi(D_{\underline{t}}(u)) - \eta(u_{j,\bar{t}})\Pi(D_{\bar{t}}(u))}{\Gamma\left(\eta(u_{j,\underline{t}})^2 + \eta(u_{j,\bar{t}})^2\right)}\right) \tag{A.29b}$$

where (A.29a) corresponds to the last inequality in (A.26). To verify that also (A.29b) holds, it is sufficient to consider (A.29a) and the following inequality as a result of the Lipschitz continuity of Π established in Assumption 2.1:

$$\begin{aligned}\dot{W}(z) &\leq \eta(u_{j,\bar{t}})\left[\Pi\left(D_{\bar{t}}(u)\right) + \Gamma\eta(u_{j,\bar{t}})z\right] - \eta(u_{j,\underline{t}})\left[\Pi\left(D_{\underline{t}}(u)\right) - \Gamma\eta(u_{j,\underline{t}})z\right] \\ &= \dot{W}(0) + \Gamma\left[\eta(u_{j,\bar{t}})^2 + \eta(u_{j,\underline{t}})^2\right] z\end{aligned}$$

To verify that (A.25a) holds, it is sufficient to consider the following:

$$V(f^{(s_j)}(u)) - V(u) = \int_0^{\Delta(u,j,\bar{t},\underline{t})} \dot{W}(z)\, dz < 0$$

where the inequality follows from expressions (2.16) and (2.17), which ensure that Δ is always within the interval considered in (A.29b) when $\gamma(u, j, \bar{t}, \underline{t}) > 0$. In order to also verify (A.25b) and conclude the proof of (2.23a), one can follow a similar reasoning, showing that $\Delta(u, j, \bar{t}, \underline{t}) = 0$ when $\gamma(u, j, \bar{t}, \underline{t}) \leq 0$. As a result, we have $f^{(s_j)}(u) = u$ and $V(f^{(s_j)}(u)) = V(u)$.

Proof of (2.23b): As it has been proven that V is non decreasing when any F_j is applied, it follows that (A.25b) must hold for all $j \in \mathcal{N}$ when $u = \phi(k)$ and $V(\phi(k+1)) = V(\phi(k))$. As previously established, this implies $\Delta(u, j, \bar{t}, \underline{t}) = 0$ for all j and therefore $\phi(k+1) = \phi(k)$.

Proof of (2.23c): This straightly follows from (2.23a) and the boundedness of V.

A.3 Proof of Theorem 2.1

The theorem can be verified by showing that, from the upper semi-continuity of F, all solutions $\phi \in \Phi$ asymptotically converge to their omega-limit set $\Omega(\phi)$. From the invariance of the set $\Omega(\phi)$, it follows that $\Omega(\phi) \subseteq \Omega^*$. The rigorous analytical steps can be found in the proof of [43, Theorem 1] which also applies to the present case.

A.4 Proof of Theorem 2.2

Consider the functional $\tilde{V}(d) : \mathbb{R}^T \to \mathbb{R}$ defined as follows:

$$\tilde{V}(d) = \sum_{t=1}^{T} G(d_t) \tag{A.30}$$

with $d \in \mathbb{R}^T$ and $G(d_t) = \int_0^{d_t} \Pi(x)\, dx$. The theorem statement is equivalent to the following condition:

$$\tilde{V}(D(u^*)) \leq \tilde{V}(D(u)) \qquad \forall u \in \mathcal{U}. \tag{A.31}$$

From the strict monotonicity of the price function Π established in Assumption 2.1 it follows that $\tilde{V}$ is strictly convex. As a result, condition (A.31) holds if the following is verified:

$$\sum_{t=1}^{T} \Pi(D_t(u^*)) \left[D(u) - D(u^*)\right] = \sum_{t=1}^{T} \Pi(D_t(u^*)) \left[\sum_{j=1}^{N} y(u_{j,t}) - y(u^*_{j,t})\right] \geq 0 \quad \forall u \in \mathcal{U}. \tag{A.32}$$

A slightly stronger condition is proved:

$$\sum_{t=1}^{T} \Pi(D_t(u^*)) \left[y(u_{j,t}) - y(u^*_{j,t})\right] \geq 0 \qquad \forall j \in \mathcal{N} \tag{A.33}$$

As we have established that u^* corresponds to an aggregative equilibrium and $u^* \in \mathcal{U}$, it follows from (2.9) that (A.33) always holds, thus concluding the proof.

Appendix B

Appendix to Chapter 3

B.1 Proof of Proposition 3.1

Two key points are preliminarily shown. Firstly, the objective function in the right-hand side of (3.1) is strictly convex given the strict convexity of each f_m. Secondly, let $\mathcal{G}(D)$ denote the set of feasible active and reactive power generation, and voltage angle and magnitude vectors (G, GQ, θ, v^2) that fulfill (3.2) for a certain demand vector $D \in \mathbb{R}^{MT}$. The graph of $\mathcal{G}$ is convex. This property straightly follows from the linearity and convexity of the constraints in (3.2). As a result of the above points, the strict convexity of $\varphi(D)$ with respect to D follows from the maximum theorem under convexity [71].

B.2 Proof of Proposition 3.2

For simplicity, we consider the simplified case in which the minimized generation cost $\varphi(D)$ in (3.1) is always differentiable. As a result, prices at bus m at time t are unique and equal to:

$$\bar{p}_{m,t}(D) = \underline{p}_{m,t}(D) = p_{m,t}(D) = \frac{\partial \varphi(D)}{\partial D_{m,t}}. \tag{B.1}$$

From Proposition 3.1, we have that $\varphi(D)$ is a strictly convex function and therefore its Hessian matrix H is positive definite, with $H \succ 0$. From basic properties of positive definite matrices, the following holds for each diagonal element of H:

$$\frac{\partial^2 \varphi(D)}{\partial D_{m,t}^2} > 0 \quad \forall t, m. \tag{B.2}$$

To verify the proposition statement, it is sufficient to check the positivity of the following partial derivative:

$$\frac{\partial p_{m,t}(D)}{\partial D_{m,t}} = \frac{\partial}{\partial D_{m,t}} \left(\frac{\partial \varphi(D)}{\partial D_{m,t}} \right) = \frac{\partial^2 \varphi(D)}{\partial D_{m,t}^2} > 0 \quad \forall t, m. \tag{B.3}$$

B.3 Proof of Proposition 3.3

Each feasible power schedule u_j for agent j can be expressed as the sum of the strategy u_j^* at the candidate equilibrium solution plus a finite number Q of elementary variations:

$$u_j = u_j^* + \sum_{q=1}^{Q} \delta_q \tag{B.4}$$

where each term $\delta_q : \mathcal{T} \to \mathbb{R}$, for some $\Delta_q > 0$ and $(\bar{t}_q, \underline{t}_q) \in \mathcal{A}_j \times \mathcal{A}_j$ has the following expression:

$$\delta_{q,t} = \Delta_q \cdot \mathbb{1}_{\{\bar{t}_q\}}(t) - \Delta_q \cdot \mathbb{1}_{\{\underline{t}_q\}}(t). \tag{B.5}$$

The above expressions can represent all the elements $u_j \in \mathcal{U}_j$, since these are characterized by the same fixed sum. In addition, one can assume without loss of generality that each δ_q corresponds to a feasible power swap of Δ_q between the time instants $\bar{t}_q$ and $\underline{t}_q$. As a result, it must hold:

$$0 < \Delta_q \leq \min\left(\left\{P_j - u^*_{j,\bar{t}_q}, u^*_{j,\underline{t}_q}\right\}\right) \tag{B.6}$$

If one substitutes (B.4) in (3.10), the cost variation ΔC_j can be written as:

$$\Delta C_j = \sum_q \left[\bar{p}^*_{\mu_j,\bar{t}_q}(D(u^*)) - \underline{p}^*_{\mu_j,\underline{t}_q}(D(u^*))\right] \Delta_q \Delta t \tag{B.7}$$

Suppose that $\Delta C_j < 0$ for some $u_j \in \mathcal{U}_j$. From (B.6) and (B.7) there should exist $\hat{q} \leq Q$ such that the following holds:

$$\bar{p}^*_{\mu_j,\bar{t}_{\hat{q}}}(D(u^*)) < \underline{p}^*_{\mu_j,\underline{t}_{\hat{q}}}(D(u^*)) \quad u^*_{j,\bar{t}_{\hat{q}}} < P_j \quad u^*_{j,\underline{t}_{\hat{q}}} > 0. \tag{B.8}$$

This would imply $\gamma(u^*, j, \bar{t}_{\hat{q}}, \underline{t}_{\hat{q}}) > 0$, thus proving the proposition statement by contradiction.

B.4 Proof of Proposition 3.4

Proof of (3.21a): An equivalent condition is verified:

$$\varphi(D(u^+)) \leq \varphi(D(u)) \qquad \forall u^+ \in F(u),\ \forall u \in \mathcal{U}. \tag{B.9}$$

From (3.19), F is the composition of N elementary mapping F_j, defined in (3.17). Therefore, a slightly stronger condition can be proven by means of inequalities on each F_j:

$$\varphi(D(y)) \leq \varphi(D(u)) \qquad \forall y \in F_j(u), \forall j \in \mathcal{N},\ \forall u \in \mathcal{U}. \tag{B.10}$$

Note that (B.10) holds if, for all $s_j = (\bar{t}_j, \underline{t}_j) \in S_j(u)$, we have:

$$\varphi\left(D\left(f^{(s_j)}(u)\right)\right) < \varphi\left(D\left(u\right)\right) \qquad \textit{if } \gamma(u, j, \bar{t}_j, \underline{t}_j) > 0 \tag{B.11a}$$

$$\varphi\left(D\left(f^{(s_j)}(u)\right)\right) = \varphi\left(D\left(u\right)\right) \qquad \textit{if } \gamma(u, j, \bar{t}_j, \underline{t}_j) \leq 0 \tag{B.11b}$$

For the case of (B.11a) with $\gamma(u, j, \bar{t}_j, \underline{t}_j) > 0$, since by definition $u_{j,\bar{t}_j} \leq P_j$ and $u_{j,\underline{t}_j} \geq 0$, as a result of (3.12) it holds:

$$\underline{p}_{\mu_j,\underline{t}}(D(u)) - \bar{p}_{\mu_j,\bar{t}}(D(u)) > 0 \quad u_{j,\bar{t}_j} < P_j \quad u_{j,\underline{t}_j} > 0. \tag{B.12}$$

For the function ϵ in (3.5), given the monotonicity of $\bar{p}$ and $\underline{p}$ established in Proposition 3.2, we have:

$$\epsilon\left(D(u), \mu_j, \bar{t}_j, \underline{t}_j\right) > 0 \tag{B.13}$$

which implies positivity of Δ in (3.16), as a result of (B.12):

$$\Delta\left(u, \mu_j, \bar{t}_j, \underline{t}_j\right) = \bar{\Delta} > 0. \tag{B.14}$$

Recalling expressions (3.8) and (3.18), and applying the mean value theorem for non-smooth functions [72], the left-hand side in (B.11a) can be rewritten as follows:

$$\begin{aligned}\varphi\left(D\left(f^{(s_j)}(u)\right)\right) &= \varphi\left(D\left(u+\bar{\Delta}\left(\hat{\mathbf{e}}_{j,\bar{t}_j}-\hat{\mathbf{e}}_{j,\underline{t}_j}\right)\right)\right)\\ &= \varphi\left(D\left(u\right)+\bar{\Delta}\left(\hat{\mathbf{e}}_{\mu_j,\bar{t}_j}-\hat{\mathbf{e}}_{\mu_j,\underline{t}_j}\right)\right)\\ &= \varphi(D(u))+\left\langle \partial\varphi(\tilde{D}),\bar{\Delta}\left(\hat{\mathbf{e}}_{\mu_j,\bar{t}_j}-\hat{\mathbf{e}}_{\mu_j,\underline{t}_j}\right)\right\rangle\end{aligned} \tag{B.15}$$

where $\tilde{D}$ is some convex combination of $D(u)$ and $D\left(f^{(s_j)}(u)\right)$ and $\partial\varphi$ denotes the generalized gradient of φ. From Proposition 3.1, this corresponds to the subdifferential of φ. The above equation can now be rewritten as:

$$\varphi\left(D\left(f^{(s_j)}(u)\right)\right) = \varphi\left(D\left(u\right)\right)+\bar{\Delta}\left(\bar{p}^*-\underline{p}^*\right) \tag{B.16}$$

with $\bar{p}^* \in \frac{\partial\varphi(\tilde{D})}{\partial\tilde{D}_{\mu_j,\bar{t}_j}}$ and $\underline{p}^* \in \frac{\partial\varphi(\tilde{D})}{\partial\tilde{D}_{\mu_j,\underline{t}_j}}$. Condition (B.11a) is therefore verified by the positivity of $\bar{\Delta}$ in (B.14) and the following:

$$\bar{p}^* \overset{(a)}{\leq} \bar{\varphi}'_{\mu_j,\bar{t}_j}(\tilde{D}) \overset{(b)}{<} \bar{p}_{\mu_j,\bar{t}_j}\left(D\left(f^{(s_j)}(u)\right)\right) \overset{(c)}{\leq} \underline{p}_{\mu_j,\underline{t}_j}\left(D\left(f^{(s_j)}(u)\right)\right) \overset{(d)}{<} \underline{\varphi}'_{\mu_j,\underline{t}_j}(\tilde{D}) \overset{(e)}{\leq} \underline{p}^*. \tag{B.17}$$

The inequalities (a) and (e) follow from (3.3) and (3.4), (b) and (d) are a result of Proposition 3.2 and (c) holds by construction of $\epsilon(D(u),\mu_j,\bar{t}_j,\underline{t}_j)$ as expressed in (3.5) in Definition 3.1. We can conclude that (B.11a) holds as a result of (B.16) and (B.17). Similar arguments can be used to also verify (B.11b), thus proving (3.21a).

Proof of (3.21b): Since φ is nonincreasing when any F_j is applied, (B.11b) must hold for all $j \in \mathcal{N}$ when $u = \psi(k)$ and $\varphi(\psi(k+1)) = \varphi(\psi(k))$. As previously proved, this implies $\Delta(u,\mu_j,\bar{t}_j,\underline{t}_j) = 0$ for all j and therefore $\psi(k+1) = \psi(k)$.

Proof of (3.21c): This property straightly follows from (3.21a) and the boundedness of φ.

B.5 Proof of Theorem 3.1

Consider the omega-limit set $\Omega(\psi)$ associated to the solution $\psi \in \Psi$ and defined as follows:

$$\Omega(\psi) := \left\{ u_\infty : \exists \{k_n\}_{n\in\mathbb{N}}, \ \lim_{n\to\infty} k_n = \infty, \ \lim_{n\to\infty} \psi(k_n) = u_\infty \right\}. \tag{B.18}$$

The theorem is verified if the following holds for all $\psi \in \Psi$:

$$\lim_{k\to\infty} |\psi(k)|_{\Omega(\psi)} = 0 \tag{B.19a}$$

$$\Omega(\psi) \subseteq \Omega^*. \tag{B.19b}$$

Condition (B.19a): This result holds if the mapping F is upper-semicontinuous [73, Chapter 6.3.3]. Since F takes non-empty compact values, the upper-semicontinuity of the mapping is guaranteed by F having a closed graph $\mathcal{G}$ [74, Chapter 3B]. Accounting for the compactness of $\mathcal{U}$, it is sufficient to show that the graph $\mathcal{G}_j$ of the individual mappings F_j in (3.19) is closed [75]. The graph $\mathcal{G}_j$ can be expressed as:

$$\begin{aligned} \mathcal{G}_j &= \left\{ (u, f^{(s_j)}(u)) : u \in \mathcal{U}, \ f^{(s_j)}(u) \in F_j(u) \right\} \\ &= \bigcup_{s_j \in \mathcal{A}_j \times \mathcal{A}_j} \mathcal{G}^{(s_j)} = \bigcup_{s_j \in \mathcal{A}_j \times \mathcal{A}_j} \left\{ (u, f^{(s_j)}(u)) : u \in U^{(s_j)} \right\}. \end{aligned} \tag{B.20}$$

where $U^{(s_j)} \subseteq \mathcal{U}$ has the following expression:

$$\begin{aligned} U^{(s_j)} &= \{ \ u \in \mathcal{U} : s_j = (\bar{t}_j, \underline{t}_j) \in S_j(u) \ \} \\ &= \{ u \in \mathcal{U} : s_j = (\bar{t}_j, \underline{t}_j), \gamma(u, j, \bar{t}_j, \underline{t}_j) \geq \gamma(u, j, \bar{t}, \underline{t}) \ \ \forall (\bar{t}, \underline{t}) \in \mathcal{A}_j \times \mathcal{A}_j \}. \end{aligned} \tag{B.21}$$

One can verify that $\mathcal{G}^{(s_j)}$ is closed since the state-space subset $U^{(s_j)}$ is closed (defined by a set of non-strict inequalities) and each component $f_{i,t}^{(s_j)}(u)$ of $f^{(s_j)}(u)$ in (3.17) is continuous with respect to u. This means that also $\mathcal{G}_j$ is closed (union of a finite number of closed sets), thus proving the closedness of $\mathcal{G}$, the upper semi-continuity of F and condition (B.19a).

Condition (B.19b): To verify that each point in $\Omega(\psi)$ also belongs to the set of variational aggregative equilibria Ω^*, it is preliminarily shown that, as a result of (3.21c) and continuity of φ and D, the following holds for all $u_\infty \in \Omega(\psi)$:

$$\varphi(D(u_\infty)) = \varphi\left(D\left(\lim_{n\to\infty}\psi(k_n)\right)\right) = \lim_{n\to\infty}\varphi(D(\psi(k_n))) = \lim_{k\to\infty}\varphi(D(\psi(k))) = \varphi_\infty. \tag{B.22}$$

Moreover, as a result of the outer-semicontinuity of the mapping F, weak-forward invariance of $\Omega(\psi)$ is also guaranteed [73, Chapter 6.3.3]:

$$F(u_\infty) \cap \Omega(\psi) \neq \varnothing \qquad \forall u_\infty \in \Omega(\psi). \tag{B.23}$$

As (B.22) establishes that all points $u_\infty \in \Omega(\psi)$ have equal costs φ_∞ and φ is non decreasing along all trajectories ψ, there must exist $s_1 = (\bar{t}_1, \underline{t}_1) \in S_1(u_\infty)$ such that:

$$\varphi\left(D\left(f^{(s_1)}(u_\infty)\right)\right) = \varphi(D(u_\infty)) \qquad \gamma(u_\infty, 1, \bar{t}_1, \underline{t}_1) \leq 0. \tag{B.24}$$

If this were not the case, from (3.19) and (3.21a), we would have $\varphi(D(u^+)) < \varphi(D(u_\infty))$, $\forall u^+ \in F(u_\infty)$, which contradicts (B.23) if one considers (B.22). As γ is maximized by all $s \in S_1(u_\infty)$ from (3.15), we have:

$$\gamma(u_\infty, 1, \bar{t}, \underline{t}) \leq 0 \quad \forall s = (\bar{t}, \underline{t}) \in S_1(u_\infty). \tag{B.25a}$$

$$\Delta(u_\infty, 1, \bar{t}, \underline{t}) = 0 \quad \forall s = (\bar{t}, \underline{t}) \in S_1(u_\infty) \tag{B.25b}$$

where (B.25b) also implies $F_1(u_\infty) = \{u_\infty\}$. Recursive application of the same arguments for $j = 2, \ldots, N$ yields:

$$\gamma(u_\infty, j, \bar{t}, \underline{t}) \leq 0 \quad \forall s_j = (\bar{t}, \underline{t}) \in S_j(u_\infty), \forall j \in \mathcal{N}. \tag{B.26}$$

The proof of (B.19b) is concluded by noting that, from (3.15), conditions (B.26) and (3.13) in Proposition 3.3 when $u^* = u_\infty$.

B.6 Proof of Theorem 3.2

Given the differentiability of $\varphi(D(u^*))$, the following gradient vector can be derived from (3.3):

$$\nabla_m \varphi(D) = \left[\frac{\partial \varphi(D)}{\partial D_{m,1}}, \ldots, \frac{\partial \varphi(D)}{\partial D_{m,T}}\right] = \left[\varphi'_{m,1}(D), \ldots, \varphi'_{m,T}(D)\right]. \tag{B.27}$$

From the strict convexity of $\varphi(D)$ in Proposition 3.1, it is sufficient to prove the following local condition for any $u \in \mathcal{U}$:

$$\begin{aligned} &\langle \nabla_m \varphi(D(u^*)), D_m(u) - D_m(u^*) \rangle \\ &\quad = \sum_{t=1}^{T} \varphi'_{m,t}(D(u^*)) \cdot [D_{m,t}(u) - D_{m,t}(u^*)] \qquad \forall m \in \mathcal{M}. \\ &\quad = \sum_{t=1}^{T} \varphi'_{m,t}(D(u^*)) \left[\sum_{j:\mu_j = m} u_{j,t} - u^*_{j,t}\right] \geq 0 \end{aligned} \tag{B.28}$$

We recall that any $u \in \mathcal{U}$ can be characterized as the sum of u^* and a finite number Q of power swaps δ_q, as presented in equations (B.4)-(B.5) in the proof of Proposition 3.3. Therefore, condition (B.28) holds if the following is verified for all $j \in \mathcal{N}$:

$$\begin{aligned} \sum_{t=1}^{T} \varphi'_{\mu_j,t}(D(u^*)) \left[u_{j,t} - u^*_{j,t}\right] &= \sum_{t=1}^{T} \varphi'_{\mu_j,t}(D(u^*)) \left[\sum_{q=1}^{Q} \delta_{q,t}\right] \\ &= \sum_{q=1}^{Q} \Delta_q \left[\varphi'_{\mu_j,\bar{t}_q}(D(u^*)) - \varphi'_{\mu_j,\underline{t}_q}(D(u^*))\right] \\ &= \sum_{q=1}^{Q} \Delta_q \left[\bar{p}_{\mu_j,\bar{t}_q}(D(u^*)) - \underline{p}_{\mu_j,\underline{t}_q}(D(u^*))\right] \geq 0. \end{aligned} \tag{B.29}$$

Consider now the equilibrium condition (3.13) in Proposition 3.3. From expression (3.12) of γ and recalling (B.6) from the feasibility of δ_q, one can conclude that $\underline{p}_{\mu_j,\underline{t}_q}(D(u^*)) \leq \bar{p}_{\mu_j,\bar{t}_q}(D(u^*))$ at the equilibrium $u^* \in \Omega^*$, thus proving (B.29) and the theorem.

Appendix C

Appendix to Chapter 4

C.1 Proof of Proposition 4.1

Note that (4.29a) can be verified by construction and the proposition holds if there exists $\bar{\Delta} > 0$, different in general for (4.29b) and (4.29c), such that these conditions are satisfied when $\nabla_{u_j} C(u, u_j) \left(\hat{\mathbf{e}}_{j,\bar{t}} - \hat{\mathbf{e}}_{j,\underline{t}}\right) < 0$ and $\Delta \in [0, \bar{\Delta}]$.

Proof of (4.29b): When $j \in \mathcal{N}^{EV}$, the only term in (4.18) which depends on u_j is the derivative of the discomfort cost $\partial\psi(u_j)/\partial u_{j,t}$. Since $\hat{E}(u_j, t)$ in (4.17) is piecewise linear, the same holds for $\psi(u_j)$ in (4.16). This means that $\partial\psi(u_j)/\partial u_{j,t}$ and the cost derivative $\partial C(u, u_j)/\partial u_{j,t}$ are piecewise constant $\forall t \in \mathcal{T}$. As a result, there always exists $\bar{\Delta} > 0$ such that:

$$\frac{\partial C(u, u_j + \hat{\mathbf{e}}_{j,\bar{t}} s - \hat{\mathbf{e}}_{j,\underline{t}} s)}{\partial u_{j,\bar{t}}} = \frac{\partial C(u, u_j)}{\partial u_{j,\bar{t}}} \qquad \forall s \in [0, \bar{\Delta}] \tag{C.1a}$$

$$\frac{\partial C(u, u_j + \hat{\mathbf{e}}_{j,\bar{t}} s - \hat{\mathbf{e}}_{j,\underline{t}} s)}{\partial u_{j,\underline{t}}} = \frac{\partial C(u, u_j)}{\partial u_{j,\underline{t}}} \qquad \forall s \in [0, \bar{\Delta}]. \tag{C.1b}$$

To take into account the possibility of u_j being a discontinuity point (where the cost derivative switches between two constant values), it is assumed that the left and right derivative are considered in (C.1a) and (C.1b), respectively. Given $\bar{\Delta}$ and the

associated modified strategy $u_j^+ = u_j + \left(\hat{\mathbf{e}}_{j,\bar{t}} - \hat{\mathbf{e}}_{j,\underline{t}}\right)\bar{\Delta}$, it holds:

$$C(u, u_j^+) - C(u, u_j) = \int_0^{\bar{\Delta}} \nabla_{u_j} C(u, u_j + \hat{\mathbf{e}}_{j,\bar{t}} s - \hat{\mathbf{e}}_{j,\underline{t}} s)\left(\hat{\mathbf{e}}_{j,\bar{t}} - \hat{\mathbf{e}}_{j,\underline{t}}\right) ds$$
$$= \int_0^{\bar{\Delta}} \nabla_{u_j} C(u, u_j)\left(\hat{\mathbf{e}}_{j,\bar{t}} - \hat{\mathbf{e}}_{j,\underline{t}}\right) ds = \nabla_{u_j} C(u, u_j)\left(\hat{\mathbf{e}}_{j,\bar{t}} - \hat{\mathbf{e}}_{j,\underline{t}}\right)\bar{\Delta}. \quad \text{(C.2)}$$

Equation (C.2) also holds in the case $j \in \mathcal{N}^S$ by considering r instead of ψ in the proof above.

Proof of (4.29c): Consider the following parametrized expression W for the variation of the function V:

$$W(\Delta) = V(u + \left(\hat{\mathbf{e}}_{j,\bar{t}} - \hat{\mathbf{e}}_{j,\underline{t}}\right)\Delta) - V(u) = V(u^+) - V(u)$$
$$= \varphi(\tilde{D}(u^+), \tilde{R}(u^+)) - \varphi(\tilde{D}(u), \tilde{R}(u)) + \psi(u_j^+) - \psi(u_j) \quad \text{(C.3)}$$

When $j \in \mathcal{N}^{EV}$, we have $\partial D_{\mu_j,t}(u)/\partial u_{j,t} = \partial R_{\mu_j,t}(u)/\partial u_{j,t} = 1$. Therefore, if we consider $\tilde{u}(s) = u + \left(\hat{\mathbf{e}}_{j,\bar{t}} - \hat{\mathbf{e}}_{j,\underline{t}}\right)s$, it holds:

$$W(\Delta) = \int_0^{\Delta} \frac{\partial\varphi(\tilde{D}(\tilde{u}(s)), \tilde{R}(\tilde{u}(s)))}{\partial D_{\mu_j,\bar{t}}} + \frac{\partial\varphi(\tilde{D}(\tilde{u}(s)), \tilde{R}(\tilde{u}(s)))}{\partial R_{\mu_j,\bar{t}}}$$
$$- \frac{\partial\varphi(\tilde{D}(\tilde{u}(s)), \tilde{R}(\tilde{u}(s)))}{\partial D_{\mu_j,\underline{t}}} - \frac{\partial\varphi(\tilde{D}(\tilde{u}(s)), \tilde{R}(\tilde{u}(s)))}{\partial R_{\mu_j,\underline{t}}}$$
$$+ \frac{\partial\psi(\tilde{u}_j(s))}{\partial u_{j,\bar{t}}} - \frac{\partial\psi(\tilde{u}_j(s))}{\partial u_{j,\underline{t}}}\, ds. \quad \text{(C.4)}$$

Recalling the price equations (4.3) and (4.14) and expression (4.19) for the cost derivative, the quantity $\dot{W}(\Delta) = dW(\Delta)/d\Delta$ evaluated at $\Delta = 0$ is equal to:

$$\dot{W}(0) = \left(\tilde{p}_{\mu_j,\bar{t}}(u) - \tilde{\rho}_{\mu_j,\bar{t}}(u) + \frac{\partial\psi(\tilde{u}_j(s))}{u_{j,\bar{t}}}\right)$$
$$- \left(\tilde{p}_{\mu_j,\underline{t}}(u) - \tilde{\rho}_{\mu_j,\underline{t}}(u) + \frac{\partial\psi(\tilde{u}_j(s))}{u_{j,\underline{t}}}\right) = \nabla_{u_j} C(u, u_j)\left(\hat{\mathbf{e}}_{j,\bar{t}} - \hat{\mathbf{e}}_{j,\underline{t}}\right). \quad \text{(C.5)}$$

As initially established in this proof, we are considering $\nabla_{u_j} C(u, u_j)\left(\hat{\mathbf{e}}_{j,\bar{t}} - \hat{\mathbf{e}}_{j,\underline{t}}\right) < 0$ and therefore we have $W(0) = 0$ and $\dot{W}(0) < 0$. For continuity of W and $\dot{W}$

(ensured by Assumption 4.1), there exists a finite $\bar{\Delta}$ such that $W(\Delta) < 0$ for all $\Delta \in (0, \bar{\Delta}]$, thus concluding the proof. Same arguments can be used to demonstrate the proposition statement when $j \in \mathcal{N}^S$, recalling that in this case $\partial D_{\mu_j,t}(u)/\partial u_{j,t} = 1$ and $\partial R_{\mu_j,t}(u)/\partial u_{j,t} = \partial r_{j,t}(u)/\partial u_{j,t}$.

C.2 Proof of Theorem 4.1

Proof of convergence: It is initially demonstrated that Algorithm 3 converges asymptotically to some final power schedule u^*. To this end, the following preliminary result is proved:

$$V(u(k)) \leq V(u(k-1)) \qquad \forall k > 0. \tag{C.6}$$

In the algorithm, when $\delta > 0$ for a device j, it is sufficient to note that the gradient $\nabla_{u_j} C(u, u_j) \left(\hat{\mathbf{e}}_{j,\bar{t}} - \hat{\mathbf{e}}_{j,\underline{t}}\right) < 0$ from (4.29a) and therefore, from (4.29b)-(4.29c), we have:

$$V(u^+) - V(u) < 0. \tag{C.7}$$

In addition, it is trivial to check when $\delta = 0$, we have $V(u^+) = V(u)$ as in this case $u^+ = u$. It is now sufficient to conclude that after a **FOR** cycle (from $k-1$-th to k-th cycle), (C.6) holds. Since V is a bounded quantity, it follows from (C.6) that $V(u(k))$ converges to some minimum value. At such minimum the **IF** condition in step 2.b.iii) is never verified, otherwise V would be further reduced. Hence the variable *conv* (set to 1 in step 2.a) does not change value throughout the **FOR** cycle and it ensures that step 3) and the final power schedule u^* is reached.

Proof of equilibrium: To verify that the final result u^* of Algorithm 3 corresponds to the aggregative equilibrium of Definition 4.1, an alternative formulation is considered for the feasible power profiles $u_j \in \mathcal{U}_j$ of device j. In particular, each u_j can be characterized as the sum of the candidate equilibrium solution u^* and a finite number M of elementary power swaps $\delta^{(m)}$:

$$u_j = u_j^* + \sum_{m=1}^{M} \delta^{(m)}. \tag{C.8}$$

Each $\delta^{(m)}$ corresponds to swapping Δ_m units of power from time $\underline{t}_m$ to time $\bar{t}_m$ and it can be expressed as follows:

$$\delta^{(m)} = \Delta_m \left(\hat{\mathbf{e}}_{\bar{t}_m} - \hat{\mathbf{e}}_{\underline{t}_m} \right). \tag{C.9}$$

The terms $\delta^{(1)}, \ldots, \delta^{(M)}$ can always be selected in order to fulfil the following feasibility conditions:

$$u_j^{(m)} = u_j^* + \sum_{i=1}^{m} \delta^{(i)} \in \mathcal{U}_j \qquad \forall m \in \{1, \ldots, M\} \tag{C.10a}$$

$$\tilde{u}_j^{(m)} = u_j^* + \delta^{(m)} \in \mathcal{U}_j \qquad \forall m \in \{1, \ldots, M\}. \tag{C.10b}$$

Furthermore, the following additional condition is assumed:

$$\nabla_{u_j} C \left(u^*, u_j^* + \epsilon \left(\hat{\mathbf{e}}_{j,\bar{t}} - \hat{\mathbf{e}}_{j,\underline{t}} \right) \right) = \nabla_{u_j} C(u^*, u_j^*) \quad \forall \epsilon \in [0, \Delta_m]. \tag{C.11}$$

This does not introduce any loss of generality since $\nabla_{u_j} C$ is piecewise continuous: any $\delta^{(m)}$ with associated Δ_m not fulfilling (C.11) can be split into multiple smaller swaps such that (C.10) and (C.11) hold.

The equilibrium result is now demonstrated by contradiction. In particular, it is assumed that u^* is not an aggregative equilibrium and there exists some $u_j \in \mathcal{U}_j$ such that $C(u^*, u_j) < C(u^*, u_j^*)$. From (C.10), if this were the case, there would exist $m \in \{1, \ldots, M\}$ such that:

$$C(u^*, u_j^* + \delta^{(m)}) < C(u^*, u_j^*). \tag{C.12}$$

From the feasibility result in (C.10b) for $u_j^* + \delta^{(m)}$, we have:

$$a(u^*, j, \bar{t}_m) > 0 \quad b(u^*, j, \underline{t}_m) > 0 \quad c(u^*, j, \bar{t}_m, \underline{t}_m) > 0. \tag{C.13}$$

From (C.12) and (C.11), it follows that $C(u, u_j) \left(\hat{\mathbf{e}}_{j,\bar{t}} - \hat{\mathbf{e}}_{j,\underline{t}} \right) < 0$. As a result of (4.29a), it also holds:

$$d(u^*, j, \bar{t}_m, \underline{t}_m) > 0. \tag{C.14}$$

We can conclude from (C.13) and (C.14) that $\delta(u^*, j, \bar{t}_m, \underline{t}_m)$ in (4.25) is also positive. This is not possible, since $u^* = u(k)$ represents the final result in step 3 of Algorithm 3, which is only reached when the variable *conv* remains equal to one through in step 2 and therefore $\delta(u^*, j, \bar{t}_m, \underline{t}_m) \leq 0$. It follows that (C.12) cannot hold, thus concluding the proof by contradiction.

C.3 Proof of Theorem 4.2

Given the strict convexity of f_m^G and f_m^R and the linearity of all the constraints in (4.2), it follows that $\varphi(D, R)$ is strictly convex. Therefore, (4.30) holds if the following sufficient condition is satisfied for all $u \in \mathcal{U}$:

$$\sum_{m=1}^{M} \nabla_{D_m}\varphi(\tilde{D}(u^*), \tilde{R}(u^*)) \left[\tilde{D}_m(u) - \tilde{D}_m(u^*)\right] + \sum_{m=1}^{M} \nabla_{R_m}\varphi(\tilde{D}(u^*), \tilde{R}(u^*)) \left[\tilde{R}_m(u) - \tilde{R}_m(u^*)\right] + \sum_{j\in\mathcal{N}^{EV}} \nabla_{u_j}\psi(u_j^*)(u_j - u_j^*) \geq 0 \quad \text{(C.15)}$$

Recalling (4.12) and (4.13), this corresponds to:

$$\sum_{m=1}^{M} \left[\nabla_{D_m}\varphi(\tilde{D}(u^*), \tilde{R}(u^*)) \sum_{\{j:\mu_j=m\}} \left(u_j - u_j^*\right)\right] + \sum_{m=1}^{M} \left[\nabla_{R_m}\varphi(\tilde{D}(u^*), \tilde{R}(u^*)) \sum_{\{j:\mu_j=m\}} (r_j(u) - r_j(u^*))\right] + \sum_{j\in\mathcal{N}^{EV}} \nabla_{u_j}\psi(u_j^*)(u_j - u_j^*) \geq 0. \quad \text{(C.16)}$$

A slightly stronger condition is considered over all $j \in \mathcal{N}$ and $u_j \in \mathcal{U}_j$. In the case $j \in \mathcal{N}^{EV}$ and $\mu_j = m$, this corresponds to:

$$\nabla_{D_m}\varphi(\tilde{D}(u^*), \tilde{R}(u^*))(u_j - u_j^*) + \nabla_{R_m}\varphi(\tilde{D}(u^*), \tilde{R}(u^*))(r_j(u) - r_j(u^*)) + \nabla_{u_j}\psi(u_j^*)(u_j - u_j^*) \geq 0 \quad \text{(C.17)}$$

Since $\nabla_{D_m}\varphi$ and $\nabla_{R_m}\varphi$ correspond respectively to the vectors of prices $\tilde{p}_m$ and $\tilde{\rho}_m$, this is equivalent to $\nabla_{u_j}C(u^*, u_j)(u_j - u_j^*) \geq 0$, which is always verified since u_j^* is an aggregative equilibrium according to Definition 4.1, thus concluding the proof.